

## LEVEL II

12

RADC-TR-81-92

Final Technical Report, 18 Jan 79-10 Feb 84

May 1981

(12) 125



# DEVELOPMENT OF BORIDE COMPOSITE MATERIALS FOR COLD CATHODE DEVICES.

Georgia Institute of Technology

⑯ EES/GIT-A-23#3

John W. Goodrum

15 F19628-79-C-0048

16 4600 17 171

APPROVED FOR PUBLIC RELEASE: DISTRIBUTION UNLIMITED

**ROME AIR DEVELOPMENT CENTER  
Air Force Systems Command  
Griffiss Air Force Base, New York 13441**

DTIC  
ELECTED  
JUL 22 1981

153850

81 7 22 0 12

FILE COPY

This report has been reviewed by the RADC Public Affairs Office (PA) and is releasable to the National Technical Information Service (NTIS). At NTIS it will be releasable to the general public, including foreign nations.

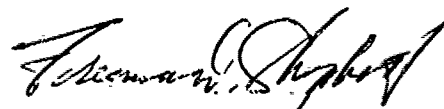
RADC-TR-81-92 has been reviewed and is approved for publication.

APPROVED:



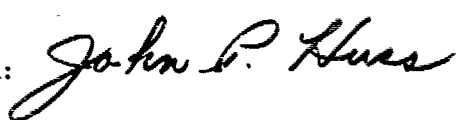
JOSEPH J. HUTTA  
Project Engineer

APPROVED:



FREEMAN D. SHEPHERD, Acting Director  
Solid State Sciences Division

FOR THE COMMANDER:



JOHN P. HUSS  
Acting Chief, Plans Office

If your address has changed or if you wish to be removed from the RADC mailing list, or if the addressee is no longer employed by your organization, please notify RADC (ESM) Hanscom AFB MA 01731. This will assist us in maintaining a current mailing list.

Do not return this copy. Retain or destroy.

UNCLASSIFIED

~~SECURITY CLASSIFICATION OF THIS PAGE (When Data Entered)~~

DD FORM 1 JAN 73 1473 EDITION OF 1 NOV 65 IS OBSOLETE

UNCLASSIFIED

**SECURITY CLASSIFICATION OF THIS PAGE (When Data Entered)**

UNCLASSIFIED

SECURITY CLASSIFICATION OF THIS PAGE (When Data Entered)

bring the most promising systems to the point where test specimens could be produced. The LaB<sub>6</sub>-B eutectic shows greatest promise, followed by LaB<sub>6</sub>-Ni and LaB<sub>6</sub>-Cu, as potentially useful composite field emission cathode material.

Accession For	
NTIS GRA&I	<input checked="" type="checkbox"/>
DTIC TAB	<input type="checkbox"/>
Unannounced	<input type="checkbox"/>
Justification	
By _____	
Distribution/	
Availability Codes	
Dist	Avail and/or
	Special
A	

UNCLASSIFIED

---

SECURITY CLASSIFICATION OF THIS PAGE/When Data Entered)

## Table of Contents

	Page
List of Illustrations	iv
List of Tables	vi
<u>Section</u>	
I. Introduction	1
II. The System $\text{LaB}_6$ -B	4
A. INTRODUCTION . . . . .	4
B. SURVEY OF LITERATURE . . . . .	6
C. PROCEDURE AND RESULTS . . . . .	19
D. DISCUSSION OF RESULTS . . . . .	34
E. CONCLUSIONS AND RECOMMENDATIONS . . . . .	43
F. APPENDIX, (SAMPLE EXAMINATION AND ANALYSIS TECHNIQUES) .	45
G. BIBLIOGRAPHY . . . . .	47
III. The System $\text{Fe}_2\text{B}$ -Fe	49
A. INTRODUCTION . . . . .	49
B. EXPERIMENTAL PROCEDURE . . . . .	49
C. EXPERIMENTAL TESTS . . . . .	52
D. BIBLIOGRAPHY . . . . .	58
IV. The System $(\text{TiB}_2, \text{LaB}_6)$ -Ni	59
A. THE Ni-TiB <sub>2</sub> SYSTEM . . . . .	59
B. THE Ni-LaB <sub>6</sub> SYSTEM . . . . .	76
C. SUMMARY . . . . .	88
D. BIBLIOGRAPHY . . . . .	89
V. The System $\text{LaB}_6$ -Cu	90
A. INTRODUCTION . . . . .	90

B. EXPERIMENTAL PROCEDURES . . . . .	90
C. EXPERIMENTS . . . . .	94
D. SUMMARY . . . . .	102
E. BIBLIOGRAPHY . . . . .	107
VI. Summary and Recommendations . . . . .	108
VII. General Bibliography (titled) . . . . .	111

## LIST OF ILLUSTRATIONS

Figure	Page
1. Structure of $\text{LaB}_6$ . . . . .	8
2. $\text{LaB}_6$ -B Phase Diagram . . . . .	9
3. Influence of Volume Fraction, V, of Minor Phase on Fibrous to Lamellae Transition, Theoretical and Actual . .	16
4. Boron Powder Ground in a WC Mill Two Minutes. x700 . . . .	21
5. Boron Powder as Received From the Supplier. x700 . . . .	21
6. Lanthanum Hexaboride Powder as Received from the Supplier. x700 . . . . .	22
7. Diagram of the Induction Heating Facilities . . . . .	24
8. Typical Pellet After RF Heating . . . . .	26
9. Typical RF Induction Furnace Power and Grid Current Curves . . . . .	27
10. Ball Milled Boron Powder. x700 . . . . .	32
11. Ball Milled Lanthanum Hexaboride Powder. x700 . . . . .	32
12. $\text{LaB}_6$ Oriented Microstructure. x1100 . . . . .	36
13. $\text{LaB}_6$ Oriented Microstructure. x575 . . . . .	36
14. EDAX Mapping of $\text{LaB}_6$ Microstructure Depicted in Figure 12 Showing Location of La. x1100 . . . . .	37
15. EDAX Mapping of $\text{LaB}_6$ Microstructure Depicted in Figure 13 Showing Location of La. x575 . . . . .	37
16. Continuous Pure Boron Area Containing Eutectic Structure. x500 . . . . .	39
17. Areas of Eutectic Microstructure. x700 . . . . .	39
18. Areas of Eutectic Microstructure. x200 . . . . .	42
19. Areas of Eutectic Microstructure. x500 . . . . .	42
Fe-1. Phase Diagram for Fe-B . . . . .	50
Fe-2. $\text{Fe}_2\text{B}$ -Fe Eutectic . . . . .	51

Fe-3. (to Fe-9) Micrographs of $Fe_2B$ -Fe Eutectic . . . . .	53
Ni-1. Eutectics of $TiB_2$ with Metals . . . . .	60
Ni-2. (to Ni-17) Micrographs of $TiB_2$ -Ni System . . . . .	63
Ni-18. (to Ni-21) Low Magnifications of $LaB_6$ -Ni Products . . . . .	78
Ni-22. (to Ni-30) Micrographs of $LaB_6$ -Ni System . . . . .	83
Cu-1. Phase Diagram for Cu-B . . . . .	91
Cu-2. Copper-Boron Eutectic . . . . .	92
Cu-3. Micrograph of $LaB_6$ Components . . . . .	95
Cu-4. (to Cu-16) Micrographs of $LaB_6$ -Cu System . . . . .	95

## LIST OF TABLES

Table	Page
1. Chemical Stability of $\text{LaB}_6$ in Boiling Acids and Bases . . . . .	10
2. Properties of Boron and Lanthanum Hexaboride . . . . .	13
3. Summary of Experimental Results . . . . .	35
Ni-1. Experimental Runs for $\text{TiB}_2$ -Ni System . . . . .	61
Ni-2. Experimental Runs for $\text{LaB}_6$ -Ni System . . . . .	77
Cu-1. Experimental Runs for $\text{LaB}_6$ -Cu System . . . . .	93

Introduction:

The purpose of this research was to conduct a study to determine and evaluate the potential of selected directionally solidified composite eutectics as electron beam sources in cathodes and other important technological applications. This project consisted of an effort to identify highly promising eutectic systems, then conduct synthesis and/or electron emission experiments to characterize the behavior of these materials.

In the search for promising eutectic systems made up of a transition metal boride plus matrix, the following selected guidelines were followed, in order of decreasing importance:

- (1) The system, matrix/metal-boride, must be either binary or pseudo-binary.
- (2) The eutectic must have a small volume fraction of metal-boride phase (to assure a fibrous metal-boride phase).
- (3) Metal-boride phase must melt at relatively high temperatures, on the order of 1500 to 2000 C minimum.
- (4) Metal-boride must have low electrical resistance.
- (5) Metal-boride phase must have good field emission properties: low work function, resistant to ion bombardment, low vapor pressure, no interactions with matrix which significantly degrade field emission.
- (6) The eutectic must produce aligned growth when directionally solidified.

(7) Other factors: must have matching of metal-boride and matrix thermal expansion coefficients, excessive volatility of matrix should be avoided, etc.

On the basis of the above criteria and other considerations based on experience, the following systems were selected for study:

- (1)  $\text{LaB}_6$  - B
- (2)  $\text{TiB}_2$  - Fe, Ni
- (3)  $\text{LaB}_6$  - Fe, Ni
- (4)  $\text{Fe}_2\text{B}$  - Fe
- (5)  $\text{LaB}_6$  - Cu

In general, little information was available on these boride systems; other eutectics had been reported but even less was known of their eutectic behavior. Therefore, the above compounds were selected as most likely to yield a candidate cathode material during the course of this project.

Approach Used for this Study:

For the several systems which were studied during this contract period, the following general approach was decided upon.

- (1) Set up and conduct screening experiments for selection of eutectics for Directional Growth studies.
- (2) Prepare apparatus and conduct Directional Growth experiments with several possible eutectic compositions.

- (3) Conduct SEM, Microprobe and other analytical studies of the above products. Particular emphasis was placed upon optical study of polished sections to identify microstructural geometrics.

## THE SYSTEM $\text{LaB}_6$ - B

### INTRODUCTION

Directionally solidified ceramic-ceramic or ceramic-metal systems have a number of possible future applications because of the intimate association of materials having different properties or extreme anisotropy. Directional solidification of two or more phases would permit a designer to choose the materials having optimum properties for a given device in order to amplify the desired effects which would otherwise be weak. There are possible optical and magnetic as well as electronic applications which would benefit from the property enhancement provided with directionally solidified materials.

As an example of one application of a directionally solidified material, Cochran, et al.<sup>1</sup> and Hill<sup>2</sup> at the Georgia Institute of Technology are presently investigating a low voltage field emission material consisting of a directionally solidified array of tungsten rods in a uranium dioxide matrix. They have demonstrated a current density capability of  $30 \text{ A/cm}^2$  from the multi-pin arrays, which is competitive with the conventional thermionic cathodes presently being used. Field emission characteristics depend on the value of the work function of the emitting surface (assuming field enhancement of the tip is constant). A decrease in the work function increases field emission. The choice of a composite consisting of electrically conducting rods having a sufficiently low work function in a semiconducting or insulating matrix

depends initially on the ability of the materials involved to form a suitable eutectic structure. According to the available literature, lanthanum hexaboride forms a eutectic or eutectoid at a composition of about 3 atomic percent lanthanum and 97 atomic percent boron at a temperature of  $2025^{\circ}\text{C} \pm 200^{\circ}\text{C}$ . Lanthanum hexaboride is a metallic-type conductor with a relatively low work function of 2.74 eV as compared to 4.5 eV for tungsten. Boron is a semiconductor.

The objective of this research was to attempt to directionally solidify lanthanum hexaboride in a boron matrix using a modified internal zone melting technique in an RF induction furnace. Pellets of the eutectic composition available from the literature were melted as well as pellets of a composition above and below the eutectic. In addition, several fabrication techniques, different furnace atmospheres and a variety of conventional crucible materials were investigated.

## SURVEY OF LITERATURE

This chapter includes a survey of the available literature concerning the properties of boron and lanthanum hexaboride, processing methods for boride powders, a brief discussion of unidirectional solidification, and multi-pin array field emission.

### Properties of Boron and Lanthanum Hexaboride

The following is a discussion of the properties of boron, lanthanum hexaboride and electron emission from lanthanum hexaboride.

#### Boron

Boron is the first and lightest element of the third group of the Periodic Table with an atomic number of five and an atomic weight of 10.82. Crystalline boron reacts very little at room temperature, but at temperatures above 1200 °C, it reacts with most metals, forming compounds with the metals and metal oxides. Pure boron is silvery gray in color.

In order to avoid reactions with other materials at high temperatures, boron is heated in crucibles made of hexagonal boron nitride or water cooled metallic crucibles of copper or silver. Even with these precautions, boron will react with trace amounts of oxygen, nitrogen or carbonaceous residues from oils of vacuum pumps if present in the system.<sup>3</sup>

Boron shows very little reaction with hydrogen. Even in the colloidal state, crystalline boron shows no reaction on soaking in water. Hydrogen peroxide, ammonium persulfate and potassium permanganate oxidize crystalline boron slowly, but amorphous boron oxidizes readily. The best oxidizing agents for crystalline boron are fused alkalies, carbonates or sodium peroxide.<sup>4</sup>

Boron is a semiconductor with a resistivity at room temperature of  $1.8 \times 10^6$  ohm-cm.<sup>4</sup> Boron occurs in several polymorphs of which  $\beta$ -rhombohedral boron is the only one grown from a melt and actually prepared in a size suitable for electrical investigation. The knowledge of the semiconducting properties of crystalline boron is limited to this polymorph. Boron plays an important role in electronic devices such as neutron detectors, high-power and high-temperature devices, and switching devices.

#### Lanthanum Hexaboride

One compound of lanthanum and boron is lanthanum hexaboride which has a  $\text{CaB}_6$ -type crystal structure of cubic symmetry and is represented in Figure 1.<sup>5</sup>

According to Spear, et al., "LaB<sub>6</sub> melts congruently at 2715 °C and a eutectoid is believed to occur at 2025 °C containing the two phases LaB<sub>6</sub> and B. A phase diagram of LaB<sub>6</sub>-B according to Spear is shown in Figure 2 with the estimated LaB<sub>6</sub>-B eutectoid temperature in parentheses.<sup>6</sup>

The compound LaB<sub>6</sub> exists over a range of composition, extending from 85.8 percent boron (LaB<sub>6</sub>), to about 88 percent boron (LaB<sub>7.8</sub>) with a variation in color from pink to blue. Primary crystals of the LaB<sub>6</sub>

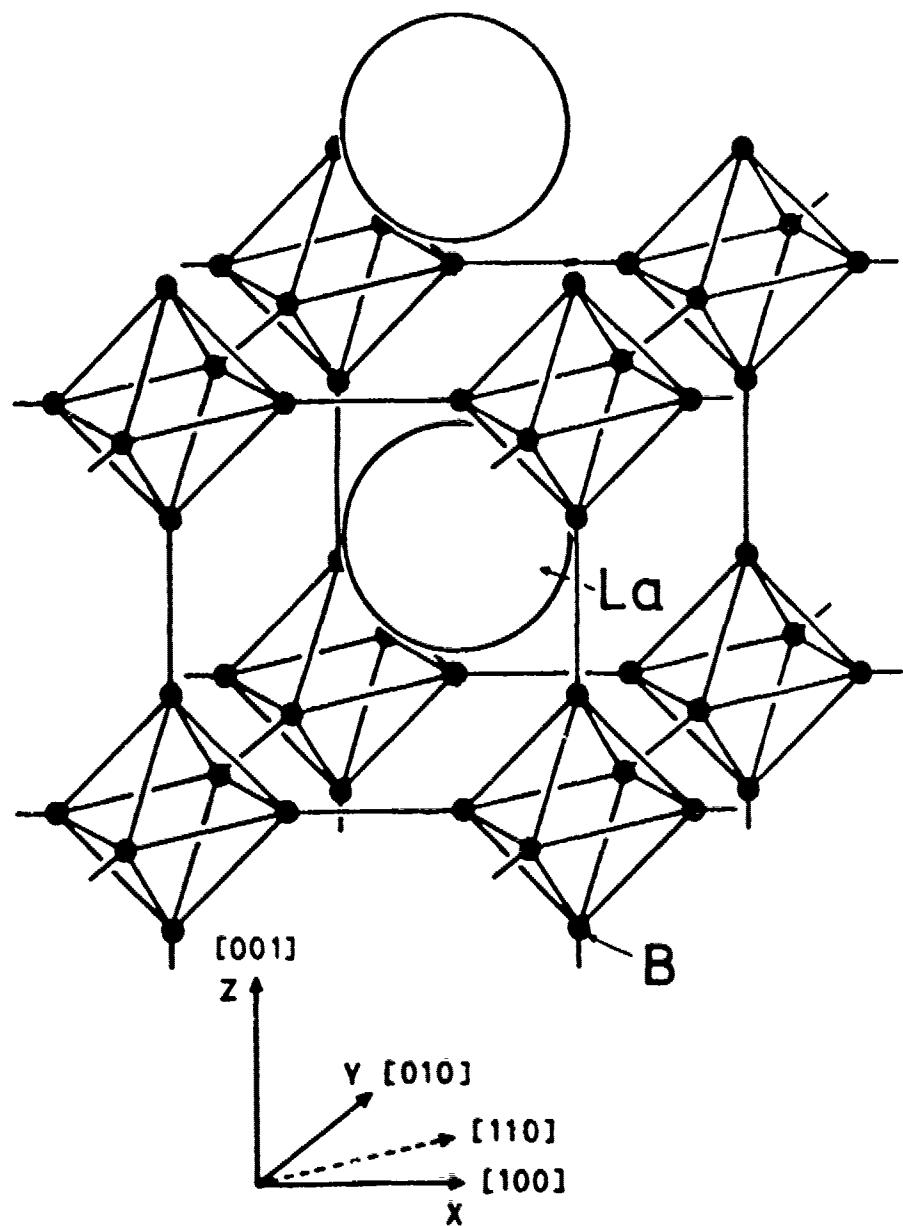


Figure 1. Structure of  $\text{LaB}_6$

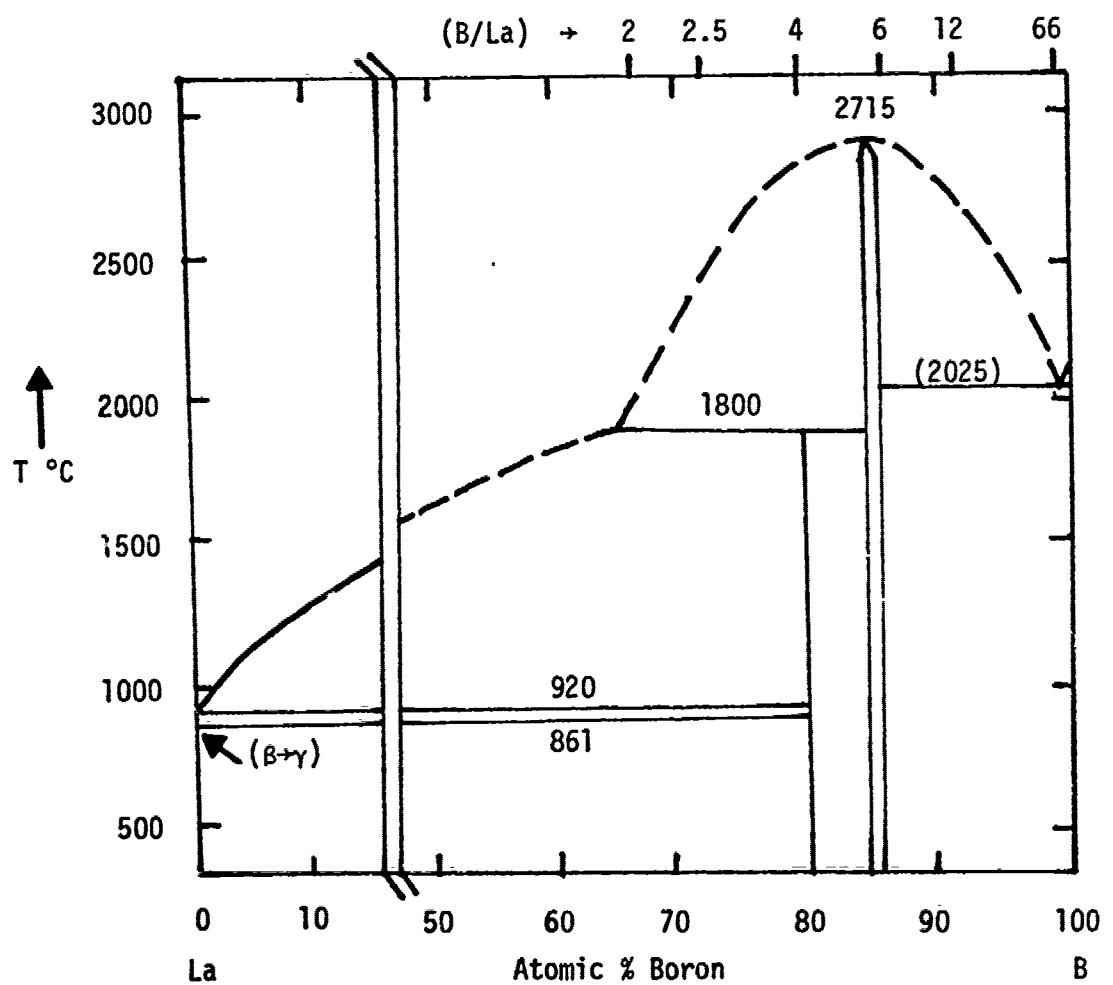


Figure 2.  $\text{LaB}_6$ -B Phase Diagram.

phase were found in a matrix phase of the  $\beta$ -rhombohedral form of boron when alloys of composition between 89 and 99.5 percent boron were arc melted.<sup>7</sup>

The chemical stability of  $\text{LaB}_6$  in boiling acids and bases according to Radzikovskaya<sup>4</sup> is shown in Table 1.  $\text{LaB}_6$  is least stable in nitric acid, and reacts only slightly with hydrochloric acid.

Table 1. Chemical Stability of Lanthanum Hexaboride in Boiling Acids and Bases.<sup>4</sup>

Reagent	Temperature, °C	Insoluble Residue, %
HCl (1:1)	110	98.2
HCl (conc.)	110	98.4
50 ml HCl (1:1)+25 ml $\text{H}_2\text{O}_2$ (30%)	107	70.2
$\text{H}_2\text{SO}_4$ (1:1)	145	98.3
$\text{HNO}_3$ (5%)	110	85.0
$\text{HNO}_3$ (1:1)	107	9.7
NaOH (15%)	106	99.6
50 ml NaOH (15%)+25 ml $\text{H}_2\text{O}_2$ (30%)	103	99.7

#### Electron Emission From $\text{LaB}_6$

Lanthanum hexaboride has received attention as a potentially high brightness electron source. Cathodes made of sintered  $\text{LaB}_6$  rods are presently being used in electron guns of scanning electron microscopes providing high brightness falling midway between that of conventional tungsten hairpins and field emission cathodes.

Studies have been made of the performances of single  $\text{LaB}_6$  points operating as field emitters with current densities at the tips of  $10^5 - 10^6 \text{ A/cm}^2$ , at residual-gas pressures of about  $10^{-9}$  Torr.<sup>8</sup>

Lanthanum hexaboride has a thermionic work function of  $2.70 \pm 0.5$  eV and a FERP (field emission retarding potential) of  $2.60 \pm 0.5$  eV.<sup>9</sup> Lafferty<sup>10</sup> explains the high thermionic emission of  $\text{LaB}_6$  is caused by the collapse of the boron framework when the boron evaporates, allowing lanthanum to diffuse to the surface. Since the rate of bulk diffusion of lanthanum is greater than the rate of evaporation, a continuous film of lanthanum is always available on the surface. Ahmed and Broers<sup>11</sup> concluded from their SEM studies, however, that theories based on the diffusion of material to selected lanthanum sites was not indicated. The cathode was believed to emit uniformly over the entire surface and there was no evidence of low work function patches as observed on some dispenser cathodes. The low thermionic work function of  $\text{LaB}_6$  is explained by Samsonov<sup>4</sup> to be a statistical transfer of electrons from lanthanum to boron, with the simultaneous presence of a sufficiently high acceptor capacity of the lanthanum atom, creating a considerable concentration of electrons which are weakly bonded to the core of the metal atom and complex of boron atoms, and are readily removed when a field is applied.

The FERP value of the work function agrees with the reported thermionic values. The advantage of this technique is the measure of the collector work function directly, contrasted to a thermionic source which measures the work function difference between the emitter and collector.<sup>9</sup>

A summary of the properties of boron and lanthanum hexaboride is contained in Table 2.

#### Fabrication Techniques From Boride Powders

The only literature available concerning boron powders was based on results obtained with diborides. The following information is based on diborides and is divided into sections on size reduction, forming and sintering.

#### Size Reduction

Ball milling of boride powders has been effective in reducing the particle size to a size suitable for forming. Due to the hardness of the borides, there is considerable contamination by the grinding media. Tungsten carbide balls are effective in reducing the particle size, but considerable contamination is produced. In one case, seven percent contamination was reported and there was no known way of removing the tungsten carbide contamination. Steel balls have proven effective if grinding time is at least 20 hours, and the iron contamination can be removed by washing with hydrochloric acid.<sup>12</sup>

#### Forming

Many techniques of forming diborides have been investigated; conventional pressing in a steel die (Babick, et al.<sup>13</sup>), isostatic pressing (Bumm and Liepelt<sup>14</sup>), extrusion die pressing (Kislyi and Samsonov<sup>15</sup>), hot casting under pressure (Medvedev, et al.<sup>16</sup>), and slip casting (Reddy, et al.<sup>17</sup>), producing relative green densities of about 50-70%.

Most of the information available on the processing of boride powders is based on the results of investigations with  $TiB_2$ ,  $ZrB_2$ ,  $CrB_2$

Table 2. Properties<sup>1</sup> of Boron and Lanthanum Hexaboride.

Properties	Boron	Lanthanum Hexaboride
Crystal Structure	$\beta$ -rhombohedral	Cubic
Lattice Constant ( $\text{\AA}$ )	10.145	$4.156^*$
Density ( $\text{gm/cm}^3$ )	2.29	4.74
Melting Point ( $^{\circ}\text{C}$ )	2300	2715
Coefficient of Thermal Expansion ( $\alpha \cdot 10^6 / ^{\circ}\text{C}$ )	$8.3 \times 10^{-6}^{***}$	$6.4 \times 10^{-6}^*$
Work Function (eV)	-	$2.70 \pm .05$ (thermionic) <sup>**</sup> $2.60 \pm .05$ (FERP)
Color	Silvery Gray	Pink-Blue <sup>*</sup>
Resistivity ( $\text{ohm-cm}$ @ rm. temp.)	$1.8 \times 10^{6***}$ (semiconductor)	$24 \pm 12 \times 10^{-6}^*$ (metallic-type conductor)

1. Most properties were reported in Ref. (3)

\* Ref. (7)

\*\* Ref. (9)

\*\*\* Ref. (4)

and  $W_2B_5$ . According to Pastor<sup>12</sup>, springback of these materials is very important and its relationship to pressure is associated with their brittleness and lack of ductility. Stratification phenomenon occurs in the pressure range above three or four tons/cm<sup>2</sup>. Holding under pressure has practically no effect on the density of the blanks. The ideal pressure may be taken as three tons/cm<sup>2</sup>.

#### Sintering

Sintering of boride powders is usually carried out in either a vacuum resistance furnace using graphite, tantalum or tungsten elements, or in an induction furnace in a stream of Ar or  $H_2$  gas. Graphite plates are used as supports with boride powder sprinkled on the plate to inhibit the boron-carbon reaction around 2200-2500 °C.<sup>12</sup>

Because the melting point of the boride powders is high, two kinds of activated sintering have been employed to lower the sintering temperature: 1) Activation by a small amount of fine powders of transition metals (e.g., Fe, Ni, Co) and 2) use of submicron powders with extremely high surface areas and thus high reactivity.<sup>12</sup>

Meersom, et al.<sup>12</sup> have investigated the sintering characteristics of  $LaB_6$  powder and found up to 15% weight loss occurs at 2207 - 2407 °C due to evaporation of boron. By embedding the sample in excess  $LaB_6$  powder, the weight loss was reduced to 4.7%. Sintering in a hydrogen atmosphere tended to have an activating effect on the samples, thus lowering the reaction temperature to 1800 °C.

#### Unidirectional Solidification

Two of the most common forms of directionally solidified eutectic

structure are the growth of rods and lamellae in a surrounding matrix. After the material is melted, lateral concentration gradients are established in the melt at the solid-liquid interface, and for any particular growth rate, these gradients provide for the diffusion of the two species of atoms, which, in turn, stabilizes the steady-state rod or interlamellar spacing.<sup>18</sup>

The eutectic microstructure will be in the form of rods or lamellae, depending on the volume fraction of the minor phase. A graph of surface area vs volume fraction is depicted in Figure 3 showing that rods will occur when the volume fraction of the minor phase is less than  $1/\pi$  (0.318) and lamellae will occur when the minor phase is more than  $1/\pi$ .<sup>19</sup>

Directional solidification can occur only if the melt solidifies under plane-front cooling with no supercooling of either phase (in a binary system). Supercooling causes one phase to grow more rapidly than the rest of the melt which disrupts the structure. According to Mollard and Fleming,<sup>20</sup> an equation defining the criterion for plane-front growth in binary systems containing a eutectic is

$$G/R = -M(C_E - C_0)/D \quad (1)$$

where  $G$  is the thermal gradient,  $R$  is the growth rate,  $M$  is the slope of the liquidus,  $C_E$  is the eutectic composition,  $C_0$  is the starting composition of the melt and  $D$  is the diffusion coefficient of solute in the melt. Equation (1) may also be expressed as

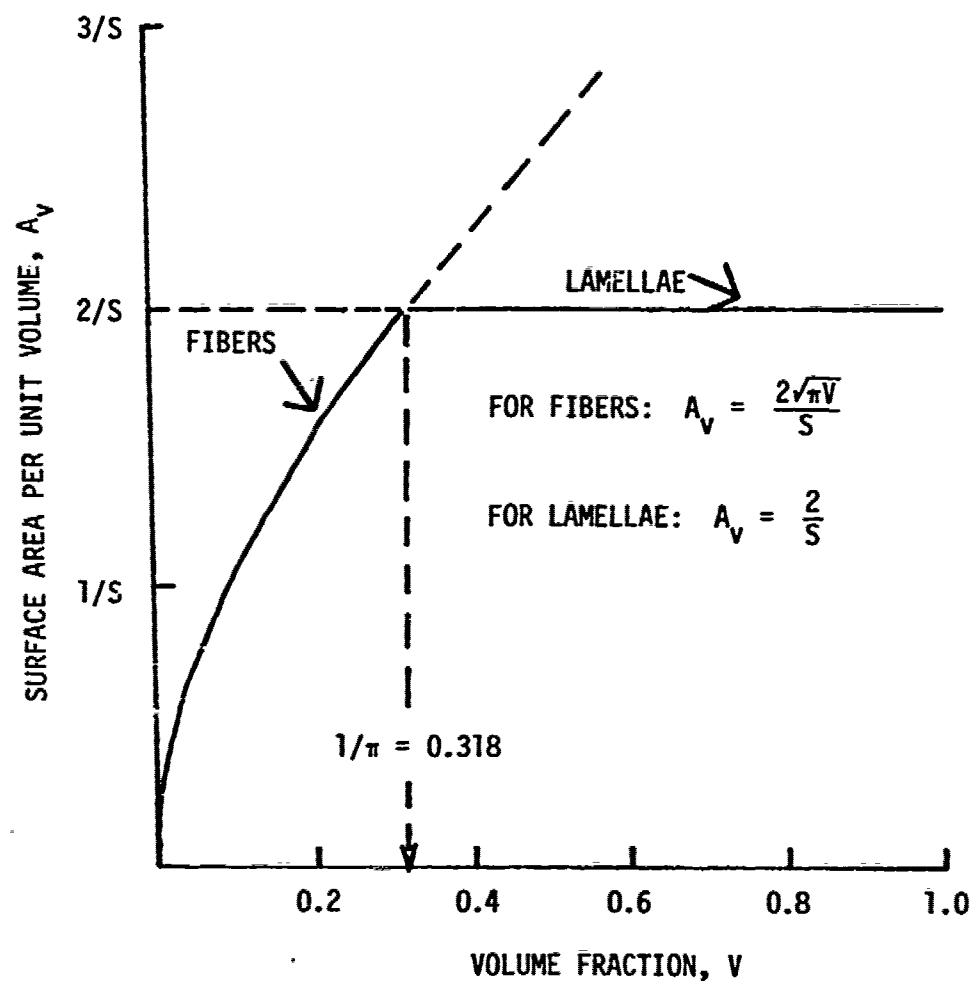


Figure 3. Influence of Volume Fraction  $V$  of Minor Phase on Fibrous-to-Lamellae Transition, Theoretical and Actual;  $S$  is Spacing Between Lamellae or Between Idealized Fibers in a Square Array.<sup>19</sup>

$$G/R = k\Delta T \quad (2)$$

where  $k$  is a constant and  $\Delta T$  is the temperature difference between the liquidus and the solidus.<sup>19</sup> As  $G/R$  increases, the structure of a two phase eutectic alloy varies from equiaxed grains to a two phase eutectic, then finally to an aligned two phase composite.

It is not necessary to have exact eutectic compositions to achieve directional solidification as long as the mixture is relatively close to the eutectic composition and there is a steep temperature gradient, a slow growth rate, and the absence of convection.<sup>19</sup>

#### Multi-Pin Array Field Emission

The majority of thermionic or dispenser cathodes presently in use require an external heating source in order to bring the material to a temperature sufficient for emission. The advantages in operating cold cathode field emitters over conventional thermionic emitters are listed as follows: a longer lifetime due to the lower operating temperature, greater current densities (more than  $30 \text{ A/cm}^2$ ),<sup>2</sup> instant turn on time, operating temperatures close to room temperature, and more ruggedness due to the lack of need for a heating device. The progress in the development of cold cathodes has been limited because of the lack of suitable materials. There have been some multi-pin arrays developed from directionally solidified W pins in a  $\text{UO}_2$  matrix by Chapman, et al.<sup>21</sup> The W- $\text{UO}_2$  composites are being used as low voltage field emitter material by Cochran, et al.<sup>1</sup> with current densities being achieved up to  $30 \text{ A/cm}^2$ .

For a fiber to be suitable for use as a cold cathode material,

it must meet the following criteria:<sup>22</sup>

- (1) High melting point (more than 2000 °C).
- (2) Low vapor pressure.
- (3) High strength.
- (4) Low sputter yield.
- (5) Electrically conducting (but not necessarily a good conductor).
- (6) Chemical inertness to allow selective etching of the matrix.
- (7) Low work function.

Lanthanum hexaboride meets the requirements for use as a cold cathode material, and compared with tungsten, would have the potential of a higher current density because of its lower work function.

## PROCEDURE AND RESULTS

The following chapter contains both the experimental procedure used in the attempts to achieve directional solidification of lanthanum hexaboride in a boron matrix, and the results obtained during the various phases of the investigation. As the investigation proceeded, modifications were necessary in sample fabrication and melting procedure to attempt to compensate for extreme shrinkage in the  $\text{LaB}_6$ -B pellet during melting. The shrinkage during melting caused the walls of the pellet to crack and separate, allowing the molten  $\text{LaB}_6$ -B mixture to spill. Sometimes the sample deformed to the extent that molten material touched, and melted through the quartz containment tube. Attempts were made to compensate for the instability of the sample during melting by using a supporting crucible technique. Attempts were also made to compensate for the shrinkage by increasing the pre-melt density of the  $\text{LaB}_6$ -B pellet using various forming techniques; ball milling and agglomeration of the  $\text{LaB}_6$  and B powders before mixing and forming; and electrically arc melting partially sintered  $\text{LaB}_6$ -B mixtures. This combined procedure and results section is a chronological description of the experimental efforts to achieve directional microstructures during the freezing of near eutectic  $\text{LaB}_6$ -B mixtures. In the following chapter, a discussion of the relative merits of these various techniques (efforts) is presented along with the conclusions and recommendations for future work.

The techniques of sample examination and analysis are described in Appendix A.

#### Internal Zone Melting

The following section describes the basic procedure and results obtained during the initial attempts to directionally solidify  $\text{LaB}_6$  in a B matrix using RF heated internal zone melting. This section is subdivided into the main processing steps of powder preparation, pre-melt pellet fabrication and internal melting.

#### Powder Preparation

The powders were supplied by CERAC, Inc., in the form of -325 mesh lanthanum hexaboride powder, typically 99.9% pure; and -325 mesh crystalline boron, typically 99.5% pure. The boron powder, as-received from the supplier, was too coarse to be formed into a suitable pellet, so it was necessary to reduce the particle size.

The boron powder was ground two minutes in a tungsten carbide mill. It was examined in a transmission electron microscope to determine the degree of particle size reduction. The average particle size of the ground boron powder was about  $5\mu$  (see Figure 4). The particle size of the as-received boron powder ranged from about  $1\mu$  to  $35\mu$  (see Figure 5). Comparison of the as-received  $\text{LaB}_6$  particle size (see Figure 6) with the ground boron powder shows these powders were of about equal particle size.

The  $\text{LaB}_6$  and B powders were weighed on an analytical balance to obtain 58 w/o boron and 42 w/o  $\text{LaB}_6$ . This weight ratio was necessary to obtain the 3 atomic percent lanthanum/97 atomic percent boron eutectic composition indicated by the phase diagram.<sup>6</sup>

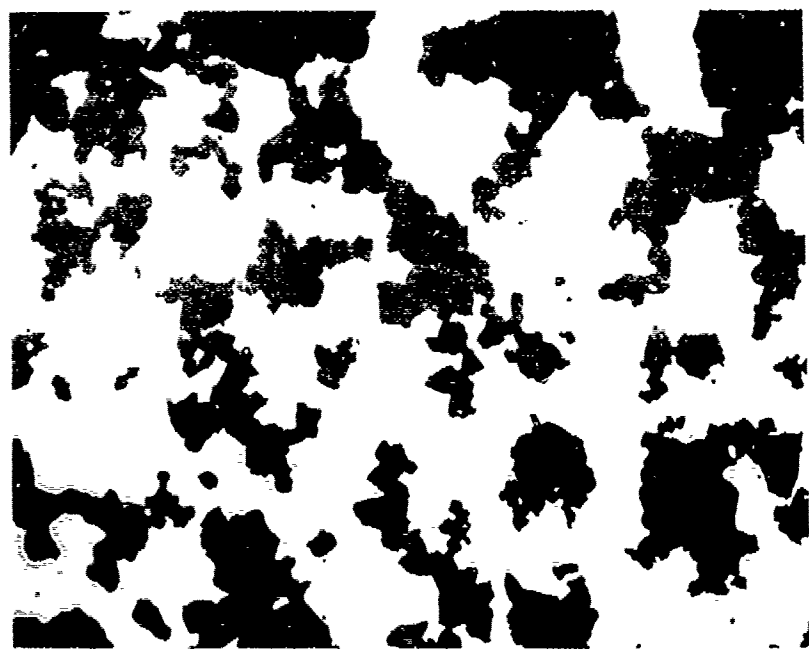


Figure 4. Boron Powder Ground in a WC Mill Two Minutes. x700.



Figure 5. Boron Powder As-Received From the Supplier. x700.

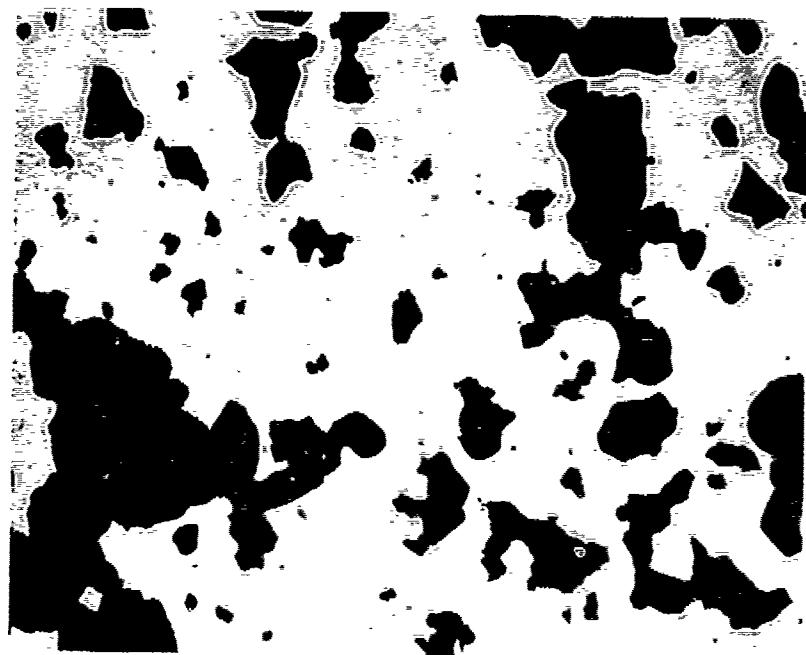


Figure 6. Lanthanum Hexaboride Powder As-Received From the Supplier. x700.

### Pre-melt Pellet Fabrication

The powders were manually mixed with a spatula, and 30 grams of the mixture was placed in a 0.75 inch (1.9 cm) double action steel die. The powder mixture was pressed in a single action hydraulic press at 6800-9000 psi and held at that pressure for about five minutes. The pressed sample was then weighed, measured, and immediately positioned in the RF induction furnace. The pressed compacts were typically 3.5 - 5 cm in height and had a pre-melt density of 1.3 - 1.5 gm/cm<sup>3</sup>. The theoretical density of a compact containing 42 w/o LaB<sub>6</sub> and 58 w/o boron was 3.32 gm/cm<sup>3</sup> so the pre-melted density was about 42% of theoretical density. The samples were strong enough for handling and placement in the furnace.

### Internal Melting

A ten kilowatt, 3-4 megahertz RF induction furnace was chosen as the primary method of heating to achieve melting and thus investigate the possibility of directional solidification. The basic furnace set-up is shown in Figure 7. A molybdenum sleeve pre-heater was used to pre-heat the pellet to a temperature high enough to allow the sample to become electrically conductive typically at 1450 - 1500 °C. The molybdenum sleeve was quickly lowered out of the coil and the RF power was immediately reduced (to prevent arcing) to about one-half the power achieved during pre-heating. Due to extreme fogging of the fused quartz tube, the runs were made "blind" until the power levels needed to melt the material could be determined. A pure hydrogen atmosphere of 100 - 200 cc/min was maintained throughout the melting run. An optical pyrometer was used to measure the temperature of the molybdenum sleeve

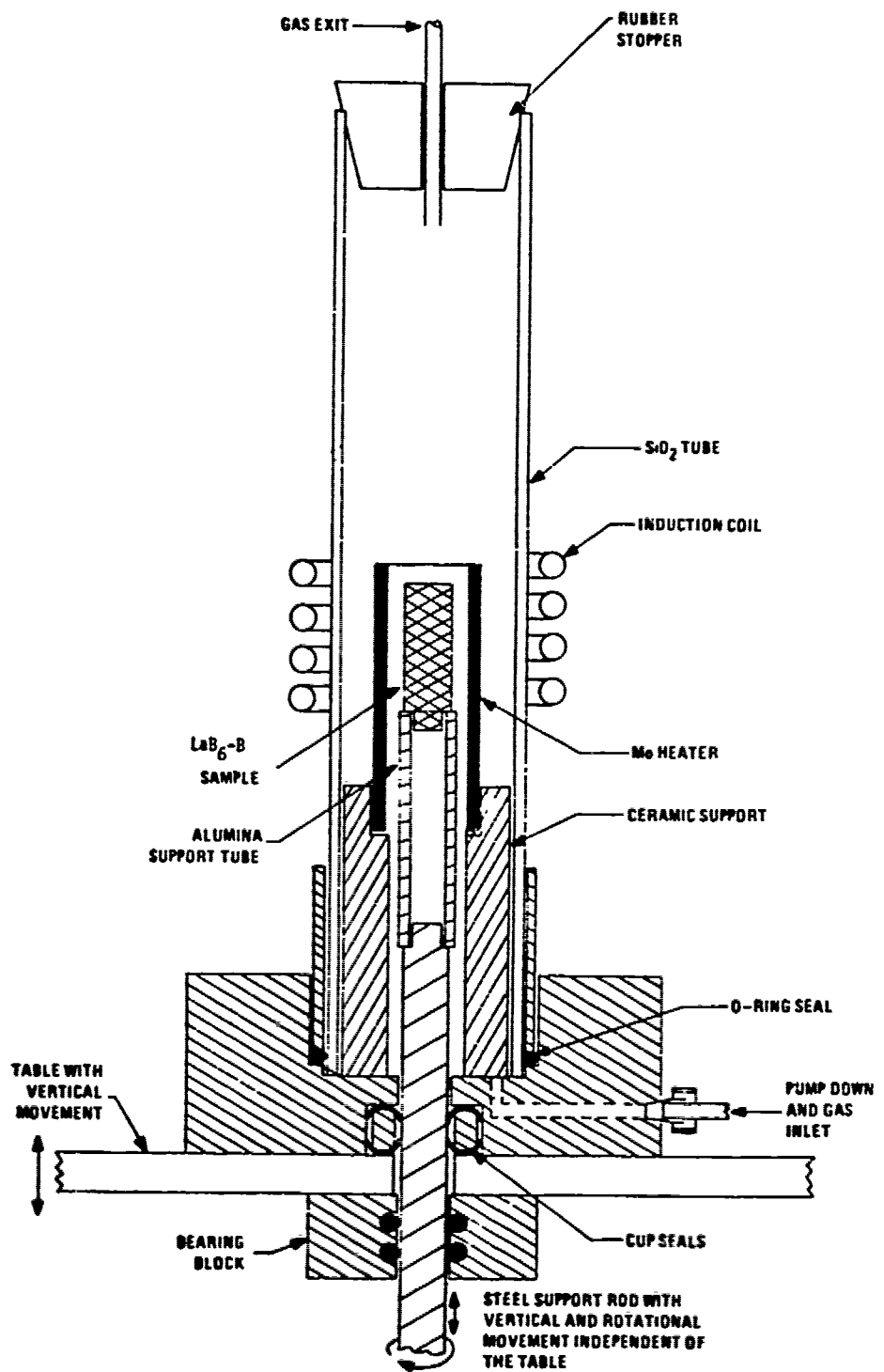


Figure 7. Diagram of the Induction Heating Facilities

and the pellet until fogging of the quartz tube prevented readings.

During the melting process, excessive shrinkage caused the samples to crack and fall off the platform before uniform melting could be achieved. A typical pellet after melting is shown in Figure 8. Note the molten center surrounded by a shell of unmelted material forming the walls of a self-contained crucible.

Typical power and grid current settings for the RF generator versus time are shown in Figure 9 for a pellet which contained evidence of eutectic microstructure. Times at which process changes were made are indicated. Most of the RF heating cycles were made under nearly identical conditions, all giving approximately the same results.

### B. Crucible Melting

Because the  $\text{LaB}_6$ -B pellets broke into pieces and fell against the quartz tube during the internal zone melting experiments, techniques of melting in a crucible were investigated. This section includes a discussion of the various types of crucible materials and melting techniques which were investigated and also describes changes made in the basic sample fabrication procedures. The different crucibles were all heated using the 10 kW RF unit. The crucibles studied were a molybdenum tube open at both ends, a graphite crucible with a lid, and a coil of tungsten wire. The  $\text{LaB}_6$  and B powders were prepared as described in the Internal Zone Melting section.

#### Molybdenum Tube

The crucible and sample consisted of a Mo tube 1/4 inch ID, 3/8 inch OD and three inches long which was filled with four or five  $\text{LaB}_6$ -B



**Figure 8. Typical Sample After RF Run.**

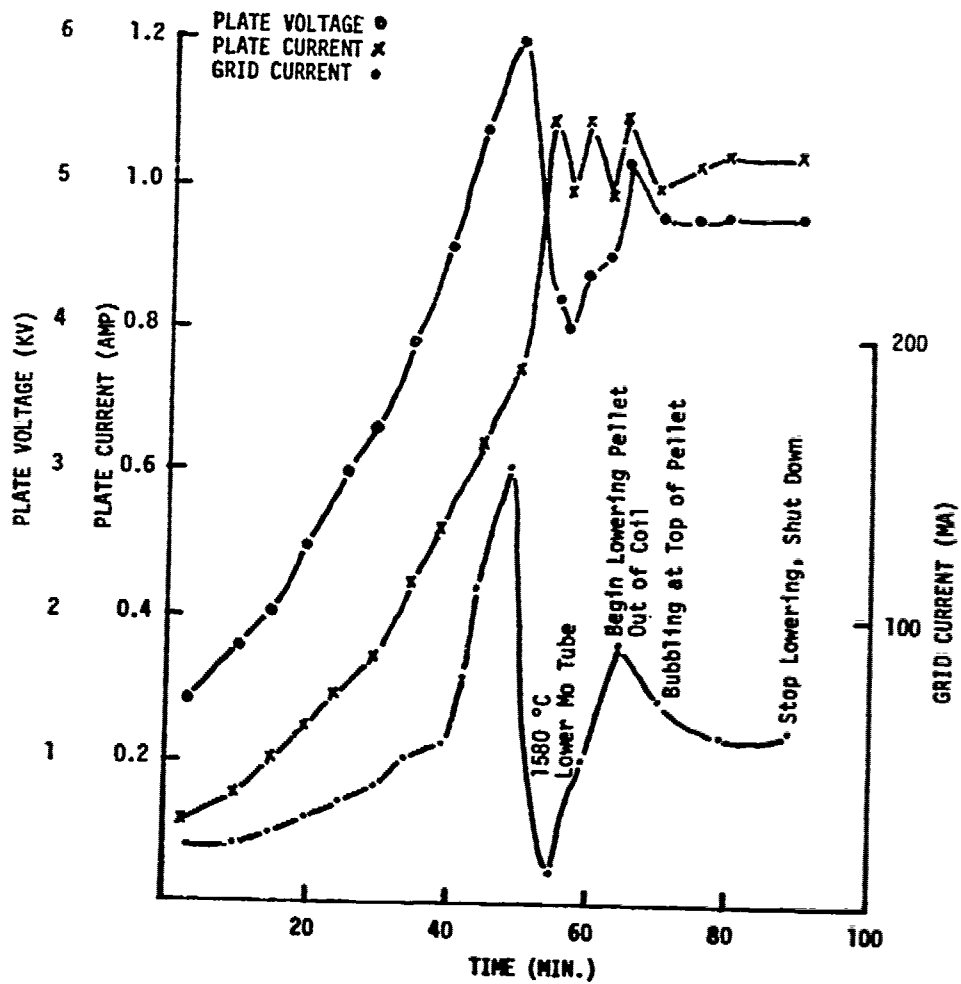


Figure 9. Typical RF Induction Furnace Power and Grid Current Curves.

pellets, 1/4 inch OD and 1/4 inch thick. Two RF induction heating experiments were made using the Mo tube crucible and, in each case, the RF power was increased continually until melting of the Mo tube occurred. The molybdenum tube crucible melted each time following the appearance of a white vapor in the vicinity of the tube. There was no melting of the  $\text{LaB}_6\text{-B}$  but sintering of the  $\text{LaB}_6\text{-B}$  pellet occurred.

#### Graphite Crucible

A graphite crucible 1/2 inch ID, 3/4 inch OD, and 1-3/4 inches in height was machined from spectrographic grade graphite. The crucible was capped with a graphite lid and heated with the crucible empty in a  $\text{H}_2$  atmosphere in the RF induction furnace. At approximately 1400 °C, a black deposit formed on the quartz tube from an apparent reaction between the graphite and hydrogen atmosphere. The crucible was cooled, and several pellets of  $\text{LaB}_6\text{-B}$ , 1/4 inch OD, 1/4 inch thick were placed in the crucible. A graphite lid was used to seal the crucible and the crucible was reheated using flowing nitrogen as the furnace atmosphere (about 400 cc/min). The temperature was increased at ~ 15 °C/min to 1750 °C, then cooled. The sample enlarged and became light gray in color. X-ray diffraction analysis indicated the presence of BN and other crystalline phases.

#### Tungsten Coil

A coil of 0.025 inch diameter tungsten wire was wound on a lathe into a 3/4 inch ID right circular cylinder, one inch in height. A  $\text{LaB}_6\text{-B}$  pellet, 3/4 inch in diameter was placed inside the coil and heated in the RF induction furnace until the maximum power of the furnace (10 kw) was reached. At maximum power, the pellet reached a red heat

(~ 800 °C). After cooling, the sample was examined showing no evidence of melting.

C. Melting Characteristics of Increased Density

LaB<sub>6</sub>-B Samples

Since a means of melting the sample in a crucible was not found, the decision was made to again use the self-contained crucible technique, and to try to reduce the shrinkage during melting by increasing the pre-melting density of the LaB<sub>6</sub>-B pellets. Techniques investigated included isostatic pressing and hot pressing, electrically arc melting of partially sintered LaB<sub>6</sub>-B pellets, ball milling and agglomeration.

Isostatic Pressing

The LaB<sub>6</sub> (as-received) and B (ground) powder was mixed, then placed in a one-half inch ID, three-quarter inch OD, rubber hose about three inches long, and pressed isostatically at 33,500 psi. The sample was not considered suitable for melting in the RF induction furnace because of its resulting non-uniform shape and severe laminations, so a hot pressing technique was investigated.

Hot Pressing \*

Approximately 60 grams of the LaB<sub>6</sub>-B mixture was hot pressed at 1700 °C in a one inch ID graphite die at 80 psi. The pressed height of the ingot was about 2-1/2 inches giving a hot pressed density of 2.0 gm/cm<sup>3</sup> and some reaction with the graphite punch. The sample appeared to be partially sintered after pressing. Heating was attempted in the RF induction furnace without using a molybdenum tube pre-heater. The LaB<sub>6</sub>-B coupled successfully and melting was attempted by increasing the temperature about 100 °C/min until fogging of the quartz tube prevented

\*The hot forging facility of the Solid State Sciences Division of RADC at Hanscom AFB was utilized to produce dense compacts for these experiments.

further direct observation of the  $\text{LaB}_6$ -B pellet. The temperature read from the optical pyrometer was 1450 °C. The RF power was increased until the interior of the  $\text{LaB}_6$ -B ingot was thought to be molten, based on previous results. The sample was then lowered out of the coil at a rate of five cm/hr.

#### Electric Arc-Melting

Partially sintered, irregular pieces (about 1/2 inch) of  $\text{LaB}_6$ -B which had been previously heated in the RF induction furnace were placed in the water-cooled copper hearth of an electric arc furnace and melted under a DC arc in air. Melting of the sample was achieved in one or two minutes in the area of the arc. The arc melted  $\text{LaB}_6$ -B sample showed a tendency to thermal shock on cooling.

There was microstructural evidence of melting and recrystallization of the sample due to the blocky nature of the crystallites. The largest arc melted pieces were heated in the RF induction furnace without using the molybdenum susceptor. Dendrites formed on the cooler exterior with the blocky crystallite structure occurring generally throughout the sample. However, there was no evidence of eutectic microstructure.

#### Ball Milling

Fifty grams  $\text{LaB}_6$  and fifty grams B, as-received from the supplier, were each placed separately in a 500 cc wide-mouth Nalgene bottle with about 35, one-half inch plain carbon steel balls. Both bottles were packed in a one gallon bottle and rolled at 57 rpm for about 19 hours. The milled powders were washed in 1N HCl and dried overnight at 100 °C.

The particle size distribution appeared to become more uniform in

size in the ball milled powders as compared to the WC ground boron and as-received  $\text{LaB}_6$ . The particle size of the milled boron powder was  $1\text{-}5\mu$  (see Figure 10), and the particle size of the milled  $\text{LaB}_6$  was about  $1\text{-}2\mu$  (see Figure 11).

It was decided at this time to change the composition slightly to see if there would be any effects on the melting behavior. A composition of 45 w/o lanthanum hexaboride and 55 w/o boron was chosen. After uniaxial cold pressing at 9000 psi, the  $\text{LaB}_6\text{-B}$  pellet was 2.0 cm in height, and had a pre-melted density of  $1.7 \text{ gm/cm}^3$ , which was about 50% of theoretical density. The pellet was heated in the RF induction using a molybdenum tube pre-heater and heating techniques described earlier. Extreme fogging of the quartz tube occurred as before upon direct coupling to the pellet, so direct observation of the sample was impossible. The apparent weight loss of the sample did not appear to be relatively large (on the order of 0.6%), but the core of the  $\text{LaB}_6\text{-B}$  pellet showed a large decrease in volume. There was a melted area about 2-3 millimeters thick lining the interior wall of the pellet, similar to the pellet shown in Figure 8.

#### Agglomerated Powders

Attempts were made to further densify the ball milled 45 w/o  $\text{LaB}_6$  and 55 w/o B powders by agglomerating with distilled water. The ball milled  $\text{LaB}_6\text{-B}$  mixture was placed in a 250 cc plastic bottle. Distilled water equivalent to one-tenth the total weight of the mixture was added six drops at a time and thoroughly blended into the mixture. Agglomeration was considered complete when the bulk volume of the powder decreased significantly and the spherical agglomerates were about one



Figure 10. Ball Milled Boron Powder. x700.

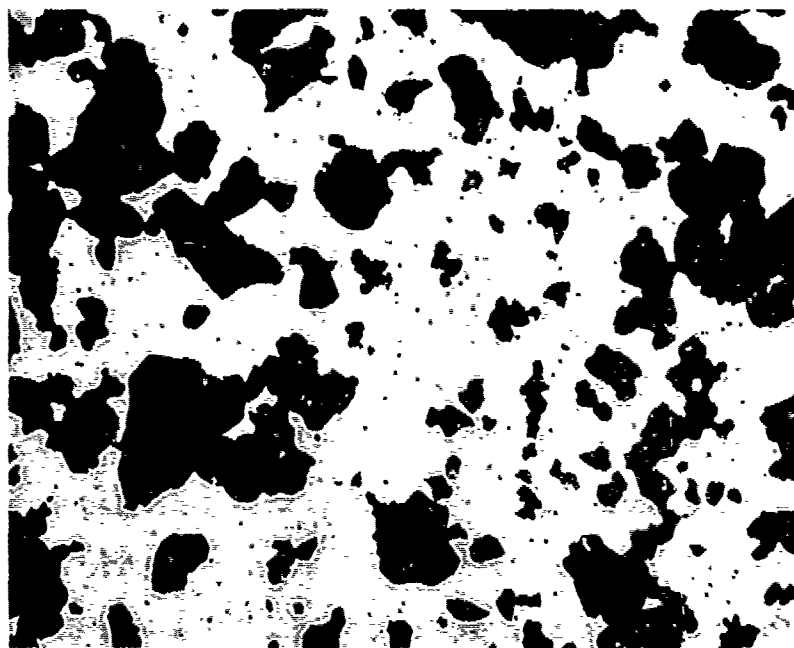


Figure 11. Ball Milled Lanthanum Hexaboride Powder. x700.

millimeter in diameter. The agglomerated powder was uniaxially pressed in a 3/4 inch die into a compact 1.9 cm in height with a pre-melted density of about 2.1 gm/cm<sup>3</sup> (62% of theoretical density). The water seemed to aid in pressing by acting as a lubricant. If additional water was added, the agglomerates increased in size to about 5 mm as opposed to 1 mm agglomerates. The LaB<sub>6</sub>-B pellet was heated in the RF induction furnace, followed by direct coupling as previously described. The pellet deformed and melted through the quartz tube before it could be lowered out of the heating zone.

The decision was then made to melt a composition richer in boron. A mixture containing 61 w/o milled boron powder and 39 w/o milled lanthanum hexaboride powder was agglomerated with distilled water, uniaxially pressed and heated in the RF furnace using the heating technique described previously. The amount of vaporization and subsequent deposits on the walls of the quartz containment tube seemed to increase significantly as compared to previous RF heating experiments. The pellet decomposed the graphite platform, partially melted the alumina support post, and finally deformed and melted through the quartz tube.

## DISCUSSION OF RESULTS

The objective of this investigation was to melt and solidify  $\text{LaB}_6$ -B mixtures close to the reported eutectic composition and examine the samples for indication of aligned (eutectic) microstructure-ideally  $\text{LaB}_6$  rods arrayed in a boron matrix. Because of the high temperature needed to melt these materials and the very reactive nature of boron, much of the research effort, of necessity, was devoted to selecting and evaluating heating techniques and sample (pellet) fabrication methods. The extent to which these objectives were met is discussed in this section and a summary of the experimental results is shown in Table III.

The most successful and informative melting experiment was the initial run using the internal zone self-contained crucible technique. The  $\text{LaB}_6$ -B pellet remained generally in one piece, with the melted zone mainly in the center of the pellet. Microscopic examination of the melted material revealed partially aligned eutectic microstructure (see Figures 12 and 13). Selected areas of the melted  $\text{LaB}_6$ -B pellet contained fibers having a  $\ell/d$  ratio of 10/1 (Figure 12) and oriented triangles showing a fairly geometric growth pattern (Figure 13). Scanning electron microscopy revealed an obvious contrast between the  $\text{LaB}_6$  fibers and B matrix with energy dispersive X-ray analysis (EDAX) confirming the presence of La as the major element in the fibers, Figures 14 and 15. Electron probe microanalysis of the individual fiber indicated an approximate

Table III. Summary of Experimental Results

Preparation Techniques	Sample Density (gm/cm <sup>3</sup> )	Attempt at RF Melting	Formation of Liquid	Eutectic Microstructure Formed	Problems
WC Grinding	N.A.	Yes	Yes	Yes	No Control over melting
Uniaxial Pressing	1.3 - 1.5	Yes	Yes	Yes	Pellet fell apart due to shrinkage
Ball Milling	1.7	Yes	Yes	Yes	Pellet fell apart due to shrinkage
Agglomeration	2.1	Yes	Yes	Yes	Pellet fell apart due to shrinkage
Mo Crucible	N.A.	Yes	No	No	No melted
Graphite Crucible	N.A.	Yes	No	No	Formation of BN
Tungsten Crucible	N.A.	Yes	No	No	Not enough furnace power
Isostatic Pressing	--	No	No	No	Laminations in pressed pellet
Hot Pressing	2.0	Yes	No	No	No melt formed

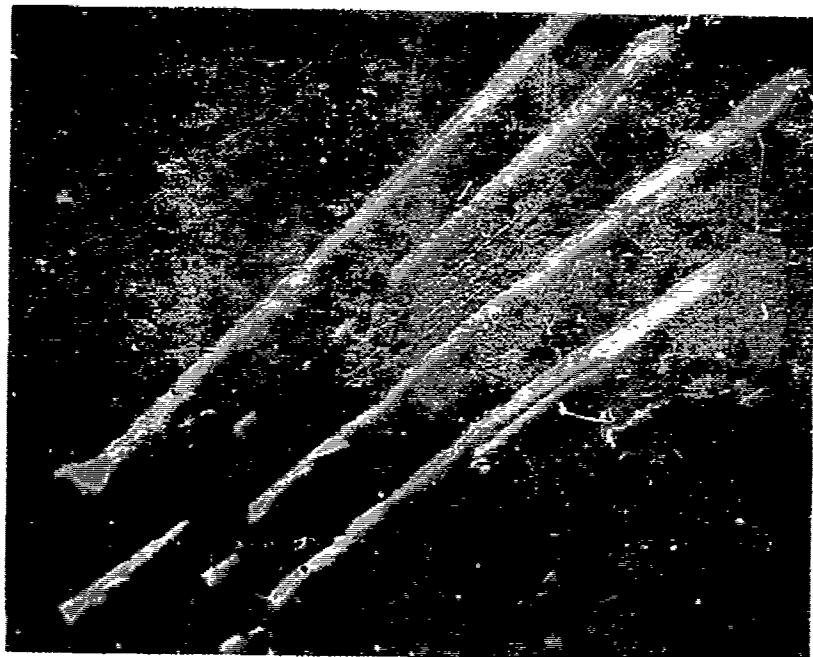


Figure 12. Lanthanum Hexaboride Oriented Microstructure. x1100.

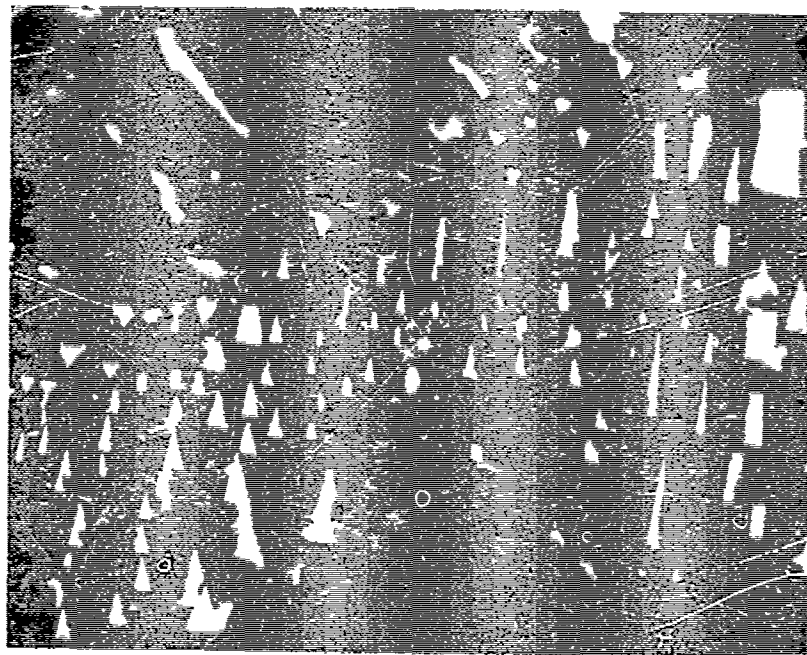


Figure 13. Lanthanum Hexaboride Oriented Microstructure. x575.

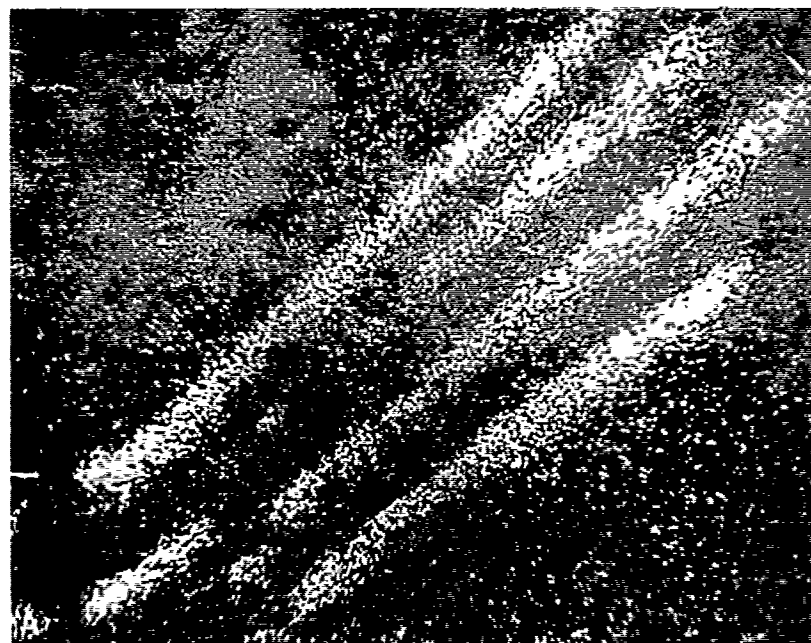


Figure 14. EDAX Mapping of Oriented Microstructure Depicted in Figure 12 Showing Location of La. x1100.

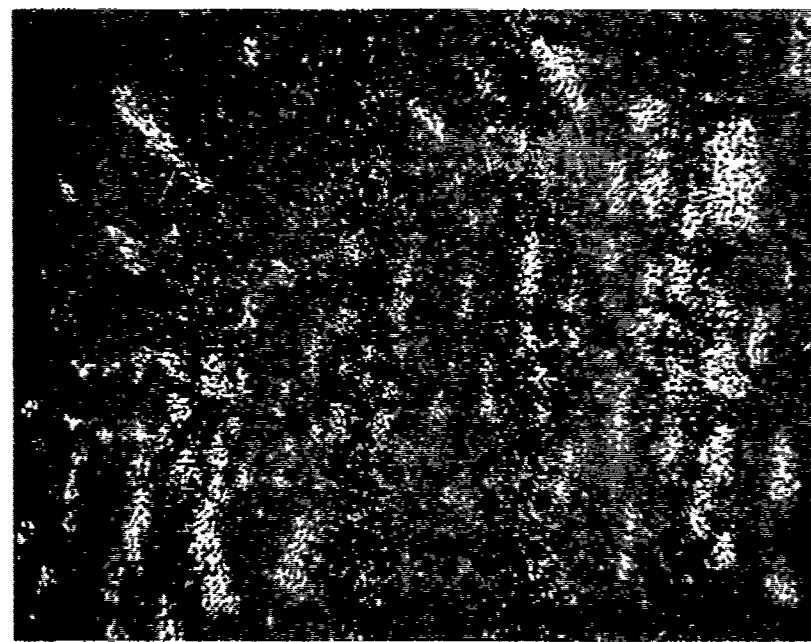


Figure 15. EDAX Mapping of Oriented Microstructure Depicted in Figure 13 Showing Location of La. x575.

$\text{LaB}_6$  composition, a trace amount of C and no Mo contamination from the Mo pre-heater. X-ray diffraction analysis indicated the presence of boron and crystalline material having d-spacings equivalent to the ASTM data for  $(\text{LaB}_6)$  7C. The remainder of the pellet showed varying micro-structure changes from the center of the pellet to the skin. The phases varied from the melted eutectic structure to melted and recrystallized blocky (cubic) forms of  $\text{LaB}_6$ , unmelted grains of  $\text{LaB}_6$  and finally sintered grains of  $\text{LaB}_6$  and B at the skin. Most of the  $\text{LaB}_6$  in the pellet was present as a blocky (cubic), recrystallized structure.

The RF heating experiments producing melted portions of the  $\text{LaB}_6$ -B pellet generally exhibited some continuous areas of pure boron containing eutectic structure (Figures 16 and 17).

In the attempts at improving the heating techniques by using the three crucible materials (molybdenum, graphite and tungsten) there was no indication of melting in the pellet because the crucibles either melted (Mo), reacted with the atmosphere (graphite), or did not allow the sample to heat enough to conduct (W).

Molybdenum melts at about 2400 °C which is above the eutectic melting point of  $\text{LaB}_6$ -B. The molybdenum probably reacted with the boron, forming a lower melting point compound causing the tube to melt before the pellet.

The graphite reacted with the hydrogen atmosphere forming a black deposit on the quartz containment tube. However, the graphite crucible technique might have provided a means of melting the pellet if the RF heating had been continued "blind".

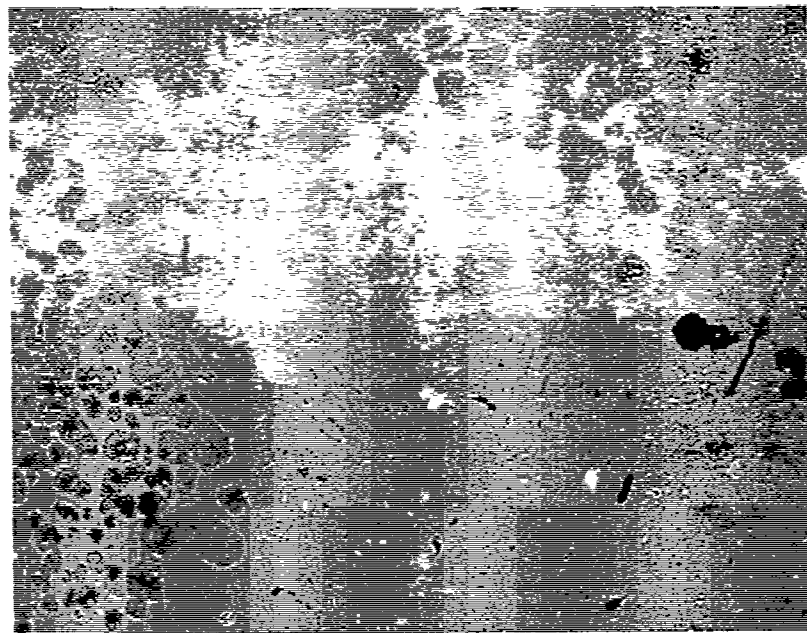


Figure 16. Continuous Pure Boron Area Containing Eutectic Structure.  
x500.

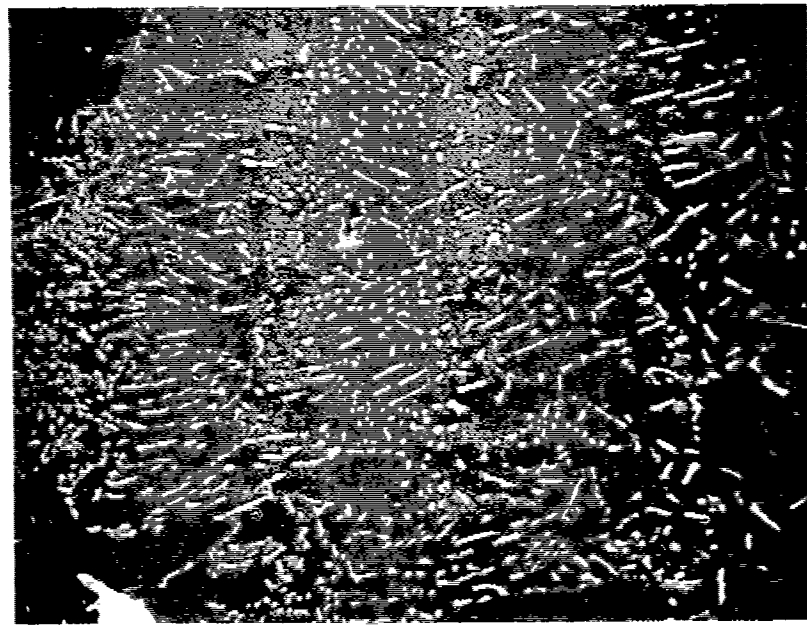


Figure 17. Areas Showing Eutectic Microstructure. x700.

The tungsten coil did not seem to generate enough heat, even at maximum furnace power. No explanation for this is apparent. Other crucible materials were not immediately available, so the self-contained crucible technique was resumed and attempts were made to increase the pre-melt density by using various fabrication techniques.

The attempts to isostatically press and hot press the powders ground in the tungsten carbide mill demonstrated the possibility of using these techniques in forming. There were several cross sectional laminations in the isostatically pressed  $\text{LaB}_6$ -B pellet possibly due to the brittleness and lack of ductility of the boron powders, or improper filling of the mold. It might be possible, with additional research, to develop a technique of isostatically pressing the  $\text{LaB}_6$ -B powders.

The hot pressed  $\text{LaB}_6$ -B pellet could be heated directly by induction from room temperature to melting. The single RF experiment made on the hot pressed pellet was not conclusive enough to evaluate the hot pressing technique. The unavailability of a local hot press capable of achieving at least 1800 °F made it difficult to hot press additional  $\text{LaB}_6$ -B pellets. There was also the disadvantage of a possible reaction with the graphite punch.

Electric arc melting of the  $\text{LaB}_6$ -B sample did not provide enough control over the heating and cooling rates to allow the formation of a solidifying front necessary for directional growth. Also, air was the only atmosphere available which would tend to form boron oxide compounds.

The attempts to increase the pre-melt density by ball milling the powders did increase the pre-melt density, but did not seem to improve the shrinkage problem. Ball milling was a disadvantage because of the

time involved (19 hours) and the need to remove possible iron contaminants with acid washes. Tungsten carbide milling was faster and produced a powder which could be formed. The possibility of tungsten contaminants from the tungsten carbide mill apparently was not a significant problem since the eutectic microstructure was present in the majority of RF melted samples regardless of the processing technique used.

Typical eutectic microstructure obtained in the melted areas of the  $\text{LaB}_6$ -B pellets are shown in Figures 17, 18 and 19. Some orientation of the structures is shown in Figures 18 and 19 indicating the possibility of additional alignment if a better solid-liquid interface could be achieved.

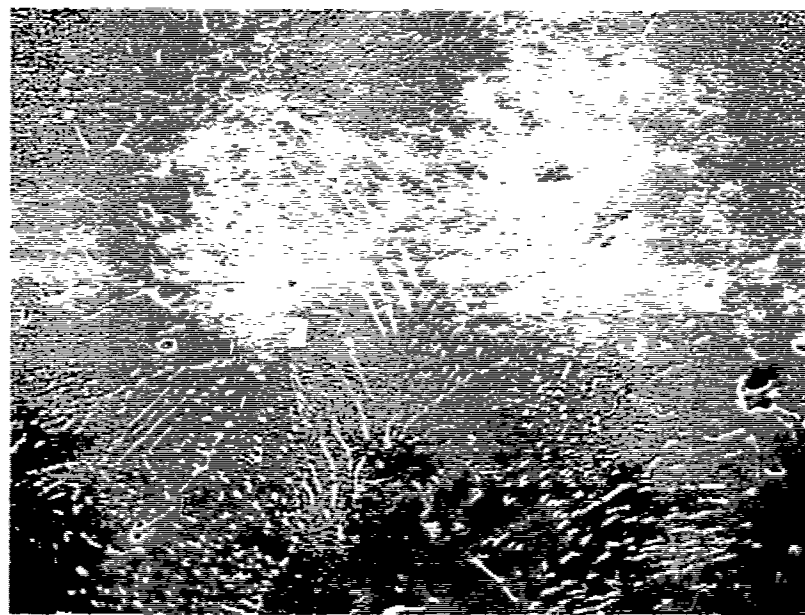


Figure 18. Area Showing Eutectic Microstructure  
x 200.

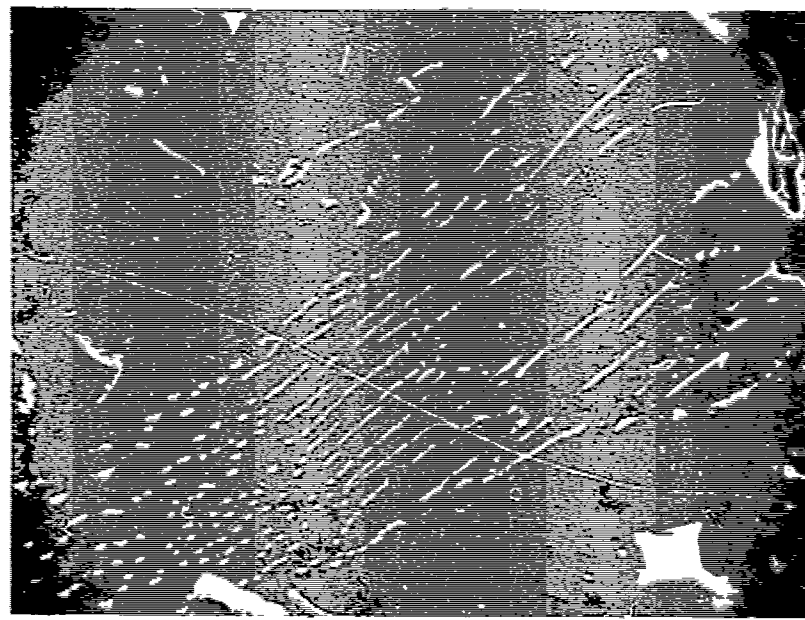


Figure 19. Area Showing Eutectic Microstructure  
x 500.

## CONCLUSIONS AND RECOMMENDATIONS

### Conclusions

1. The  $\text{LaB}_6$ -B eutectic mixture can be melted using modified internal zone melting in an RF induction furnace.
2. Eutectic microstructure showing areas of oriented structures having a  $\varepsilon/d$  ratio of about 10 to 1 was obtained in the majority of  $\text{LaB}_6$ -B pellets having melted areas.
3. A hot pressed  $\text{LaB}_6$ -B eutectic mixture can be directly heated from room temperature to melting in an RF induction furnace.
4. Ball milling  $\text{LaB}_6$  and B powders with plain carbon steel balls increased the pre-fired density of uniaxially cold pressed  $\text{LaB}_6$ -B pellets.
5. Agglomeration of a mixture of ball milled  $\text{LaB}_6$ -B powders with distilled water increased the pre-melt density of uniaxially cold pressed  $\text{LaB}_6$ -B pellets.
6. Tungsten contamination from milling the boron powder with the tungsten carbide mill did not seem to affect the formation of the eutectic microstructure.
7. An electric arc was capable of melting the  $\text{LaB}_6$ -B eutectic composition, but there was no control over the melting and cooling rates.
8. During RF heating, the  $\text{LaB}_6$ -B pellets reacted with nitrogen gas forming boron nitride compounds of varying stoichiometry.

Recommendations

The presence of small areas of an aligned  $\text{LaB}_6$  phase dispersed in the B matrix suggests the potential for achieving an ordered eutectic structure in the system  $\text{LaB}_6$ -B. Any future solidification efforts in this system must concentrate on achieving a well defined and controllable liquid-solid interface. Of the melting techniques tested in this study, the internal zone technique should be investigated further, realizing the obvious need to increase the pellet density prior to melting. The investigation of hot pressing and isostatic pressing as a means of increasing the pre-melt density should be continued with the emphasis on hot pressing because of the advantage of direct RF coupling from room temperature to melting.

## APPENDIX

### Sample Examination And Analysis Techniques

The processed powders and melted samples were examined and analyzed using metallographic techniques, electron microscopy, electron probe microanalysis and X-ray diffraction analysis where applicable.

#### Metallographic Technique

The melted pellets were prepared for metallographic examination by first mounting the pellet pieces in Quickmount or Bakelite, then grinding the surface to be examined using the following procedure. The surface was first ground with loose 120 grit SiC on a belt sander, then 400 grit loose SiC on a high speed lap. Diamond impregnated brass laps were tried, but the most effective technique was using the loose SiC grit.

#### Electron Microscopy

Three types of electron microscopy were used in analyzing the samples: scanning and transmission electron microscopy and electron probe microanalysis. Energy dispersive X-ray analysis (EDAX) was used for elemental analysis and electron probe microanalysis was used for compound analysis.

Scanning Electron Microscopy. The samples were prepared for scanning electron microscopy by first attaching the sample to a 1/2 inch aluminum stub with silver paste, then evaporating a film of carbon and a film of AuPd onto the surface of the sample in a vacuum evaporator. The samples were observed in a Cambridge Mark II Stereoscan or a Cambridge

150 Stereoscan.

Transmission Electron Microscopy. The samples were prepared for transmission electron microscopy by depositing a suspension of the powders that were -325 mesh onto a carbon coated copper grid and observed in a Philips 200 Transmission electron microscope.

Energy Dispersive X-ray Analysis (EDAX). The samples to be analyzed using energy dispersive X-ray analysis were packed into spectrographic grade carbon rods 1/4 inch in diameter in a small cavity that had been formed in the tip of the rod about 1 mm OD and 0.5 mm in depth. The samples were then analyzed in a Cambridge Mark II Stereoscan at a 45° angle, count rate of  $10^4$  and magnification of 110X, for a counting time of two minutes.

The samples that were not powders were observed and analyzed using the same procedure for SEM described above. X-ray mapping was obtained using the standard mapping techniques in energy dispersive X-ray analysis.

Electron Probe Microanalysis. The sample was analyzed with an electron probe microanalyzer by Mr. James Johnson of the Materials Characterization Branch of the EMSL of the Georgia Tech Engineering Experiment Station.

#### X-ray Diffraction Analysis

The melted or sintered samples were ground to -325 mesh and packed into a standard aluminum, X-ray diffraction powder pack. The Al holder was then placed into a rotating stage goniometer and X-rayed with Cu K $\alpha$  radiation at a scanning rate of two degrees per minute.

## BIBLIOGRAPHY

1. Cochran, et al., "Low Voltage Field Emitter Arrays," Interim Technical Report, Air Force Contract F33615-79-C-1832, Georgia Institute of Technology, School of Ceramic and Electrical Engineering, Sept. 1980.
2. Hill, D.N., "The Effect of Cathode Geometry on the Emission Characteristics of Low Voltage Field Emitters Fabricated From Uranium-Dioxide-Tungsten Composites," a thesis for Doctor of Philosophy in Ceramic Engineering, Georgia Institute of Technology, Aug. 1979.
3. Cueilleron, J., et al., "Chemical Properties of Boron," Boron and Refractory Borides, V.I. Matkovitch ed., Springer-Verlag, New York, 1977, pp. 203-226.
4. Samsonov, G.V., et al., Boron, Its Compounds and Alloys, ed. G.C. Samsonov, Publishing House of the Academy of Science, Ukrainian, U.S.S.R., Kiev, 1960.
5. Etourneau, J., "Compounds Based on Octahedral B<sub>6</sub> Units: Hexaborides and Tetraborides," Boron and Refractory Borides, V.I. Matkovitch ed., Springer-Verlag, New York, 1977, pp. 116-138.
6. Spear, K.E., "Rare Earth-Boron Phase Equilibria," in Boron and Refractory Borides, V.I. Matkovitch ed., Springer-Verlag, Berlin, Heidelberg, New York, 1977, pp. 439-456.
7. Johnson, R.W., et al., "The Lanthanum-Boron System," *J. Phys. Chem.*, 65 (1961), p. 909-915.
8. Windsor, E.E., "Construction and Performance of Practical Field Emitters From Lanthanum Hexaboride," *Proc. IEEE*, Vol. 116, No. 3, March 1969, p. 348-350.
9. Swanson, L.W., et al., "Work Functions of the (001) Face of the Hexaborides of Ba, La, Ce and Sm," to be published in *Surface Science*, Oregon Graduate Center, Beaverton, Oregon 97005, Oct. 1978.
10. Lafferty, J.M., "Boride, Cathodes," *Journal of Applied Physics*, Vol. 22, No. 3, March 1951, pp. 299-309.
11. Ahmed, H., et al., "Lanthanum Hexaboride Electron Emitter," J. Appl. Phys., Vol. 43, No. 5, May 1972, pp. 2185-2192.

12. Pastor, H., "Metallic Borides: Preparation of Solid Bodies - Sintering Methods and Properties of Solid Bodies," Boron and Refractory Borides, V.I. Matkovitch, ed., Springer-Verlag, New York, 1977, pp. 458-493.
13. Babich, B.N., Portnoi, K.I., Samsonov, G.V., "Compacting and Sintering of Boride Powders," Metalloved Term. Obrabot. Metallov, 1, 31-35 (1960). Translation in English: HB-5301, H. Brutcher, Altadena, California; or AD 273601, Washington, D.C.: O.T.S.
14. Bumm, H., Liepelt, H., "Results of Isostatic Pressing of Metallic and Non-metallic Powders Up To 15000 Atmospheres," Z. Werkstofftechnik 3, 1972, pp. 364-368.
15. Kislyi, P.S., Samsonov, G.V., "Basic Principles of the Extrusion-die Production of Pipes and Rods from Powders of Highmelting Compounds," Poroshikov. Met. (3), 31-48 (1962). Translation in English: Soviet Powder Met. (3), 1962, pp. 164-177.
16. Medvedev, O.G., Trunov, G.V., Chernyak, L.V., Shlyuko, V.Y., "Production of Parts of Complex Shape in Lanthanum Hexaboride," Poroshk. Met. (3), 101-102 (1971). Translation in English: Soviet Powder Met. (3), 250-251 (1971).
17. Reddy, R.L., Montgomery, L.C., Grulke, C.A., "Slip Casting Composition," Brit. Pat. 1052 590 (Dec. 30, 1966).
18. Salkind, M., "Metals With Grown-In Whiskers," International Science and Technology, March 1967, pp. 52-64.
19. Ashbrook, R.L., "Directionally Solidified Ceramic Eutectics," J. of Am. Cer. Soc., Vol. 60, No. 9-10, 1977, pp. 428-435.
20. Mollard, F.R., et al., "Growth of Composites From the Melt: I," Trans. AIME, 239 [10], 1967, pp. 1526-1533.
21. Chapman, A.T., et al., Final Technical Rept., U.S. Army Missile Command Contract DAAH01-75-C-1852, Georgia Institute of Technology, School of Ceramic Engineering, Dec. 1977.
22. Stewart, D., et al., "Field Emission Cold Cathode Devices Based on Eutectic Systems," Interim Report, Air Force Systems Command, Contract AFOSR-77-3292, Fulmer Research Ltd., July 1979.

### The System Fe<sub>2</sub>B-Fe

#### Introduction

The system Fe - B is reported to form a eutectic (Fe-1) at 3.6 w/o B (Figure Fe-1). This corresponds to 26 a/o Fe<sub>2</sub>B in a Fe matrix. The volume fraction of Fe<sub>2</sub>B in Fe is about 40%, a level which often leads to formation of lamellar microstructures under directional solidification conditions. However, a fibrous, aligned eutectic has been reported (Fe - 2,3), (Figure Fe-2).

This eutectic was of considerable interest to this study, since it was the only reported metallic boride which forms a fibrous or rod-type eutectic. Specimens of this composite were prepared to examine the solidification conditions required to yield aligned microstructure in a boride - containing system. The melting point and work function are marginal for an electron emission material, compared to LaB<sub>6</sub>. However, it would be of interest to conduct a brief emission test to verify this predicted performance. It is not unlikely that a Fe<sub>2</sub>B - Fe composite could find a specialized application as an electron emitter.

#### Experimental Procedure

High purity (99.9 w/o Fe, 99.99 w/o B) powdered (-325 mesh) starting materials were obtained from Cerac (B) and Fisher (Fe). Components were mechanically mixed, then pressed into pellets before melting in a closed-end alumina (sapphire) tube. The mixture coupled directly with the induction coil.

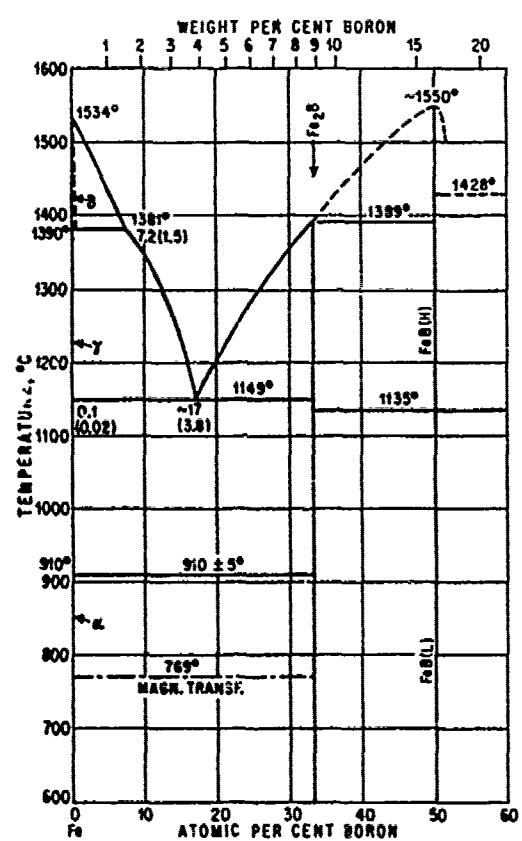


Fig. Fe-1. Phase Diagram for Fe-B from (Fe-1).

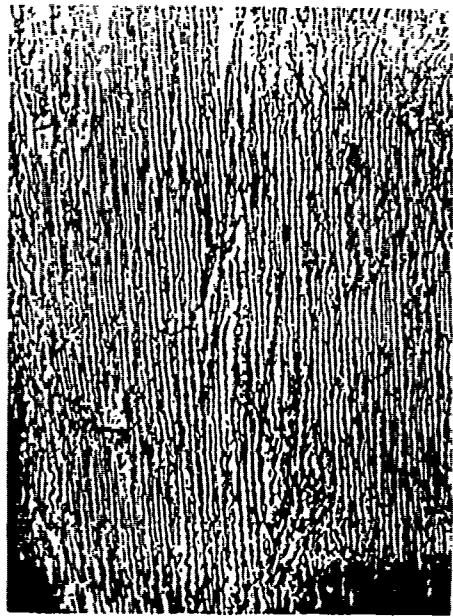


Fig. Fe-2. 280X of Fe<sub>2</sub>B-Fe. Eutectic (Ref. Fe-3).

The powder mixtures were melted and directionally solidified (D.S.) using a 3.6kW induction power supply and quartz tube furnace. The H<sub>2</sub> atmosphere in the furnace was maintained by a slow gas flow under slight positive pressure. A slow heat up rate was set to permit escape of water before melting. The lowering rate (approximate cooling rate) was adjusted to 1. cm/hr for all experiments. A schematic of the furnace is given in the Introduction.

Samples for optical microscopy were prepared by standard procedures: mounting in thermo-set polymer and mechanical polishing. Hardness of the Fe<sub>2</sub>B phase was not great enough to present polishing problems. Phase contrast was improved by chemical etching of polished sections. An ethanol, HCl, CuSO<sub>4</sub> mixture given in Petzow (Fe-4) gave very satisfactory contrast.

#### Experimental Tests

1. A mixture of 3.6 w/o B and Fe (the eutectic composition) was directionally solidified at a lowering rate of 1 cm/hr. in H<sub>2</sub> atmosphere. Specimen size was approximately 3/16" diameter by 1" long.

Optical microscopy studies showed large areas of aligned, directional microstructure. In Figure (Fe-3) may be seen the aligned Fe<sub>2</sub>B fibers (section parallel to growth direction). Figures (Fe-4) and (Fe-5) show the cross section normal to growth direction. In (Fe-4) may be seen the cellular growth pattern in which "bundles" of fibers are surrounded by irregular eutectic structures. Figure (Fe-5) is a 500X view of a single bundle of fibers. These sections were etched as discussed in an earlier paragraph.

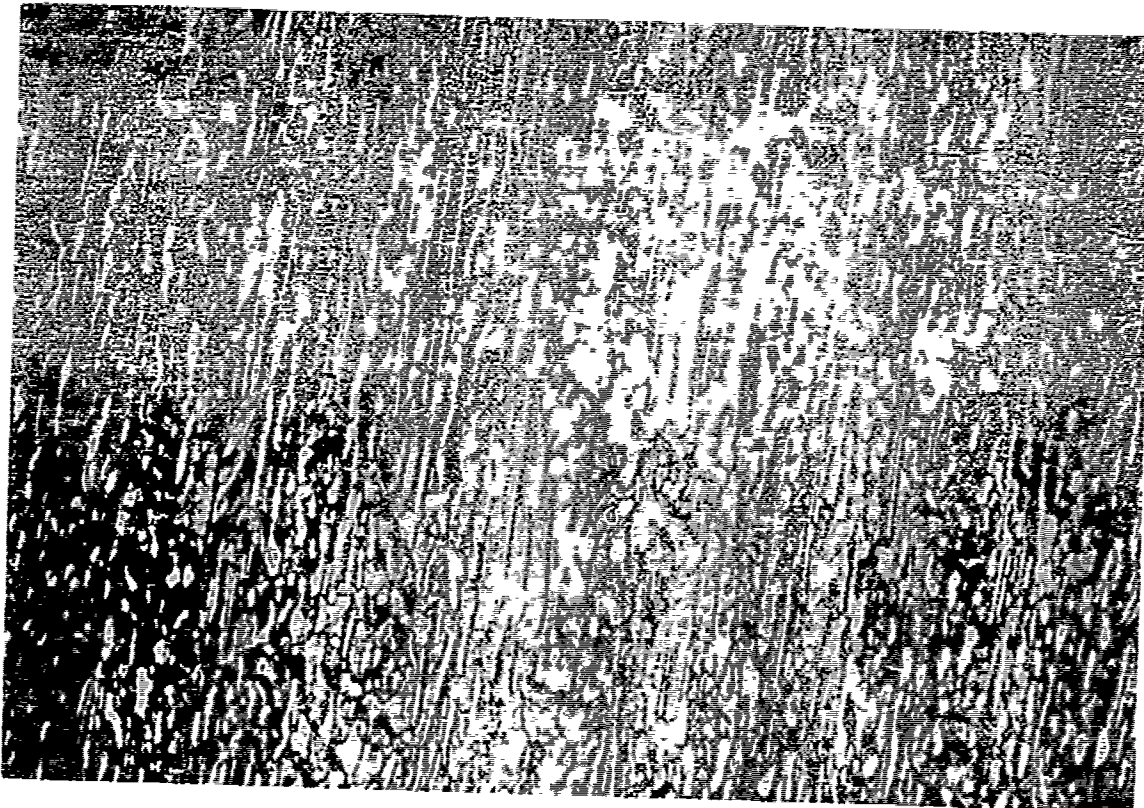


Fig. Fe-3

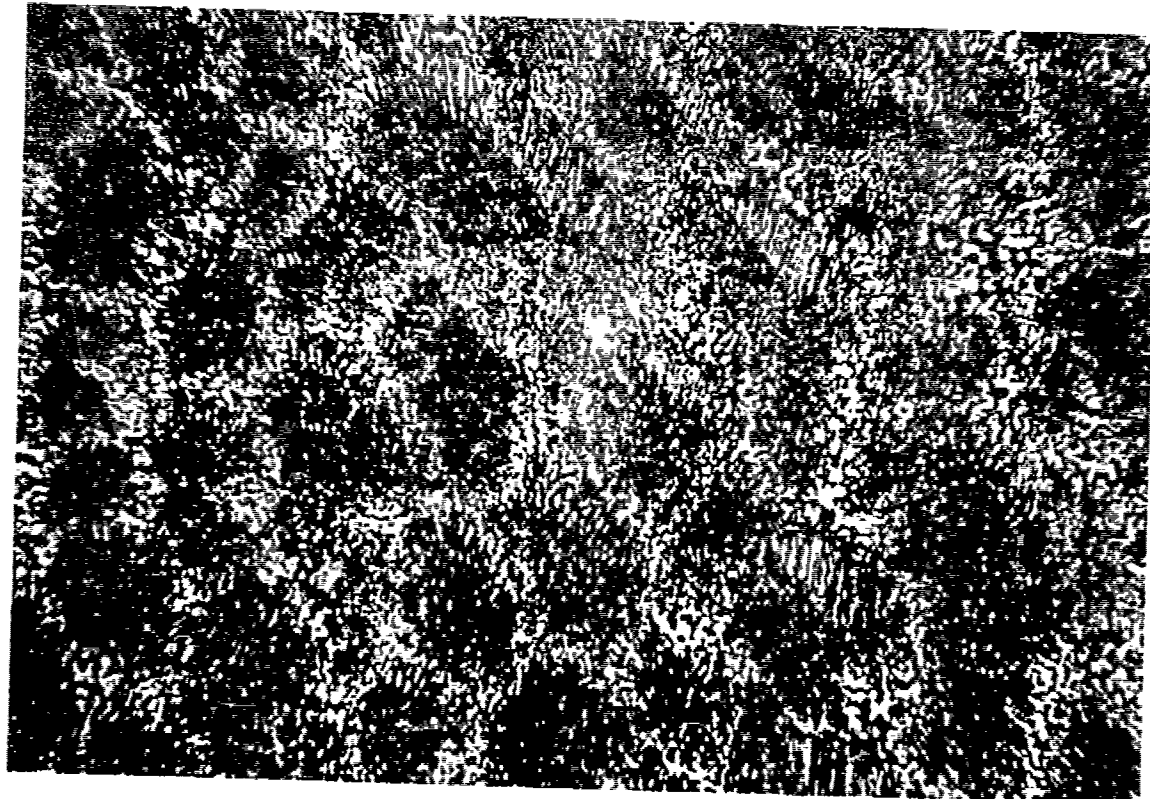


Fig. Fe-4

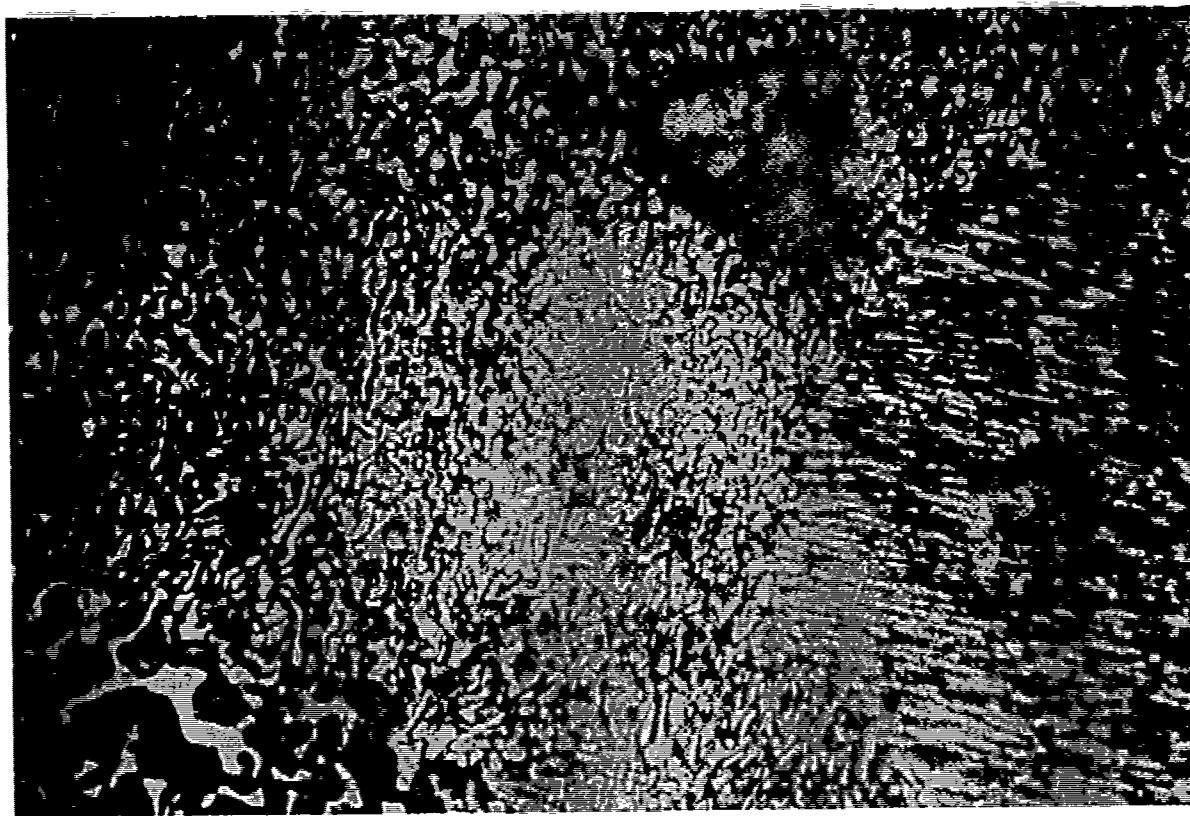


Fig. Fe-5

2. The first experiment was later repeated, using a somewhat larger charge with the intent of obtaining larger aligned areas and more fibers. The melt was held for a 1/2 hr. soak period before lowering at a carefully controlled rate of 1 cm/hr. The crucible was recrystallized alumina and specimen dimensions were 5/16" diameter by 1 1/4" long.

Micrographs of this D.S. product indicated dendritic growth for the first half of the product. (Figure Fe-6). Dendritic structures became smaller (Figure Fe-7), then were replaced by an aligned microstructure in the last (upper) half of the product (Figures (Fe-8), (Fe-9)). The most regular microstructures appeared at the top of the specimen. It is suggested that either the cooling rate was initially too slow, or an incorrect mixture was prepared which "rected itself" as the melt moved toward eutectic composition during the solidification process.



Fig. Fe-6



Fig. Fe-7



Fig. Fe-8

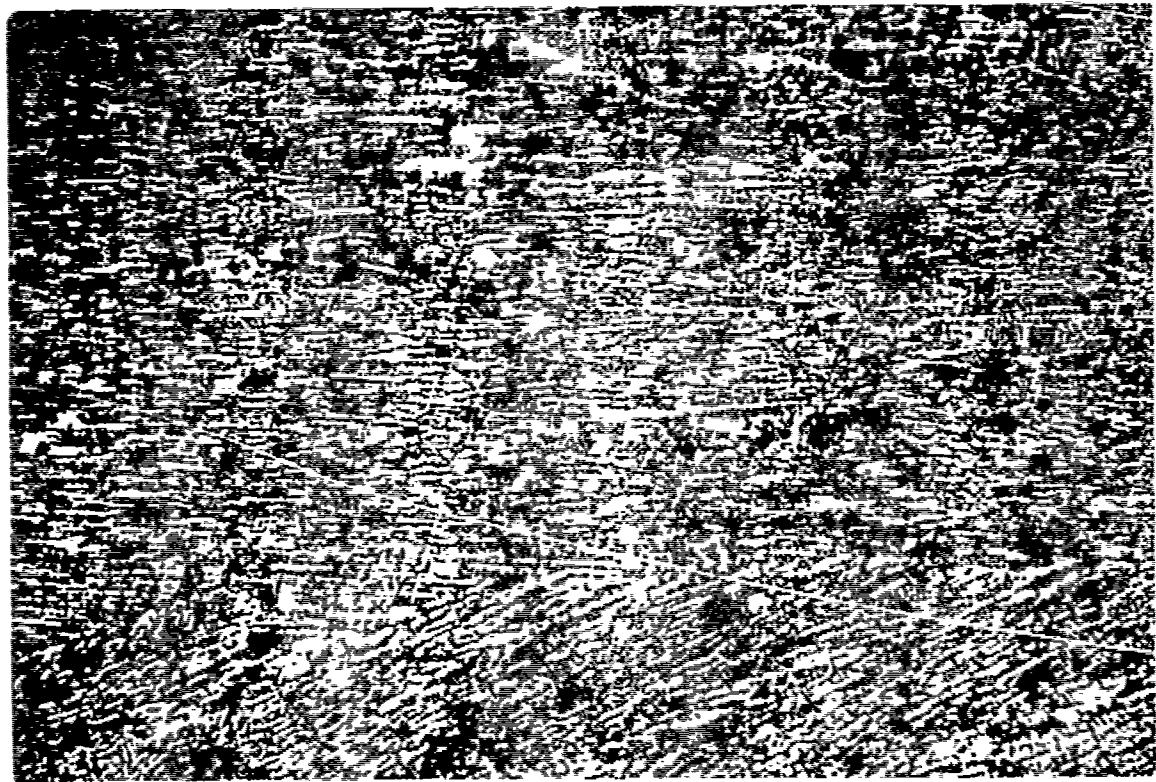


Fig. Fe-9

References

- (Fe-1). Hansen, M., Constitution of Binary Alloys, McGraw-Hill Co. 1958, p. 250.
- (Fe-2). Silva de, A.R.T., Metal Science Journal, 3 (1969), p. 63
- (Fe-3). Silva de, A.R.T., J. Metal Society, 4 (1970), P. 90.
- (Fe-4). Petzow, Gunter, Metallographic Etching, Amer Soc. for Metals, Metals Park, Ohio, 1978. p. 76.

### THE SYSTEMS (TiB<sub>2</sub>, LaB<sub>6</sub>) - Ni

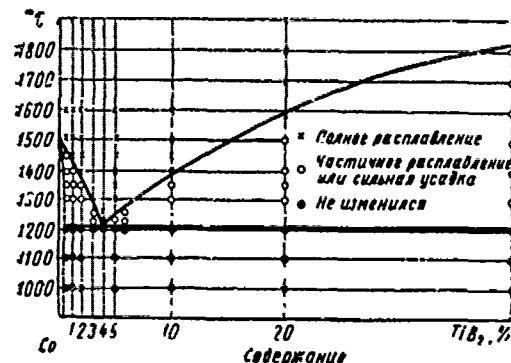
#### A. The Ni-TiB<sub>2</sub> System

Studies by Samsonov (Ni-1) (Fig. Ni-1) and Matkovitch (Ni-2) have indicated the presence of a eutectic in the Ni-TiB<sub>2</sub> system at 3.50Wt% TiB<sub>2</sub>. This pseudo-binary system, based on the interface area criteria given by Lemkey (Ni-3) and others, could yield TiB<sub>2</sub> fibers when directionally solidified. TiB<sub>2</sub> has a number of properties which suggest it could serve as an electron emission material similar to LaB<sub>6</sub>. However, its work function at 3.9eV makes it less attractive than LaB<sub>6</sub> (Ni-4).

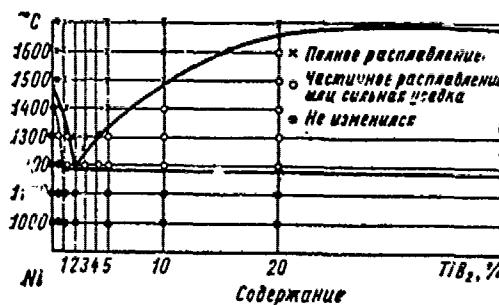
In light of the properties of TiB<sub>2</sub> and the published data showing a eutectic whose composition would favor fiber-type geometry for the TiB<sub>2</sub> phase, it was decided that directional growth should be investigated. Table (Ni-1) summarizes the experimental runs made for the Ni-TiB<sub>2</sub> system.

Early experiments (#1 thru 4) were based on use of 3/16" id. sapphire tubes to contain the melt. a slow hydrogen flow was maintained through the furnace to avoid oxidation and moisture effects on the melt. In later experiments a larger 5/16 id. recrystallized alumina tube confined the melt.

1. The first experiment yielded a poorly melted, poorly mixed product containing zones of Ni (SEM Edax analysis) and zones with Ni and Ti present. Directional growth was not attempted on this run.



Фиг. 3. Пробная диаграмма системы  $\text{TiB}_2$ — $\text{Co}$ .



Фиг. 4. Пробная диаграмма системы  $\text{TiB}_2$ — $\text{Ni}$ .

Fig. Ni-1. Reported eutectics of  $\text{TiB}_2$  with metals (Ni-1).

TABLE (Ni-1). Experimental Runs for Ni-TiB<sub>2</sub> System

No	Composition	Solidification Rate (Cm/hr)	Results	Comments
1. (27-4-79)	3.5 W/0 TiB <sub>2</sub>		on surface or mixed) (TiB <sub>2</sub>	Eduap: Metallic & non-metallic (porous) areas.
2. (24-5-79)	3.5 W/0 TiB <sub>2</sub>	Quenched	2-phase microstructure	sapphire tube, H <sub>2</sub>
3. (29-5-79)	3.5 W/0 TiB <sub>2</sub>	20 cm/hr	2-phase microstructure Ti, hi uniformly dis- tributed	sapphire tube H <sub>2</sub> ,
4. (11-6-79)	12 W/0 TiB <sub>2</sub>	Crucible/Quench	looks like 3.5 w/o	Sm. alumina cruc. prod. did not adhere when cold.
5. (10-7-79)	3.5 W/0 TiB <sub>2</sub>	1 Cm/hr	"2-phase" microstruct: large grains w/porous electric between them Ti & hi = uniform	Sapphire tube, H <sub>2</sub>
6. (24-7-79)	12 W/0 Ti B <sub>2</sub>	1 cm/hr	Large voids in product uniform melt	Gold color on exterior (air cooled)
7. (1-8-79)	3.5 W/0 Ti B <sub>2</sub>	22 cm/hr		Sapphire tube
8. (15-8-79)	12 W/0 Ti B <sub>2</sub>	22 cm/hr	Poor melt @ 1300°C	alumina tube
9. (22-8-79)	3.5 W/0 Ti B <sub>2</sub>	1 cm/hr	Good melt	alumina tube ("prefired w/moly heater")

2. At a higher temperature (estimated at 1400°C Via optical pyrometer), a two-phase microstructure resembling that shown by Samsonov (Ni-1) was seen with polished sections. Etching was very helpful in developing contrast between the phases. A standard Ni etchant was used (Ni-8).

3. A relatively rapid lowering rate of 20.cm/hr was next tried. The resulting product did not show directional growth patterns; it closely resembled the previous product when viewed optically. SEM/EDAX data showed a uniform dispersion of Ni and Ti through the specimen. It appears that the rapid lowering permitted solidification in all directions, as in normal solidification. Figures (Ni-2) and (Ni-3) are characteristic of large areas of the section parallel to the growth direction. One contains a dendritic pattern and the other figure shows a polyphase structure in which are distributed "arrays" of rounded and elongated structures. These structures were too small for individual analysis by the SEM/EDAX.

Generally, the variation in microstructures appeared to result from uneven heating of the melt at various points. Cross sections of this product also contained areas of dendrites (Fig Ni-4) and areas of primary grains having a eutectic-like matrix (Fig. Ni-5). All of the above structures were chemically etched to show phases present.

4. A 12.w/o TiB<sub>2</sub>-Ni mixture was melted in an alumina crucible, This melt was very low viscosity and did not adhere to the crucible when cooled to room temperature. The microstructure closely resembled



(Fig. (Ni-2) Longitudinal Section of Sample 3 at 50X.

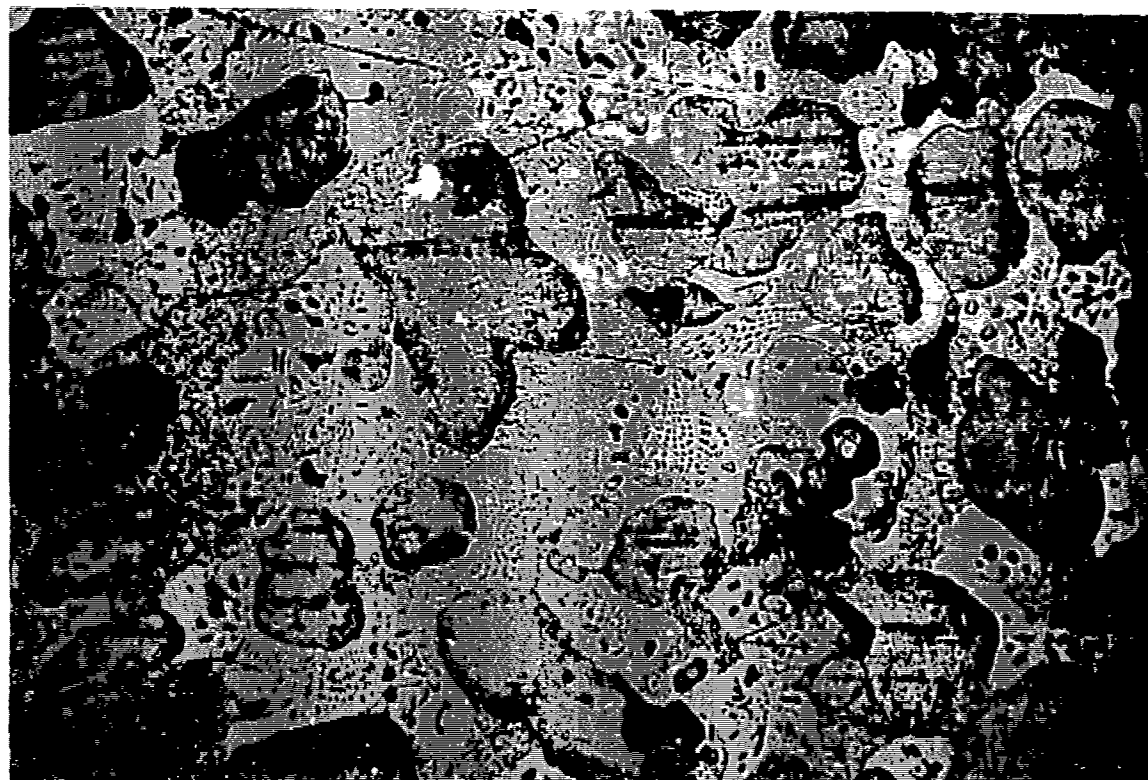


Fig. Ni-3. Longitudinal Section of Sample 3 at 200X.

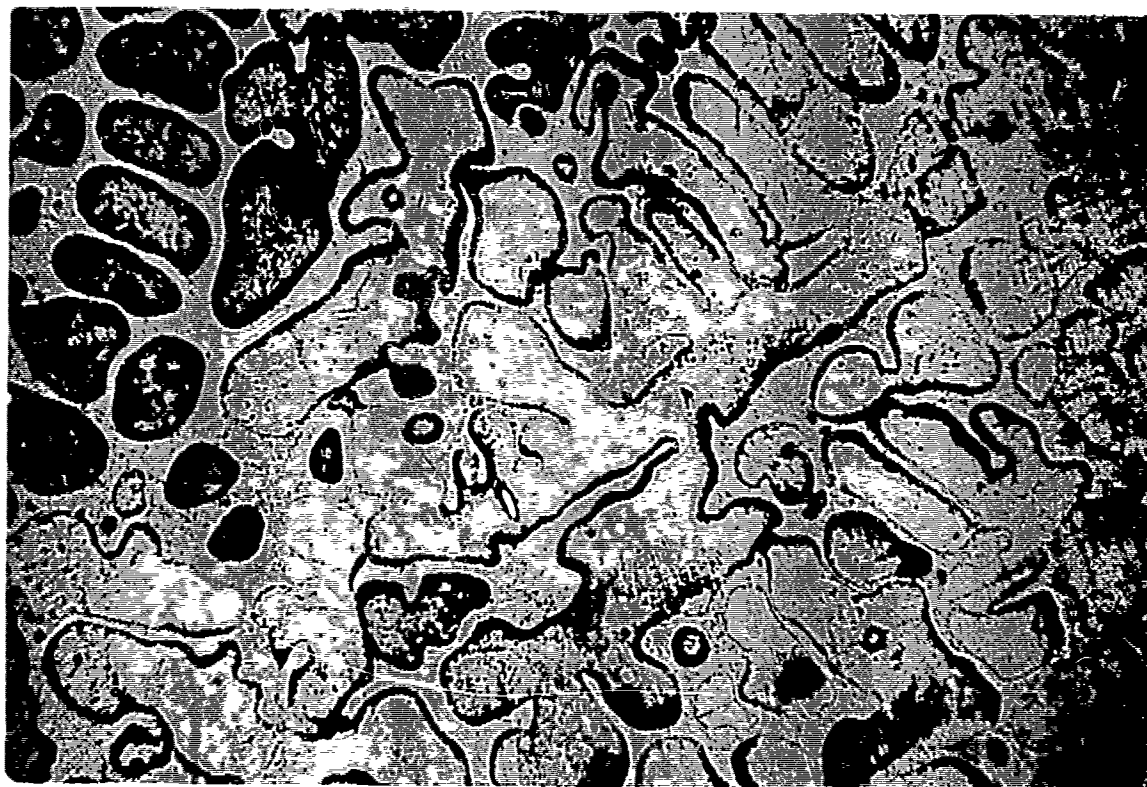


Fig. Ni-4. Transverse Section of Sample 3 at 50X.

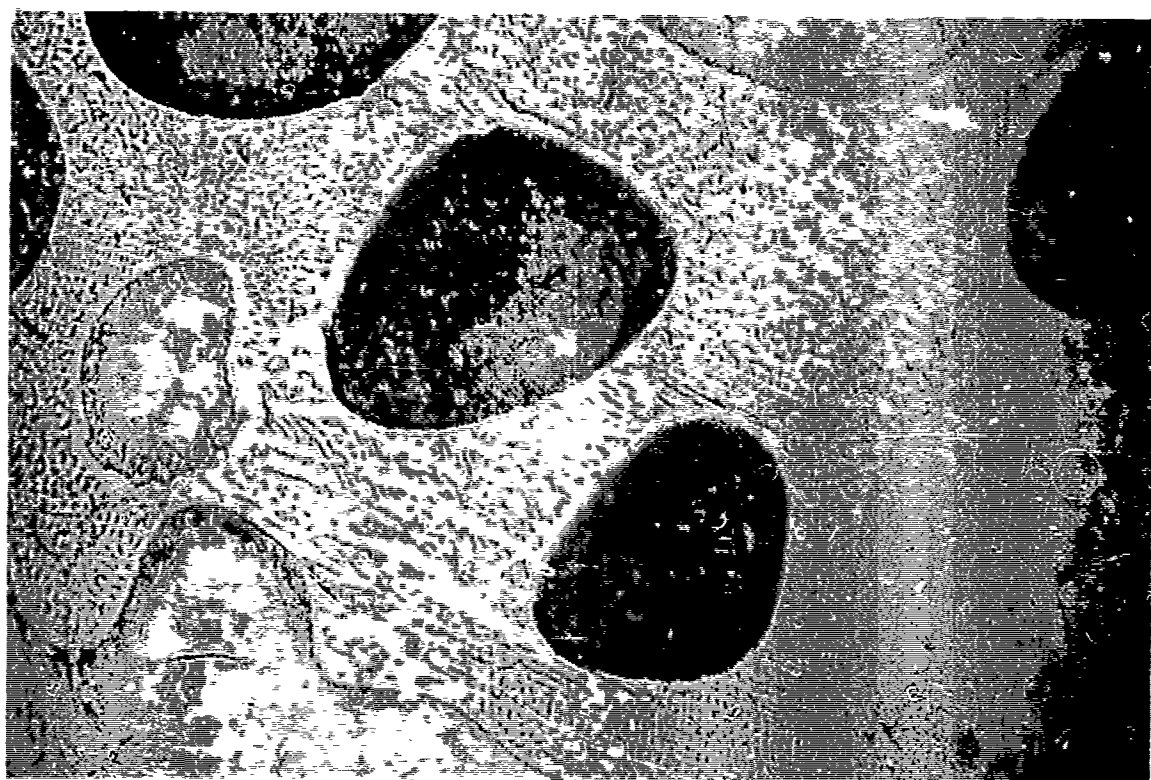


Fig. Ni-5. Transverse Section of Sample 3 at 200X.

that of the 3.5 W/O material.

5. A 3.5 W/O mixture was now lowered at a rate of 1.cm/hr (a satisfactory rate for the  $Fe_2B$ -Fe eutectic). A sapphire tube and hydrogen were used for this experiment. The microstructures are shown in Figures (Ni-6 to 8). Note the two-phase character which was seen in most previous  $TiB_2$ -Ni products. The SEM/EDAX studies (Fig. Ni-9,10) show a uniform distribution of Ti and Ni. However, this reflects the resolution limits of the equipment and does not preclude the existence of distinct phases.

6. A further run at 1 cm/hr was made with a 12 W/O mixture. Again, efforts were being made to identify trends in behavior, or differences in behavior which could assist in interpreting the behavior of the 3.5 W/O eutectic composition. This product apparently was overheated; large voids were found when the specimen was sectioned lengthwise.

7. In order to improve composite quality, a larger growth tube of alumina was used for this run. The mixture was lowered at a rapid rate (22.cm/hr) since it was uncertain whether (1) the alumina tube might react with the charge, or if (2) the larger tube might permit more rapid solidification rates. Figures (ni-11) and Ni-12) show microstructures observed. In Figure (Ni-11) the mid-point of the product is shown. Here, an apparent phase segregation has occurred. Near the top of the product (Fig. Ni-12),



Fig. Ni-6. Longitudinal Section of Sample 5 at 240X.

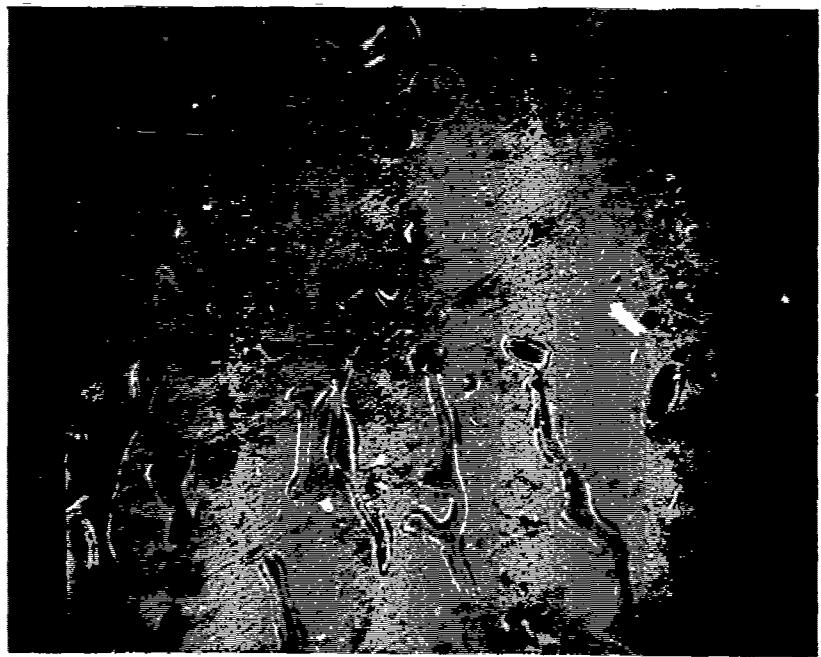


Fig. Ni-7. Longitudinal Section of Sample 5 at 125X.



Fig. Ni-8. Longitudinal Section of Sample 5 at 250X.

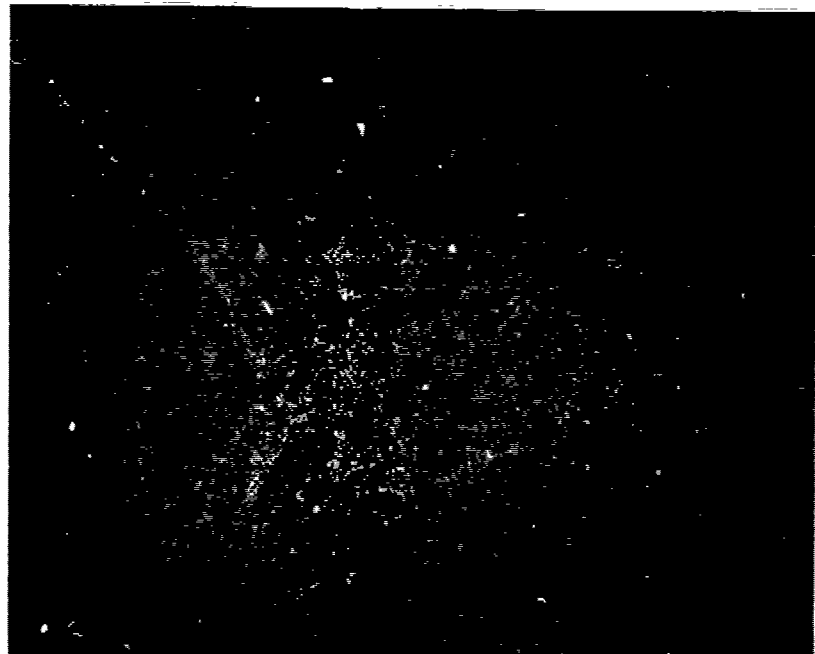


Fig. Ni-9. Edax Scan for Ni on Fig. Ni-8. 250X.

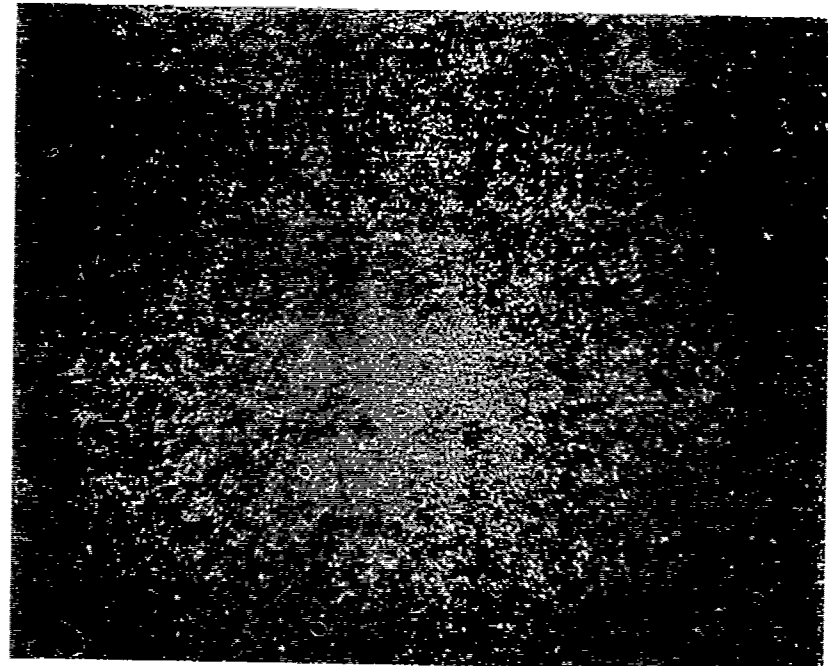


Fig. Ni-10. Edax Scan for Ti on Fig. Ni-8. 250X.



Fig. Ni-11. Middle Region, Longitudinal Section of Sample 7 at 200X.



Fig. Ni-12. Top area, Longitudinal Section of Sample 7 at 500X.

a more equal volume distribution of the phases is seem. It was not possible to establish what components make up the granular "eutectic phase", but it is suggested that the darker, minor component is  $TiB_2$ . If so, the apparent elongated structures suggest that a rod or fibrous type composite is possible under D.S. conditions.

8. A 12.W/O  $TiB_2$  was also lowered at 22 cm/hr in the larger alumina tube. A somewhat lower temperature (Ca. 1300°C on the outside of the alumina tube) was maintained to eliminate the voids seem in experiment 6. However, this temperature was too low, and the polished section had large areas of poorly-melted material.

9. A 3.5 W/O  $TiB_2$  D.S. run was made, using a slow growth rate (1 cm/hr) and large alumina tube. A good melt was seen in the polished section. The alumina tube was carefully dried by pre-firing in hydrogen. This product may be seen in Figures (Ni-13) to (Ni-17). Figures (Ni-13) and (Ni-14) are lower magnifications. Elongated structures following the growth direction are seen in (Ni-18). These are tentatively identified as  $TiB_2$  with occasional Ni inclusions. The Ni was partially removed by the etchant, leaving small pits in the  $TiB_2$  phase. In (Ni-13) a more uniform upper surface was observed. Presumably, this change in morphology was due to different thermal gradients at the surface of the specimen.

Figures (Ni-15) and (Ni-16) are higher magnifications of the upper surface. One sees colonies of rounded and rod-like structures.

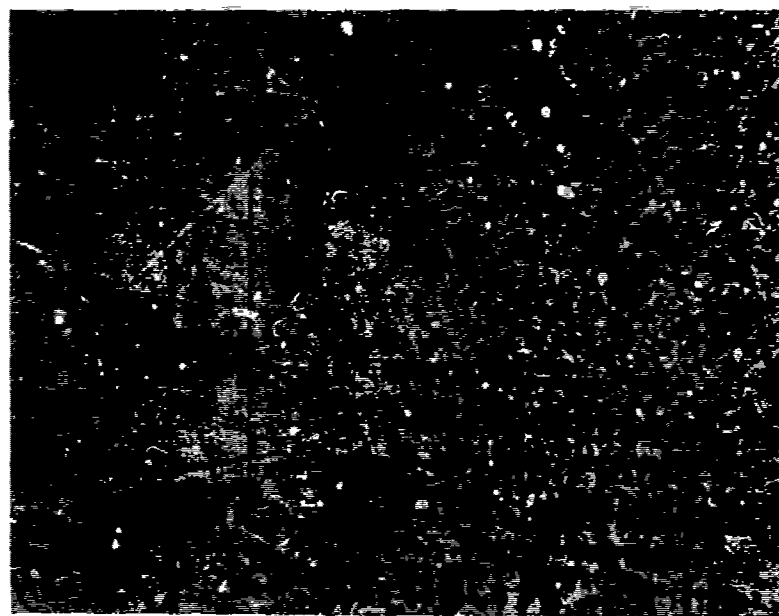


Fig Ni-13. Longitudinal Section Near Top of Sample 9 at 200X.

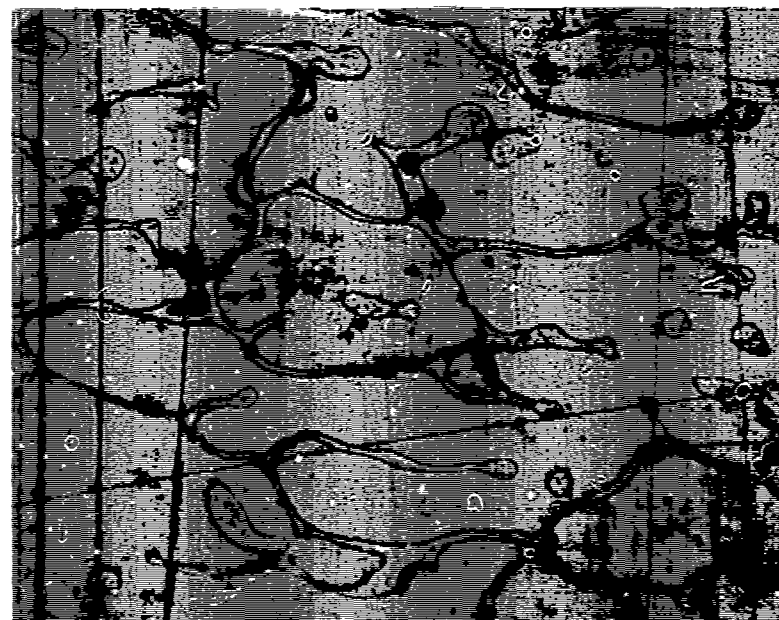


Fig. Ni-14. 200X showing structure making up most of sample 9.  
Longitudinal Section.



Fig. Ni-15. 500X of 3.5 W/O  $TiB_2$  in Ni. Note Fields of Circular and Elongated Structures. Top Region of D.S. Sample 9.

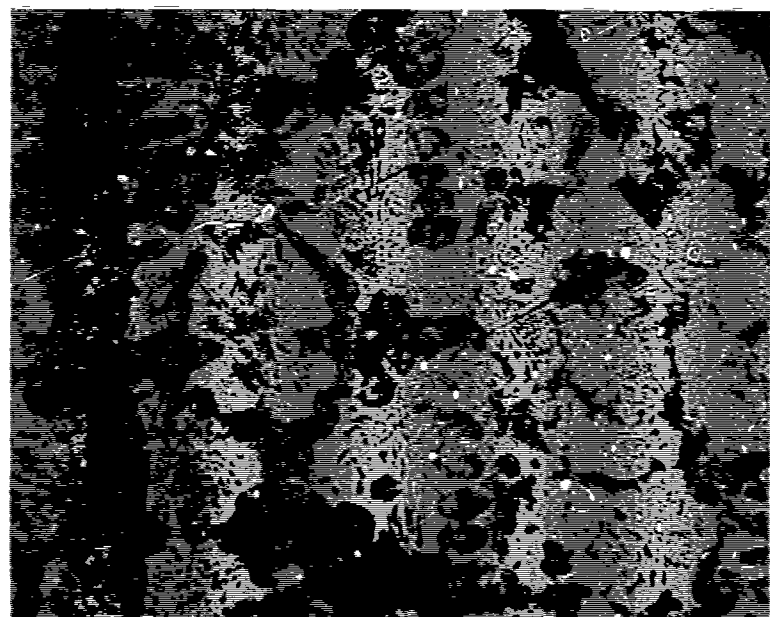


Fig. Ni-16. 500X of 3.5 W/O  $TiB_2$  in Ni. Note Circular and Elongated Structures. Top Region of D.S. Sample 9.

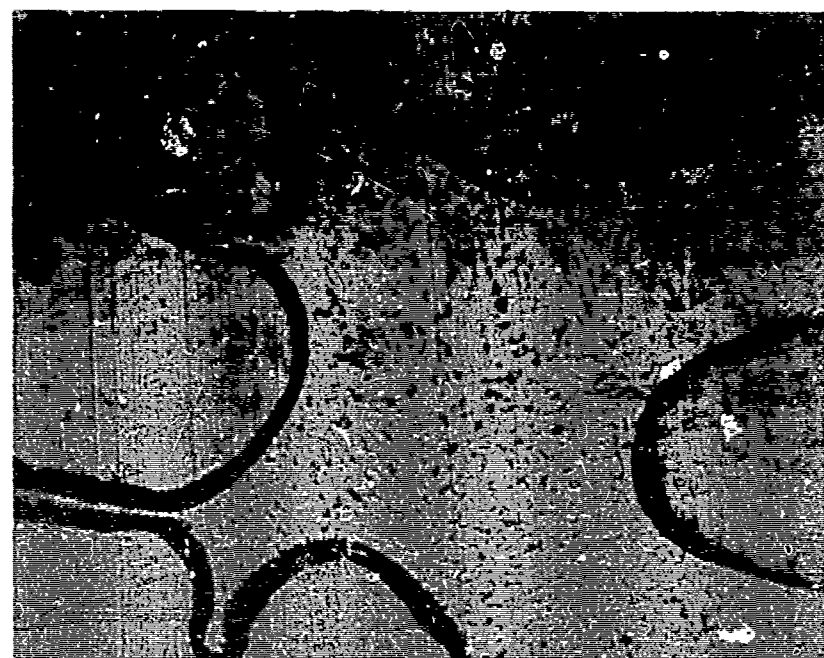


Fig. Ni-17. 500X of 3.5 W/O  $TiB_2$  in Ni. Bottom Region of D.S. Sample 9.

These are regarded as potential aligned structures of  $TiB_2$ , if proper control of thermal gradients can be maintained during D.S. Figure (Ni-21) is a high magnification of the lower region of the 3.5 W/O  $TiB_2$  specimen. The structures are similar to (Ni-14) and again show etch pits where Ni inclusions were.

### B. The LaB<sub>6</sub>-Ni System

Due to the many similarities between TiB<sub>2</sub> and LaB<sub>6</sub>, it was decided that some studies of the LaB<sub>6</sub>-Ni system should be made. There was no published information on LaB<sub>6</sub> - metal systems except the reports that Al acts as a solvent for both LaB<sub>6</sub> and TiB<sub>2</sub>. High purity single crystals of the two borides were grown from Al solutions. The lack of reactivity with Al attests to the great chemical stability of these borides. Other references (Ni-5) (Ni-6) report that at high temperatures LaB<sub>6</sub> has little if any chemical reaction with Rh, Ta, or Mo.

LaB<sub>6</sub> has a reported (Ni-7) free energy of

$$\Delta F = 0.071T - 351 \text{ KJ/mole (1700K-2100K)}$$

So that at 2100K,  $\Delta F = 0.48.0 \text{ Kcal/mole}$ . At 273K,  $\Delta F$  for LaB<sub>6</sub> is 0.79 Kcal/mole and  $\Delta H$  is 69 Kcal/mole. Samsonow (Ni-7) reports a value of 70.07 Kcal/mole for TiB<sub>2</sub>.

Since LaB<sub>6</sub> shares a number of chemical properties with TiB<sub>2</sub>, initial experiments were conducted on that assumption that LaB<sub>6</sub> forms a eutectic with Ni as TiB<sub>2</sub> does. TiB<sub>2</sub> also forms similar eutectics with both iron and cobalt, so these were regarded as alternate matrix candidates for use with LaB<sub>6</sub> also. The experimental equipment and procedures were the same as those used for Ni-TiB<sub>2</sub> studies. Powdered starting materials (-325 mesh) of 99.9% purity were obtained from the Cerac Company. The experiments conducted are summarized in Table (NI-2).

Figures Ni-22 to Ni-25 show evidence of microstructural alignment at about 10X. The sharp change from a random dendritic structure to an aligned structure may be clearly seen.

Table (N1-2). Experimental Runs for Ni-LaB<sub>6</sub> System

Sample No.	Composition	Solidification rate cm/hr	Results	Comments
1. (11-6-79)	10 w/o LaB <sub>6</sub>	melt in open crucible	2-phase microstructure like Ni-Ti B <sub>2</sub> products	melt in alumina crucible low viscosity melt
2. (17-7-79)	4 w/o LaB <sub>6</sub>	1 cm/hr	good melt, Rx w/sapphire LaB <sub>6</sub> whiskers observed	sapphire tube
3. (26-7-79)	10 w/o LaB <sub>6</sub>	1 cm/hr	Inc. melting, no directional microstructures observed	sapphire tube
4. (31-7-79)	4 w/o LaB <sub>6</sub>	22 cm/hr	well melted, partly aligned microstructure	sapphire tube
5. (10-8-79)	10 w/o LaB <sub>6</sub>	10 cm/hr	some microstructural align- ment, large voids in sample	alumina tube
6. (13-8-79)	10 w/o LaB <sub>6</sub>	5 cm/hr	several phases visible	alumina tube
7. (16-8-79)	10 w/o LaB <sub>6</sub>	22 cm/hr	good melt @ Ca. 1375C	alumina tube
8. (20-8-79)	10 w/o LaB <sub>6</sub>	1 cm/hr	"	alumina tube
9. (23-8-79)	10 w/o LaB <sub>6</sub>	5 cm/hr	Rx w/alumina tube	alumina tube



Fig. Ni-18. Section parallel to growth axis of sample "b".



Fig. Ni-19 Center section parallel to growth axis of sample #7.



Fig. Ni-20 Section transverse to growth axis, near top of sample #6.



Fig. NI-21 Section parallel to growth axis of sample #9.

In Figures Ni-22 to Ni-27 are shown microstructures of a relatively non-aligned sample (due to low temperatures in part). Figures Ni-22 to Ni-24 show equiaxed structures and some evidence of eutectic. Figures Ni-25 to Ni-27 at a higher magnification clearly suggest the sample is near a eutectic composition.

In Figures Ni-28 to Ni-30 some relatively aligned structures resulting from  $\text{LaB}_6$ -Ni mixtures are shown. These sections are in the same plane as the growth axis. More nearly aligned structures were observed for 4 w/o samples. However, it was not clearly established whether  $\text{LaB}_6$  phases were present after the  $\text{LaB}_6$ -Ni mixture was directionally solidified. Solid solubility may be a significant factor. At 10 w/o,  $\text{LaB}_6$  was identified by microprobe in the D.S. product.

The following observations were made when a series of experiments were conducted to examine the effect of lowering rate on microstructure. Rates of 1, 5, 10, and 22 cm/hr were compared for 10 w/o  $\text{LaB}_6$  + Ni mixtures:

1. One (1) cm/hr was the most uniformly aligned of this test series.  
Long cells, parallel to the growth direction were observed.  
Note that this sample was also pre-heated to dry the mixture before heating to melt temperature.
2. 5 cm/hr = less uniform rod structure than above, less parallel to growth direction than above, long cells.
3. 10 cm/hr = large areas of uniformly striated (rod) structure, but poor directionality, cells shorter than above.
4. 22 cm/hr = large areas of striated structure. Several "secondary structures" long cells, but random orientation of striated

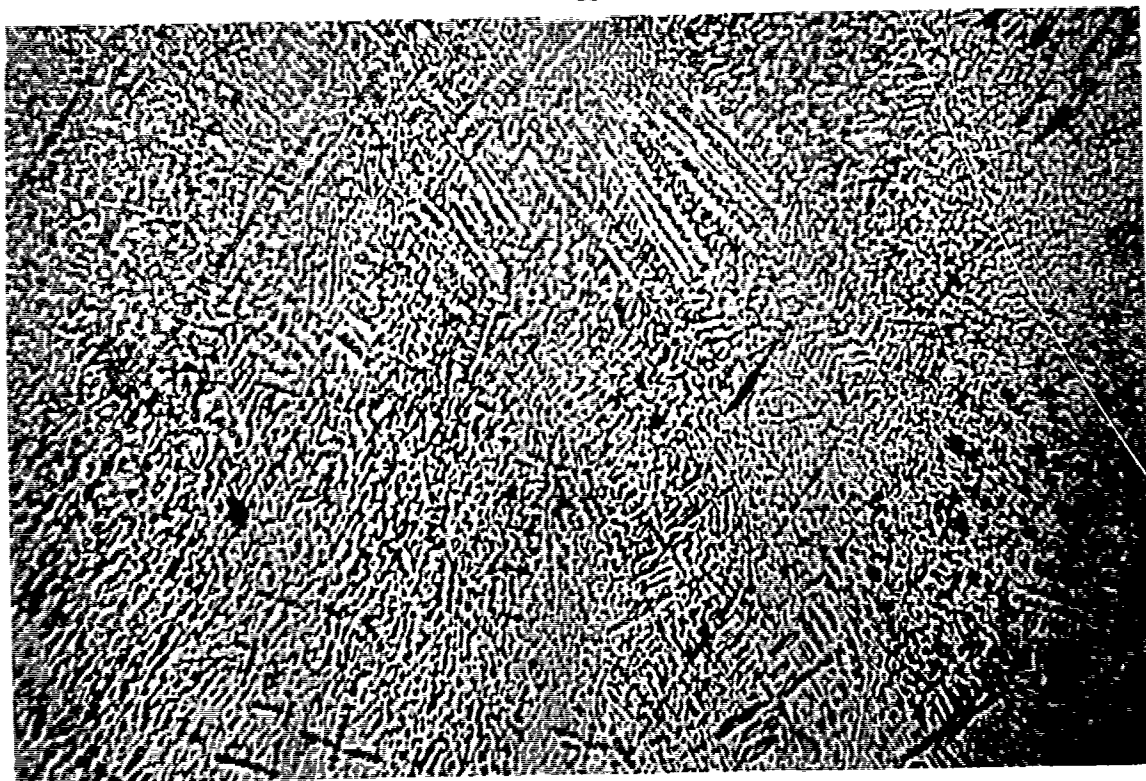


Fig. Ni-22 Sample #4 at 200X.



Fig. Ni-23 Sample #4 at 200X.

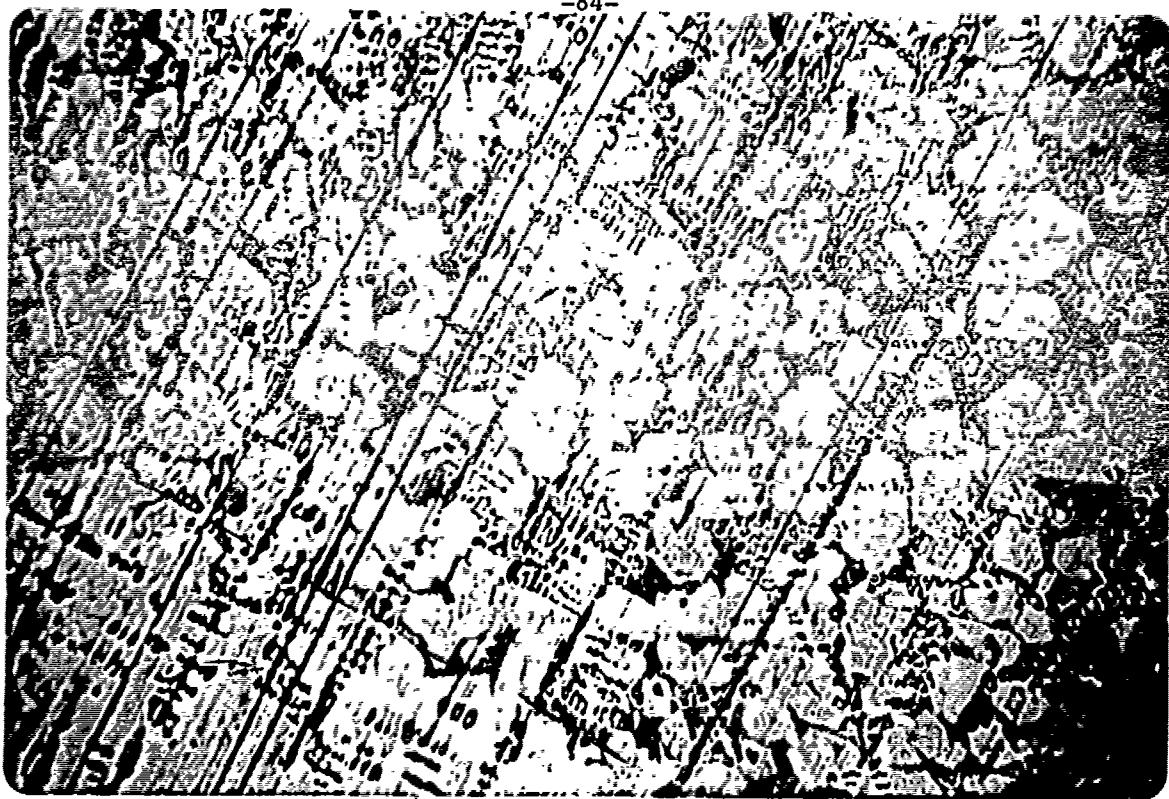


Fig. Ni-24 Sample #4 at 200X.



Fig. Ni-25 Sample #4 at 500X.



Fig. Ni-26 Sample #4 at 500X.

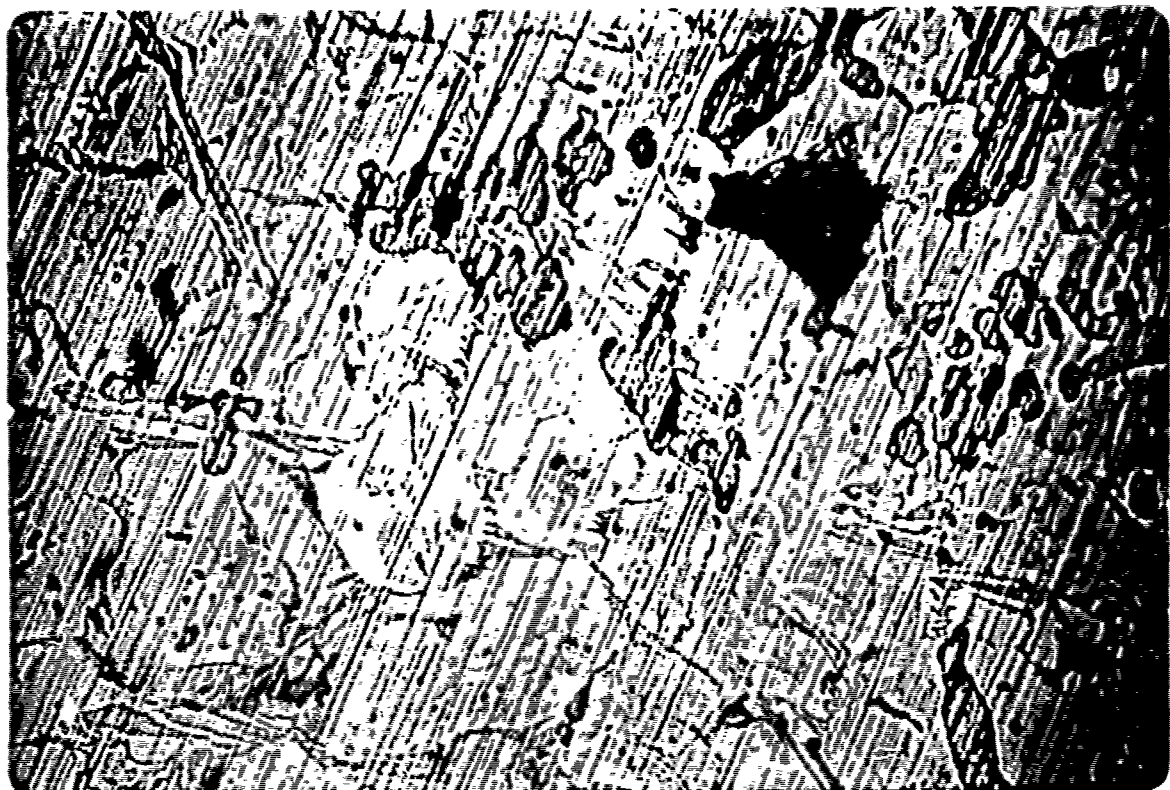


Fig. Ni-27 Sample #4 at 500X.

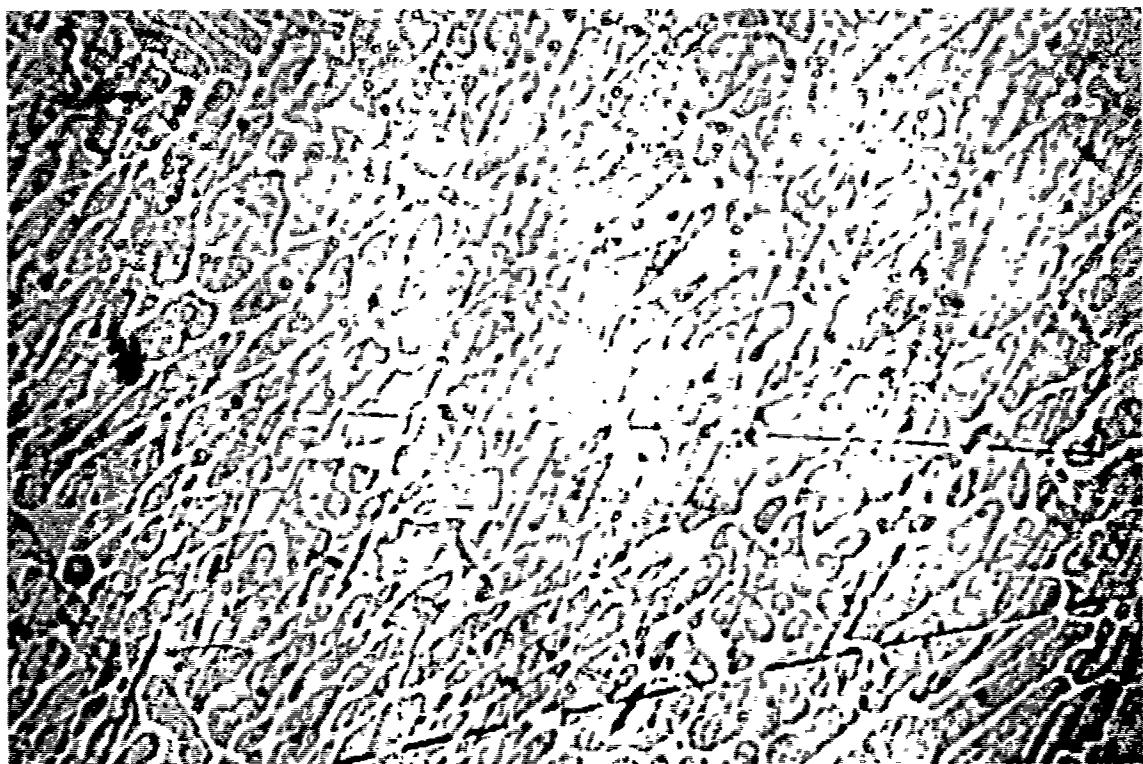


Fig. Ni-28 Sample #5 at 500X.

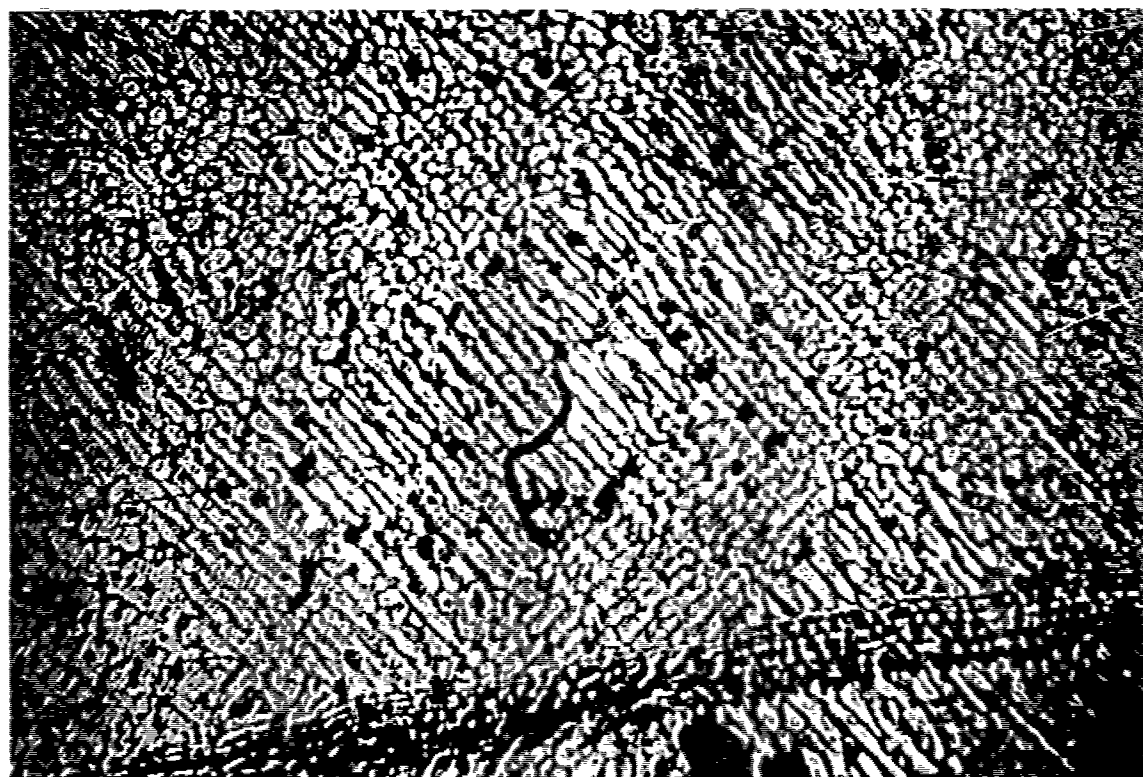


Fig. Ni-29 Sample #5 at 500X.

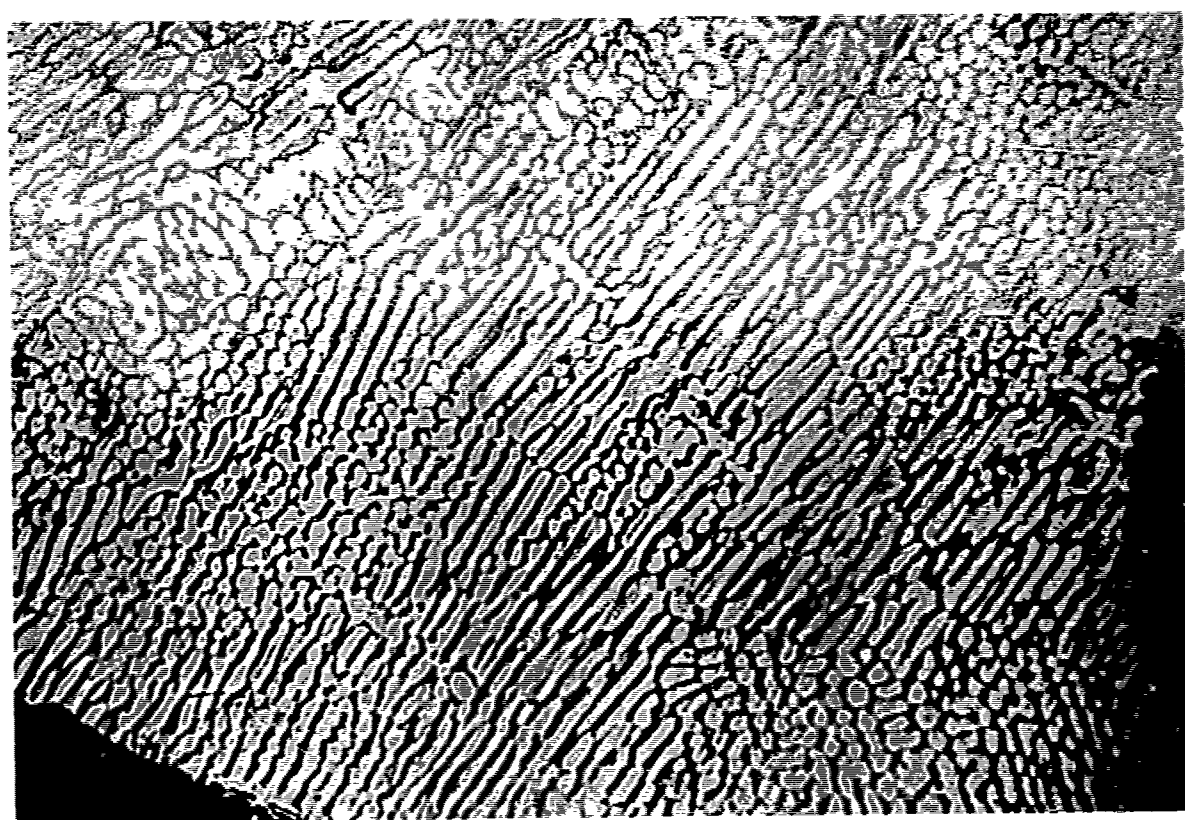


Fig. Ni-30 Sample #5 at 500X.

material in cells and much dendritic material over whole specimen.

Summary

Many questions remain about the presence of a  $\text{LaB}_6$ -Ni eutectic at low volume fractions of  $\text{LaB}_6$ . In this work we have observed (1) that  $\text{LaB}_6$  remains a separate phase in mixtures heated to 1600°C, (2) directional solidification tests show that the mixtures of phases form aligned microstructures.

It would be necessary to determine a segment of the phase diagram for La-B-Ni before prospects for a  $\text{LaB}_6$ -Ni pseudo-eutectic can be reasonably evaluated. As with the  $\text{LaB}_6$ -Cu system, a ductile electrical and heat conductive matrix such as Ni would be of interest for exploiting the cathode potential of  $\text{LaB}_6$ .

References for Systems (TiB<sub>2</sub>, LaB<sub>6</sub>) - Ni

- (Ni-1) Samsonov, G.V., Boron, ITs Compounds and Alloys, Publishing House of Academy of Science, USSR, Kiev, 1960.
- (Ni-2) Matkovitch, V.I., (ed), Boron and Refractory Borides, Springer-Verlag, Berlin, 1977.
- (Ni-3) M. Salkind and F. Lemkey, International Science and Technology, March 1967, p. 52.
- (Ni-4) Fomenko, V. S., Handbook of Thermionic Properties, Plenum Press, N.Y. 1966, p. 87.
- (Ni-5) Schmidt, P.H., J. Vac. Sci. Technol., 15(4), Jw/aug 1978, p. 1554.
- (Ni-6) Elinson, M., "Field Emission Cathodes", Radiotek. elecTRoniKA, Vol. 1, 1962, p. 1417.
- (Ni-7) Samsonov (p. 452) see Reference Ni-1.
- (Ni-8) Gunter Petzow, Metallographic Etching, Amer. Soc. for Metals, Metals Park, Ohio. 1978.

### The System $\text{LaB}_6$ -Cu

#### Introduction

The Cu- $\text{LaB}_6$  system was examined on the basis of projected behavior, and after discussions with J. M. Lemsky concerning screening experiments he had previously conducted (Cu-1).

The system Cu-B (17. a/o B, 3.8 w/o B) is reported (Cu-2, 3) (Fig. Cu-1) to form a eutectic containing B structures in a Cu Matrix. This system was directionally solidified and yielded aligned B fibers in the Cu Matrix (Cu-4) (See Fig. Cu-2). Since  $\text{LaB}_6$  may be regarded as a B lattice which contains La atoms in interstitial holes, it was not unreasonable that  $\text{LaB}_6$  could behave similarly or substitute for B where the B and Cu phases are in equilibrium. Also, if one examines the reports on the Ni- $\text{TiB}_2$  eutectic (Cu-5) it is seen that the Ni atom and Ni (II) (atomic) diameters are greater than that of Ti (II). This then suggests that physically Ni (II) is unlikely to replace Ti (II) in the  $\text{TiB}_2$  lattice. At the same time, the heat of formation of  $\text{TiB}_2$  is greater than that of reported Ni-B compounds (Cu-6). One now has a physical and energetic basis to discuss the formation of Ni- $\text{TiB}_2$  eutectic. Using the above criteria for systems (X- $\text{LaB}_6$ ), where X is a metallic ion, Cu is found to be a potential eutectic former with  $\text{LaB}_6$ . Therefore, a series of screening experiments were conducted to determine (1) reactions between  $\text{LaB}_6$ -Cu and (2) presence or absence  $\text{LaB}_6$ -Cu eutectics. Lemkey has conducted some screening experiments which also suggest that Cu could serve as matrix for a Cu/ $\text{LaB}_6$  composite. See Table (Cu-1) for the summary of experiments conducted with the Cu/ $\text{LaB}_6$  system.

#### Experimental Procedures

High purity (99.9 w/o Cu, 99.9 w/o  $\text{LaB}_6$ ) powdered (~325 mesh) starting material were obtained from Cerac Inc. These were mechanically mixed, then

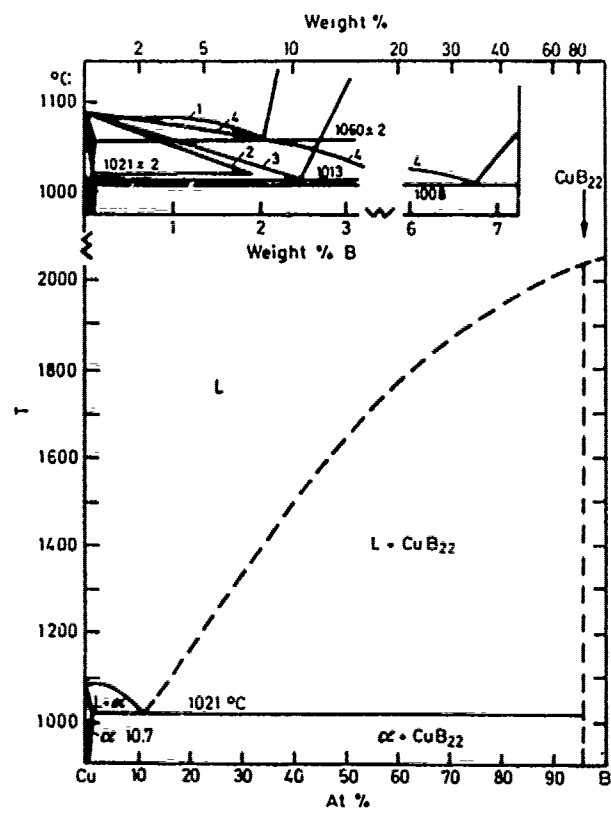


Fig. Cu-1. From Ref. Cu-2.



Fig. Cu-2. Copper-Boron Eutectic. Ref. Cu-4.

Table (Cu-1). Experimental Runs for Cu-LaB<sub>6</sub> System

No.	Composition	Solidification rate (cm/hr)	Results	Comments
1. (17-8-79)	10 w/o LaB <sub>6</sub>	24. cm/hr.	blocky LaB <sub>6</sub> grains	Pink grains identified as LaB <sub>6</sub> , alumina crucible; direct coupling with R.F.
2. (29-8-79)	2 w/o LaB <sub>6</sub>	5.cm/hr	no LaB <sub>6</sub> phases visible after etching	alumina crucible
3. (10-10-79I)	2, 10 w/o LaB <sub>6</sub>	-	some evidence of Rx w/alumina plate	melted samples on an alumina plate
4. (10-10-79II)	2, 10 w/o LaB <sub>6</sub>	-	no apparent Rx w/graphite plate	melted samples on a graphite plate
5. (11-10-79)	2, 10 w/o LaB <sub>6</sub>	-	red needles of LaB <sub>6</sub> on surface of samples; La evenly distributed in 2% sample, non-uniform in 10% sample.	graphite container (indirect heating)
6. (20-10-79III)	4, 6 w/o LaB <sub>6</sub>	-	red needles on surface of samples, 6 w/o was very volatile above M.P. 4% was less volatile.	M.P. 1150°C (est.), graphite container
7. (15-1-80)	(2 w/o LaB <sub>6</sub> )	5.cm/hr.	blocky LaB <sub>6</sub> phases at top of boul. 2-phase areas at lower section of sample. Distinct interface during d.s. suggests a phase boundary was crossed, or cooling rate changed.	graphite crucible

pressed into pellets before induction melting.

Mixtures were melted and directionally solidified (D.S.) using a Lepel 3.2 Mc r.f. generator and quartz tube furnace. The furnace atmosphere of  $H_2$  was maintained by a slow gas flow under slight positive pressure. Lowering rate (nominal cooling rate) could be varied over a wide range. A schematic of the furnace is given in the Introduction to the  $LaB_6$ -B section.

Samples for optical microscopy were prepared using conventional polishing methods. For the Cu-base specimens extreme hardness was not a problem, and a good polished section could be quickly prepared. Several chemical etchants and polishing solutions were found helpful in increasing phase contrast. These included  $HNO_3$ -based mixtures given by Petzow/(Cu-7).

Generally, the polished specimens could be de-mounted and used for SEM characterization. The SEM was used both to resolve phase structures and to make elemental analyses of selected areas. The electron microprobe was used to detect elemental concentrations below the capabilities of the SEM.

#### Experimental Tests

1. Initially a 10.w/o  $LaB_6$  - Cu mixture was directionally solidified at a rapid rate in an alumina tube to examine interactions, crucible reactions, etc. The approximate melting temperature (optical pyrometer) and volatility were recorded. Optical microscopy of mounted and polished sections revealed the degree of melting and the presence of major phases. Scanning electron microscopy and electron microprobe elemental analyses of specific sites were conducted on a limited basis.

Large grains of  $LaB_6$  were the most prominent features visible in optical studies. In Figure (Cu-3) are shown at 500X the two phase structures making up most of the first product. There was a rather uniform

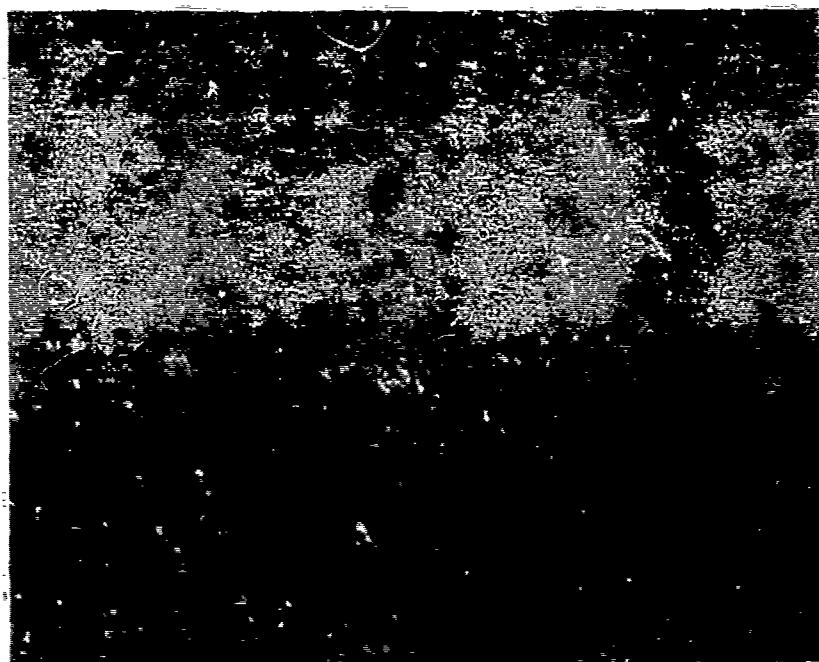


Fig. Cu-3. 10%  $\text{LaB}_6$ -Cu. Dark  $\text{LaB}_6$  Visible. Sample 17-8-79.



Fig. Cu-4. 2%  $\text{LaB}_6$ -Cu. Near top of sample 29-8-79.

dispersion of pink-red grains (shown by SEM analysis to be  $\text{LaB}_6$ ) in a copper matrix. It appeared that  $\text{LaB}_6$  and Cu (starting materials) had reacted very little. Figure Cu-4 (Ca 500X) shows a dentritic, directional growth of copper observed in a narrow band across the upper surface of the specimen. The copper matrix contained about 2% La, presumably in solid solution.

2. Next a mixture of 2.w/o  $\text{LaB}_6$  in Cu was directionally solidified in an alumina crucible. In this experiment the lowering rate was reduced from 25 cm/hr to 5 cm/hr. When viewed optically, there were no visible two-phase areas, the specimen appeared uniform and resembled copper in color and ease of grinding. Aligned dendrite structures were visible after polishing with a  $\text{HNO}_3$ ,  $\text{HCl}$ ,  $\text{H}_3\text{PO}_4$ , HAC mixture given in Petzow (Cu-7).

SEM measurements showed that a small level of La was uniformly distributed throughout the Cu matrix. However, there was also visible reaction with the alumina crucible. It was uncertain whether this reaction was due to traces of moisture in the alumina cement used to attach the crucible or if the higher reaction temperature and longer reaction duration led to the crucible-charge reaction. These possibilities were examined in later experiments.

3. In this next experiment, small amounts of 2.w/o and 10.w/o  $\text{LaB}_6$  - Cu mixtures were heated simultaneously in separate depressions on an alumina block to compare melting behavior, reactivity with alumina, and microstructural properties.

At the melting point of  $1150\text{-}1200^\circ\text{C}$ , both compositions seemed to react slightly with the alumina block. After cooling, it was apparent that a significant reaction with the alumina had occurred. It was concluded that other crucible materials should be tried.

4. Small amounts of 2 w/o and 10 w/o  $\text{LaB}_6$  - Cu were now heated simultaneously in depressions on a graphite block. The observed melting temperatures were again in the range  $1150\text{--}1200^\circ\text{C}$ , with the 10 w/o apparently melting at a higher temperature than the 2 w/o mixture.

There was little if any reaction with the graphite block. The 10% mixture seemed to "wet" the graphite container more than the 2%. Upon optical examination of the products, large areas of red needles were observed on the surface. Sections through the products revealed a random dispersion of red needles and blocky red-pink particles in a copper matrix. The 10 w/o product contained a much higher fraction of distinct  $\text{LaB}_6$  particles.

5. The products from the previous experiment were heated in the same apparatus for a longer period of time, then carefully examined for micro-structural features and elemental composition. Again melting was at approx.  $1150\text{--}1200^\circ\text{C}$ . If the temperature was raised to  $1300^\circ\text{C}$ , rapid vaporization started, depositing a red-brown film on the cool portion of the quartz tube. Red needles were visible on areas of the specimen surfaces. SEM measurements on polished sections showed a uniform distribution of La in the 2 w/o product and a non-uniform La distribution in the 10 w/o product. La concentrations could be directly correlated with observable  $\text{LaB}_6$  particles. 250X and 500X micrographs and elemental distribution density are shown in Figures (Cu-5-10).

Precipitate-like particles observed in several areas of the 10 w/o product. It was not possible to resolve these features to determine if they were  $\text{LaB}_6$  or other La-rich phases.

6. Intermediate compositions of 4 w/o and 6 w/o  $\text{LaB}_6$  in Cu were melted on a graphite block in  $\text{H}_2$ . The intent was to learn if greater



Fig. Cu-5. 2%  $\text{LaB}_6$ -Cu. Randomly Oriented  $\text{LaB}_6$  Needles in Sample 11-10-79.



Fig. Cu-6. 2%  $\text{LaB}_6$ -Cu. 500X of  $\text{LaB}_6$  Needles in Sample 11-10-79.

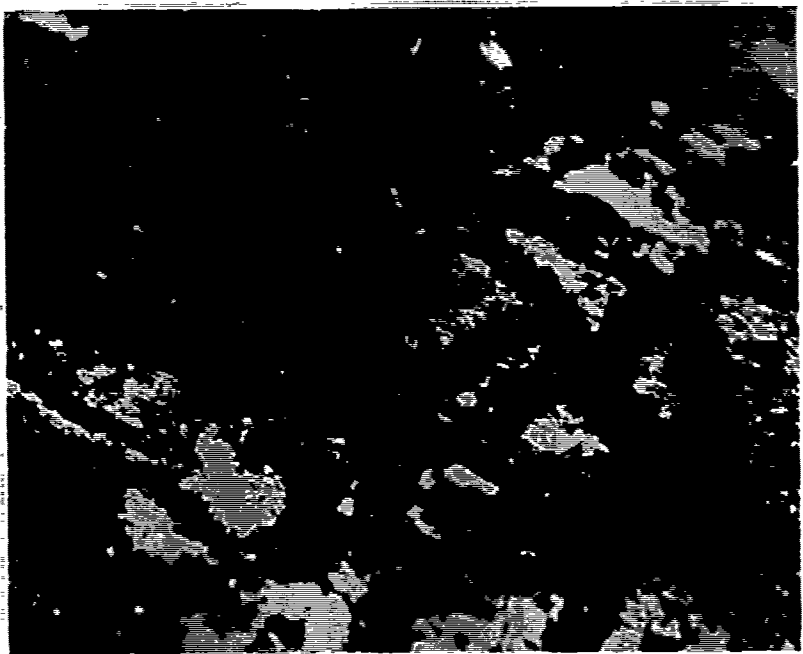


Fig. Cu-7. 10% LaB<sub>6</sub>-Cu. 200X of Large LaB<sub>6</sub> Needles in Sample 11-10-79.

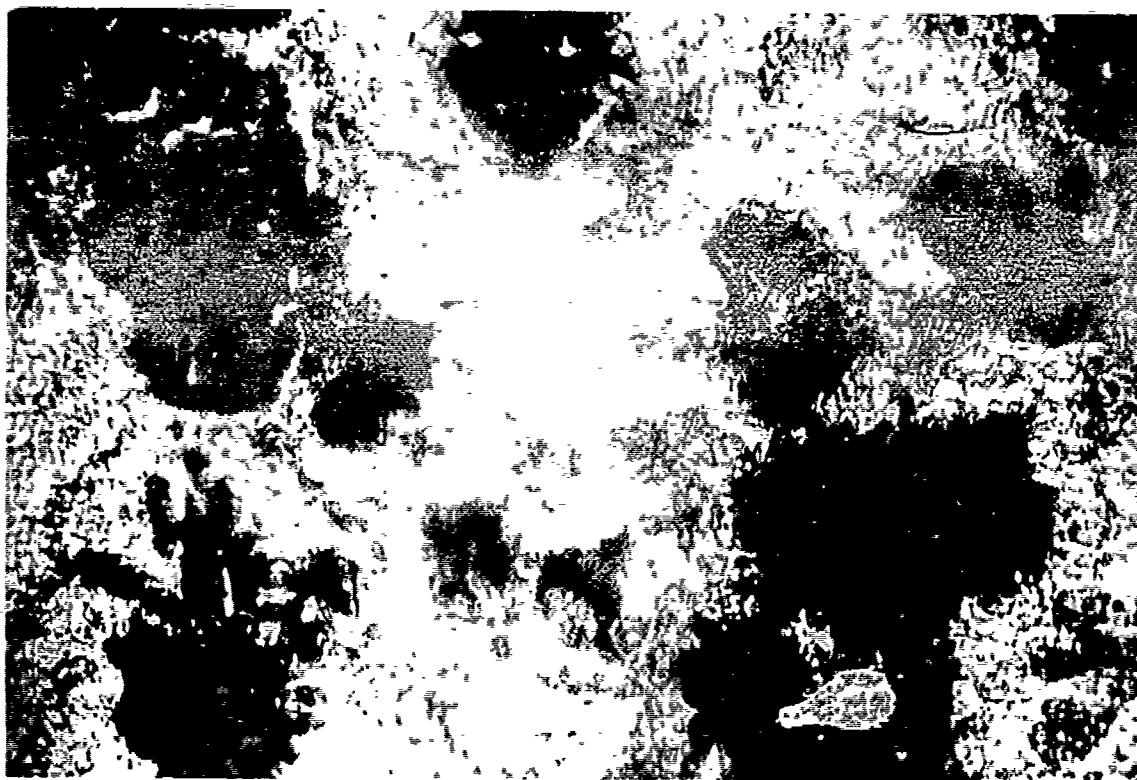


Fig. Cu-8. Sample 11-10-79.

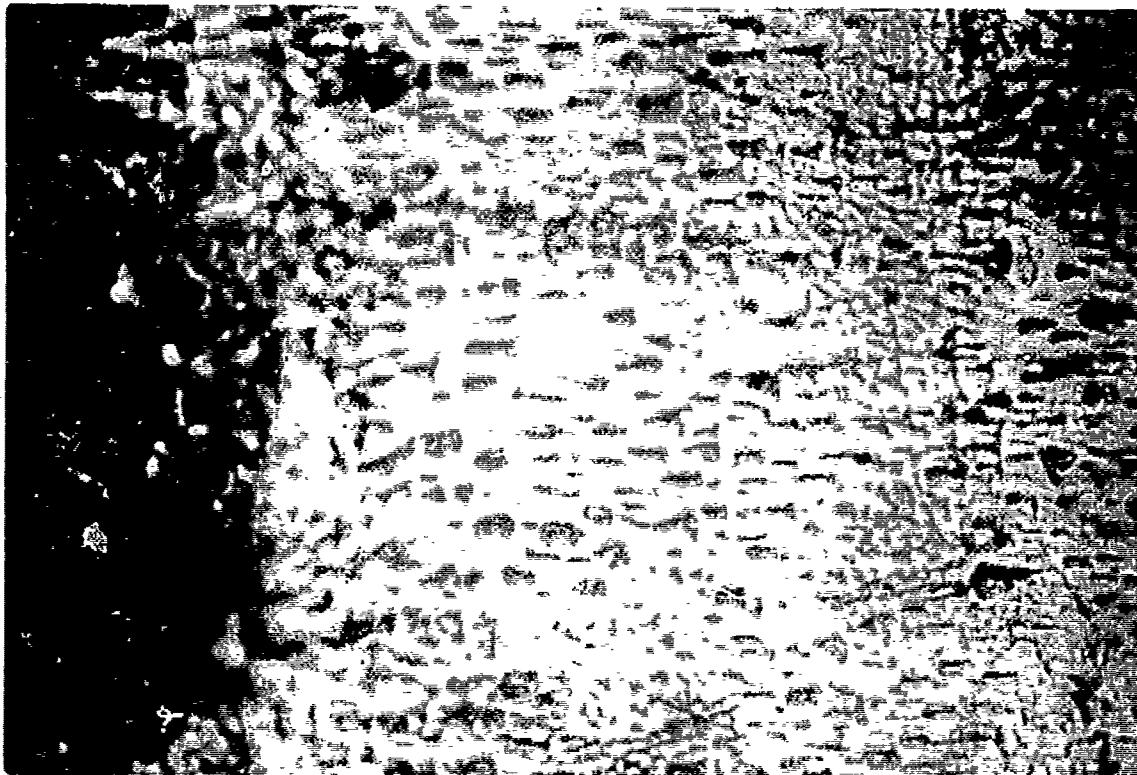


Fig. Cu-9. (500X) Sample 11-10-79.

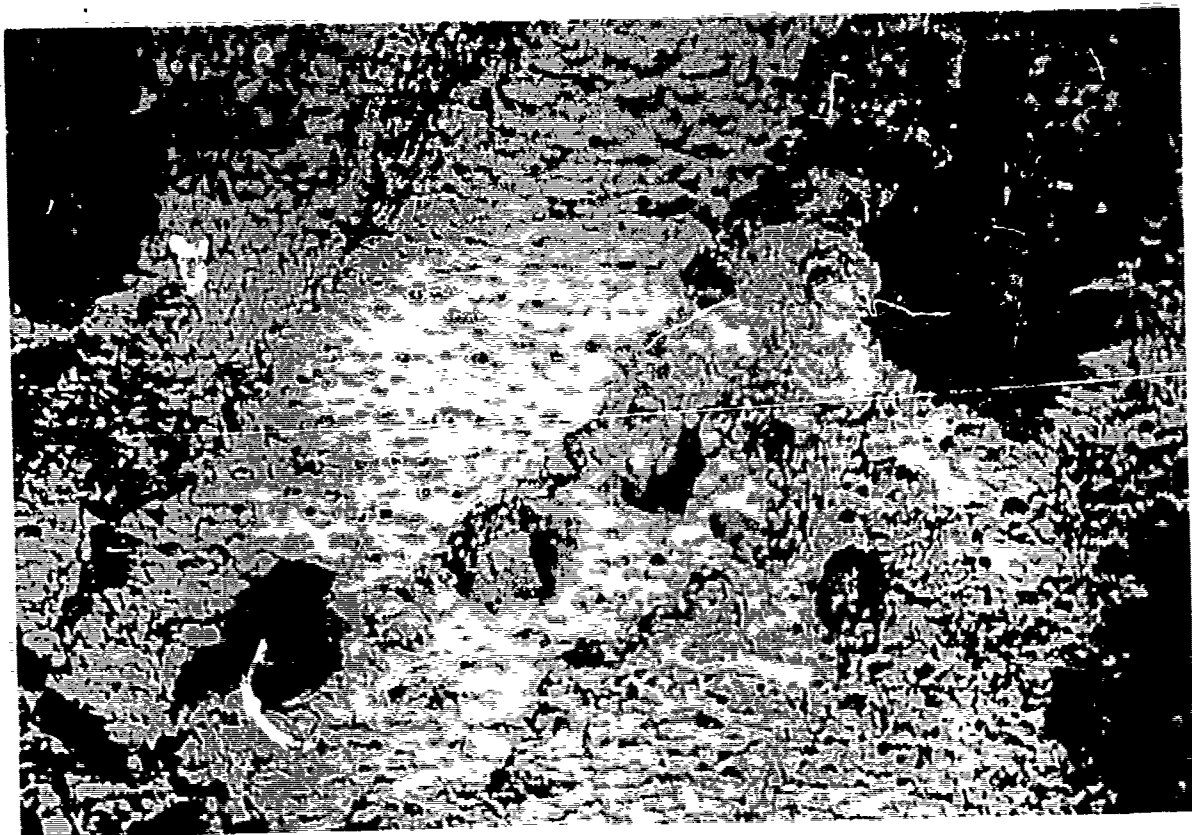


Fig. Cu-10. (500X) Sample 11-10-79.

concentrations of  $\text{LaB}_6$  would lead to a greater density of needle-like  $\text{LaB}_6$  particles in the product. The 2 w/o appeared to be forming a solid solution while the 10 w/o clearly contained a large excess of pure  $\text{LaB}_6$  particles. Therefore, at some intermediate point, all the  $\text{LaB}_6$  could dissolve, then solidify as a eutectic or two-phase system containing precipitated  $\text{LaB}_6$  as needles or blocky particles.

During melting, mixtures with higher  $\text{LaB}_6$  content were the more volatile at temperatures above the M.P. Red needle were visible on product surfaces and some red particles were observed on polished sections. SEM/Edax data showed that the needles were  $\text{LaB}_6$ .

7. After review of the results of several experiments on alumina and graphite, a further D.S. run was conducted. A mixture of 2 w/o  $\text{LaB}_6$  in Cu was solidified at 5 cm/hr in a graphite crucible of 1/4" i.d.

Micrographs at 250X and 500X of the product are shown in Figures (Cu-11-16). The first zone solidified contained an irregular dispersion of  $\text{LaB}_6$  particles with no visible microstructural features (Figures 11 and 12). At midpoint of the specimen, a sharp phase boundary is seen (Figures Cu-13-16). Note the distinct dendritic growth present in the last segment to solidify. Note also the randomly dispersed  $\text{LaB}_6$  particles in the dendritic structure. It is suggested that the "dendritic" region is a eutectic composition for the Cu/ $\text{LaB}_6$  pseudo-binary system.

#### Summary

Cu has several attractive properties as a matrix for  $\text{LaB}_6$  emitting fibers; Cu is ductile, an excellent heat conductor, and relatively inert to oxidation at low temperatures. Also, electrical contact to fibers could easily be made via the Cu matrix. Further study of the  $\text{LaB}_6$ -Cu system will better define the phase diagram. Possibly a

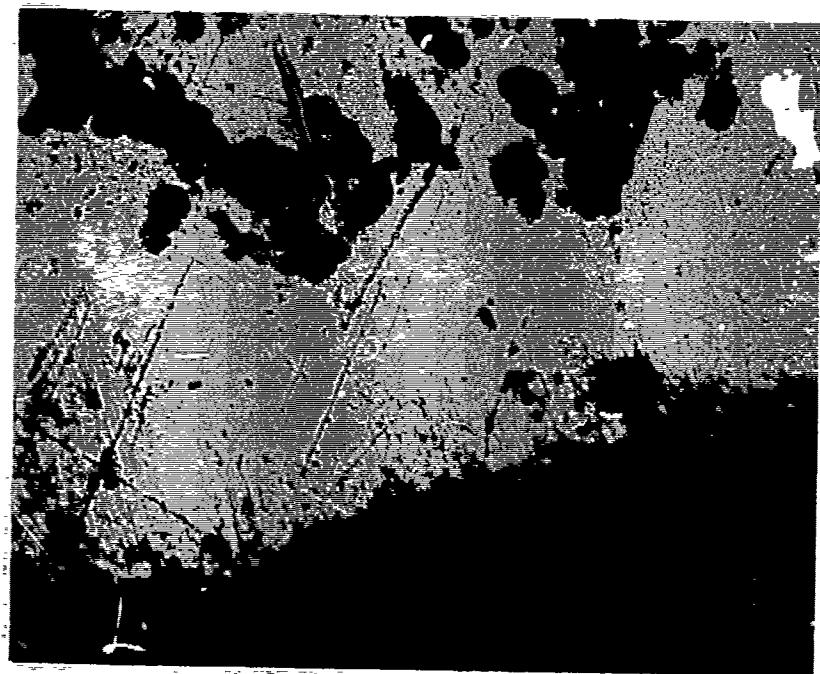


Fig. Cu-11. 150X of Sample #15-1-80.



Fig. Cu-12. 150X of Sample #15-1-80.

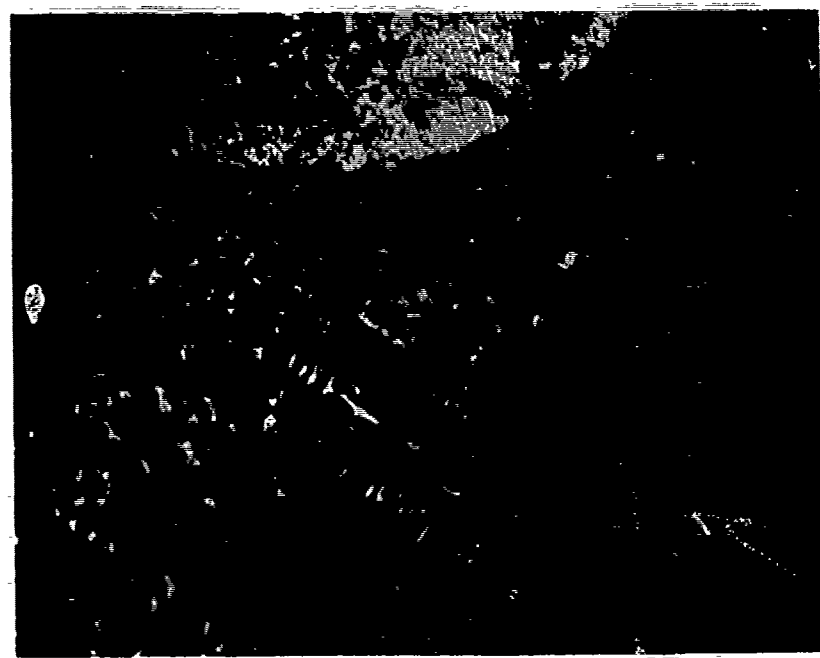


Fig. Cu-13. 50X of Sample #15-1-80 at the Interface.

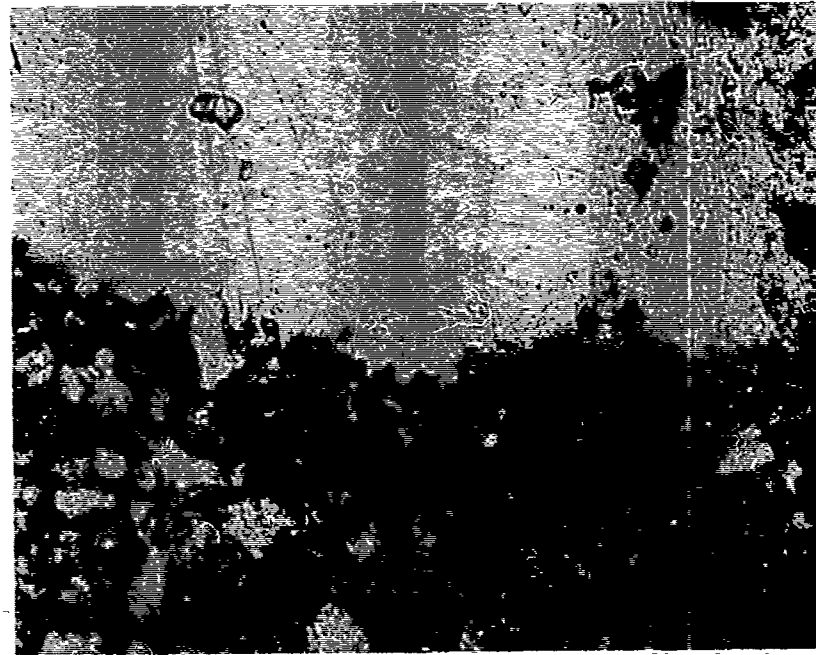


Fig. Cu-14. 150X of Sample #15-1-80.

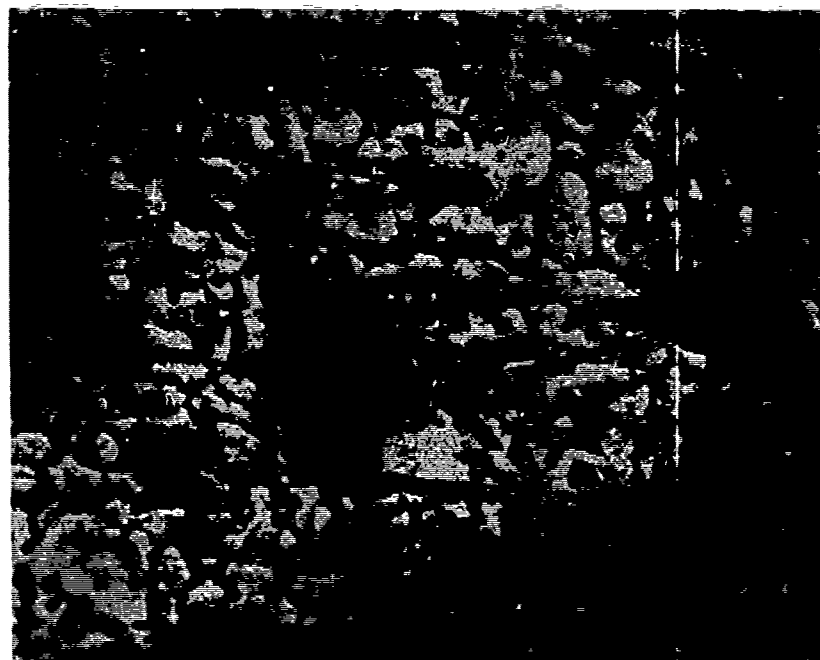


Fig. Cu-15. 150X of Sample #15-1-80 Near Top.

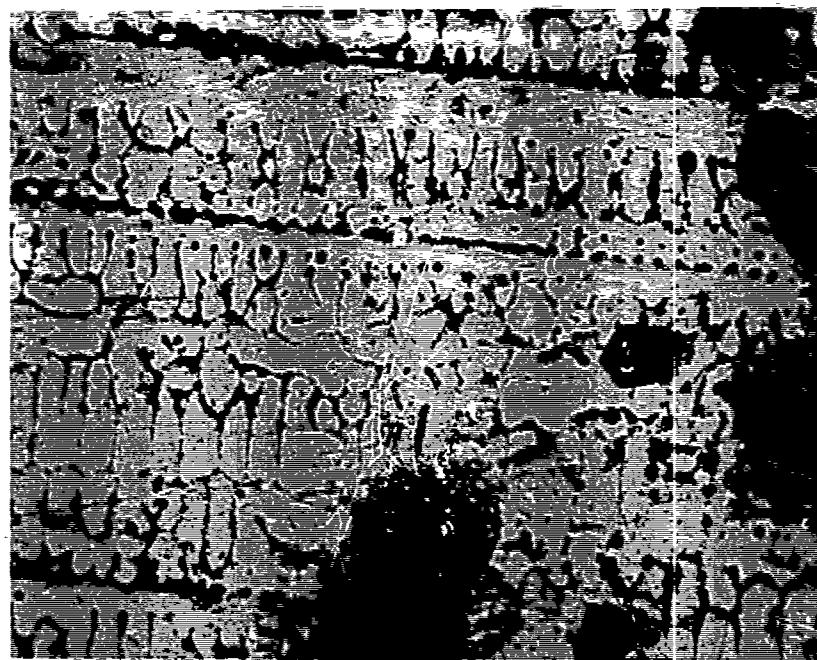


Fig. Cu-16. 150X of Sample #15-1-80 Near the Top.

study of the  $\text{LaB}_6$ -Cu system will better define the phase diagram. Possibly a pseudo-binary composition will be found which can yield a high density of the observed  $\text{LaB}_6$  fibers in a composite material.

References - Cu/LaB<sub>6</sub>

- (Cu-1) Lemsky, J. R., Private Communication, June 1979.
- (Cu-2) Matkovitch, V. I., "Boron and Refractory Borides," Springer-Verlag, 1977, p. 298.
- (Cu-3) Hansen, M., Constitution of Binary Alloys, McGraw-Hill Co., 1958, p. 250.
- (Cu-4) Perry, A. J., J. of Material Science, 8(1973), p. 1340.
- (Cu-5) Yen, C. F., Private Communication, May 1979.
- (Cu-6) Samsonov G., Boron, ITs Compounds, Springer Verlag, 1960.
- (Cu-7) Petzow, Gunter; Metallographic Etching, American Society for Metals, Metals Park, Ohio, 1978, p. 58-59.

### Summary and Conclusions

During the period covered by this study, the project team conducted directional growth experiments for  $\text{LaB}_6$ -B,  $\text{Fe}_2\text{B}$ -Fe,  $\text{LaB}_6$ -Cu,  $\text{TiB}_2$ -Ni and  $\text{LaB}_6$ -Ni systems, seeking regular microstructures containing metal-boride fibers in a stable matrix.

An effort was made to identify lower melting metal matrix systems containing  $\text{LaB}_6$  fibers. The presence of a  $\text{Ni-TiB}_2$  eutectic at 1200°C suggested that eutectic exists for  $\text{LaB}_6$  with Ni or other metallic elements. Experimentation is much easier and a metallic matrix has desirable electrical conductivity and mechanical ductility.

Much of the effort during this study has gone toward development of suitable preparation and analysis techniques in the several eutectic systems listed above. For the lower melting systems such as  $\text{TiB}_2$  - Ni, alumina or sapphire tubes were used for melting and directional growth. For the higher melting temperature of  $\text{LaB}_6$ -B, the floating zone technique was used. Many of the boride materials were hard and required special polishing techniques.

#### The System $\text{LaB}_6$ - B:

This system to date continues to be the most promising of those examined in this study. Attempts were made to directionally solidify lanthanum hexaboride as uniformly spaced rods, less than one micron in diameter, in a boron matrix. Lanthanum hexaboride and boron powders were combined in a near eutectic mixture, formed into right circular cylinders and melted by RF induction heating in a pure hydrogen atmosphere using a modified internal zone melting technique.

Ball milling, uniaxial cold pressing, isostatic pressing, hot pressing and electric arc melting were investigated as possible means of increasing the sample density before melting in the RF induction furnace. RF coupling was achieved directly in the hot pressed pellet, and indirectly through the use of molybdenum pre-heater in the uniaxially cold pressed pellets. Internal zone melting and various conventional crucible materials were tried.

Directional growth was observed in the pellets which were uniaxially cold pressed and pre-heated with a molybdenum pre-heater. Lanthanum hexaboride fibers with an  $\ell/d$  ratio of about ten to one and other forms of aligned microstructures were observed in selected areas of the pellet.

The System  $Fe_2B$ -Fe:

Early D. S. experiments yielded an aligned  $Fe_2B$  phase in a Fe matrix. Additional experiments in larger alumina tubes yielded somewhat more regular  $Fe_2B$  structures in both longitudinal and transverse cross section. This composite could be advanced to preliminary vacuum emission tests at this point. However, the properties of  $Fe_2B$  are not as desirable as  $LaB_6$  and other borides for electron emission applications.

The System  $LaB_6$ -Cu:

A survey of several cu-rich mixtures was made by melting mixtures of powder and examining by optical and SEM methods.  $LaB_6$  is stable in contact with liquid copper, limited solubility occurs, and needle-like  $LaB_6$  crystals were observed in two cases. It is felt that this system deserves further study.

The System  $TiB_2$ -Ni:

The reported eutectic behavior of a 3.5 w/o  $TiB_2$  in Ni has been examined by directional growth at several rates. To date, the system shows evidence of aligned microstructures. Additional tests should be made to search for conditions which promote aligned  $TiB_2$  phases.

The System  $LaB_6$ -Ni:

The presence of  $LaB_6$  phases in apparent equilibrium with Ni strongly suggests that a eutectic  $LaB_6$ -Ni composition can be identified as has been done in the case of  $TiB_2$ -Ni. Aligned microstructures were observed in D.S. specimens containing  $LaB_6$  and Ni as starting material. It is suggested that further phase studies of this system could result in composite material with potential as cathode element.

The directional solidification method apparently can be used as a tool for study of liquidus curves of unknown systems. It was repeatedly observed that the D.S. product from a two-phase region "deposits" a sequence of phases in layer fashion along the growth axis. The D.S. product can reveal the presence of congruent phases and thereby make possible an estimate of the phase diagram.

BIBLIOGRAPHY OF EUTECTIC COMPOSITES: PROPERTIES AND APPLICATIONS

Ahmed, H. "Lanthanum Hexaboride Electron Emitter," J. of Appl. Physics, Vo. 43, No 5, May 1972, p. 2185.

Aita, T., "Single Crystal Growth of Lanthanum Hexaboride in Molten Aluminum," Japan. J. Appli. Phys., Vol. 13, No. 2 1974, p. 391.

Alexander, John A., "Investigation to Produce Matrix Composites with High-Modulus, Low Density Continuous Filament Reinforcements, AFML TR 67 391. 150P. Feb 68.

Butneva, N. I., "Method of Developing Boride Phases By Color Metallography," Zavodskaya Laboratoriya, Vol. 38 No. 9, pp. 1111-1112, Sept. 1972, p. 1397.

Camcohoob, L., "Xapaktep B3A MO E CTB SOP A T TAH A C META AM PY Bl E E3A, No. 1, 1958r.

Chin, T., "Electronic Processes in Oxide Cathodes," RCA Review, Vol 35, Dec. 1974, p. 520.

Clougherty, Edward V., ET AL., "Research and Development of Refractory Oxidation Resistant DI BO RI Des., AFML TR 68 190. AF33(615) 3671 313P. Jul 68.

Donald, I. W., "Review Ceramic-Matrix Composites Journal of Materials Science 11 (1976) 949-972.

Elinson M., "Field Emission Cathodes of High-Melting Metal Compounds," Radiotekhnika Electronika, Vol. 1, p. 1417, 1962.

Elwell, D., "Surface Structure and Electrolytic Growth Stability of LaB<sub>6</sub> Crystals," J. of Crystal Growth, Vol. 29, 1975 pp. 65-68

Ethournear, J., "Structure Electronique de Quelques Hexaborures de Type CaB<sub>6</sub>," J. of Solid State Chemistry, Vol. 2, 1970 pp. 332-342.

Fisk, Z., "Preparation and Lattice Parameters of the Rare Earth Tetraborides," Mat. Res. Bull., Vol 7, 1972, pp. 285-288.

Fisk, Z., "Growth of YB<sub>6</sub> Single Crystals," Mat. Res. Bull. Vol. 11, pp. 1019-1022, 1976.

Flemings, M., Solidification Processing, McGraw-Hill Book Co. New York, 1974 p. 364.

Ford, R., "Structure of Lanthanum-hexaboride-coated rhenium filaments," J. of Appl Physics, Vol. 44, No 10, Oct 73 p. 4378.

Fursei, G., "Localization of Field Emission in Small Solid Angles," Soviet Physic-Technical Physics, Vol. 11 No 6, Dec. 1966. p. 827.

Futamoto, Masaaki, "Crystallographic Properties of  $\text{LaB}_6$  Formed in Molten Aluminum, Japanese Journal of Applied Physics, Vol. 14, No. 9, Sept. 1975.

Futamoto, Masaaki, "Field-emission and field-ion microscopy of Lanthanum Hexaboride," J of Appl. Physics, Vol 48, No. 8, Aug 1977 pp. 3541-3546.

Gardner, Fred M., Grazing Alloy for Bonding Thermonic Cathode to Support. United States Patent [15] 3,668,457 June 6, 1972.

Gibson, E., "The Preparation of Single Crystal  $\text{LaB}_6$  Cathodes for Electron Microscopes," J of Phsics E. Scientific Instruments, Vol 8, 1975 pp. 1003-1004.

Givargizov, E., "Morphology of Silicon Whiskers Grown by the VLS-Technique," J. of Crystal Growth, Vol 9, 1971, pp 326-329.

Goebel, D. M., "Lanthanum Hexaboride Hollow Cathode for Dense Plasma Production," Rev. Sci. Instrum 49(4), Apr. 78.

Gruber, Bernard A., "Process for the Production of Metal Borides," U. S. Patent #3, 096, 149 July 2, 1963.

Herzog, J. A., Filaments Fibers and Metal Matrix Composites, Air Force Materials Lab., Wright Patterson AFB, Ohio, AFML-TR-67 244, 53p Oct. 67.

Higashi, I., "Growth of Titanium Diboride Single Crystals in Molten Aluminum," J of Crystal Growth, Vol 7, 1970, pp. 251-253.

Ingold, J. H., Therminoic Properties of Some Refractory Metal Carbides. J. of Applied Physics Vol 34, No. 7, July 1963 p. 2033.

Jen-Der Hong, K. E. Spear, "Directional Solidification of  $\text{SiC-B}_4\text{C}$  Eutectic: Growth and Some Properties." Mat. Res. Bull. Vol 14 pp. 775, 1979.

Johnson, R., "The Lanthanum-Boron System," J of Phys. Chem, Vol 65, 1961, p. 909.

Kanitkar, P., "Field Emission Studies of the Lanthanum Hexaboride/Tungsten System," J. Physics D: Appl. Phys. Vol 9, 1976 pp 1165-1168.

Kanitkar, P. L. "Field Emissian Studies of the Lanthanum Hexaboride/Tungsten System. J. Phys. D: Appl. Phys. Vol 9, 1976 p. 153.

Kumashiro, Y., et al. "TiC Single Crystals Prepared by the Radio Frequency Floating Zone, Process" J. of the Less-Common Metals, Vol. 32, 1973, p.21.

Krochmal, J. J., Fiber Reinforced Ceramics: A Review and Assessment of Their Potential Air Force Materials Lab., Wright Patterson AFB, Ohio AFML TR 67 207, 85P., Oct 67.

Lafferty, J., "Boride Cathodes," J. of Applied Physics, Vol 22, No 3, March 1951, p 299.

Lee, K. N., Exchange Interactions and Fluctuations in  $\text{CeB}_6$ , Physical Review B, Vol. 6 No. 3, Aug. 1973, p 1032.

Levine, J., "Analysis and Optimization of a Field-Emitter Array," RCA Review, Vol 32, March 71, p 144.

Levitt, Albert P., "Whisker Composites by Eutectic Solidification," Whisker Technology, Wiley Inter-Science, New York, N.W. pp 343-401, 1970.

Luchinskii, G. P., Army Foreign Science and Technology Center Charlotte ETC F/G 7/2 Titanium Compounds Containing Hydrogen, Nitrogen and other Non-ETC Sept 74

Morris, James F., "Spacecraft Charging Control By Thermal, Field Emission with Lanthanum-Hexaboride Emitter".

Morris J. F., Spacecraft Charging Control by Thermal Field Emission with Lanthanum Hexaboride Emitters, NASA TM 78990

Milek, John T., Hughes Aircraft Co. Culver City Calif. Electronic Prop--ETC Boron.

Minfore, W. J., "Crystallography and Microstructure of Directionally Solidified Oxide Eutectics," Journal of American Ceramic Society, Vol 62, 1979 p 154-157.

Motojima, Seiji, "Chemical Vapor Growth of  $\text{LaB}_6$  Whiskers and Crystals Having A Shapr Tip," Journal of Crystal Growth 44 1978 pp 1060-1099

Murr, L., Interfacial Phenomena in Metals and Alloys, Addison-Wesley Publishing Co., Reading, Mass., 1975, p 376.

Niemyski, T., "Crystallization of Lanthanum Hexaboride," J. of Crystal Growth, Vol 3, 4 1968. pp 162-165.

Pelletier, J., "Work Function of Sintered Lanthanum Hexaboride," Appl Phys. Lett 34(4) p 249, Feb. 1979.

Perry, A. J., "The Copper-boron Eutectic Unidirectionally Solidified," Journal of Material Science, 8, 1973, p.1340.

Quatinetz, Max Refractory Metal Base Allow Composites United States Patent Office 3,676,084 patented July 11, 1972.

Rachidi, I, "Surface Ionization Negative Ion Source," Applied Physics Letters, Vol 28, No 5, March 1976, p 292

Ramachandra, K. N., "Rhenium bonded LaB<sub>6</sub> Electron Source," Rev. Sci. Instrum., Vol 46, p 1662 No. 12 Dec. 1975.

Rare-Earth Information Center, "LaB<sub>6</sub> is Better" Vol. XI No. 1, March 1, 1976.

Research Materials Information Center, "Crystal Growth and Solid-State Materials Research."

Rivlin, Vivian G., Field Emission Cold Cathode Devices based on Eutectic System. A Literature Search. Contract or Grant Number, AFOSR-77-3292, p 40.

Rudy, E. I, Aerojet-General Corp. Sacramento Calif. Materials Research--ETC Ternary Phase Equilibria In Transition Metal-Boron-Carbon-Silicon SY--ETC May 69.

Salkind M. and F. Lemkey, "Metals with Grown-In Whiskers, International Science and Technology, p.52, Mar. 1967.

Samsonov, G., "Nature of Interaction Between Titanium Boride and The Iron-Group Metals," Metallovenic I Obrabotka Metalloy, Vol 1, Jan. 1958, pp 35-38.

Samsonov, G. Boron, Its Compounds and Alloys, Translation Series AEC-tr-5032 (Book 1), 1960, p 624.

Samsonov, G. V., "Preparation of the Double Boride of Lanthanum and Sodium and Study of Some of its Physical and Chemical Properties," translated from Zhurnal Prikladnoi Khimii, Vol 37, No. 9, pp 1872-1878, Sept. 1964.

Samsonov, G. W., "The Emission Properties of Zirconium Diboride." (above reference).

Schmidt, P.H., "Anisotropy of Thermionic Electron Emission Values for LaB<sub>6</sub> Single-Crystal Emitter Cathodes," Applied Physics letters, Vol 29, No. 7, 1 Oct. 76, p 400.

Schmidt, P.H., "Design and Optimization of Directly Heated LaB<sub>6</sub> Cathode Assemblies for Electron-Beam Instruments," J. Vac. Sci. Technol. 15 (4) Jul/Aug 1978 p 1554

Schmidt, P.H., "Low Work Function Electron Emitter Hexaborides," J. Vac. Sci. Technol., 15 (6) Nov./Dec 78, p 1809

Senzaki, Kiyoshi, Field Emission Studies of TiC Single Crystal. Proc. 6th Internl. Vacuum Congr. 1974 Japan J. Appl. Phys. Suppl. 2, Pt. 1, 1974. p 289.

Shimizu, R."Field Emission Pattern of LaB<sub>6</sub> Single Crystal Tip," Japan J. Appl Phys, Vol 14, No. 7, 1975 p 1089.

Shimizu, R., "LaB<sub>6</sub> Single-Crystal tips as an Electron Source of High Brightness," *Applied Physics Letters*, Vol 27, No. 3, Aug. 75, p 113.

Shimizu, R., "Stability of Beam Current of Single Crystal LaB<sub>6</sub> Cathode in High Vacuum," *Japan, J. Appl.Phys.*, Vol 16 1977, No 4, p 669.

Shrednik, V., "Investigation of Atomic Layers of Zirconium on the Faces of a Tungsten Crystal By Means of Electron and Ion Projectors," *Soviet Physics-solid State*, Vol 3, No 6, Dec. 1961, p 1268.

Shurin, A. K., Phase Diagrams and Structure of Alloys of Quasi-Binary Systems Cr-ZrB<sub>2</sub> and Cr HfB<sub>2</sub>.  
IHCITHTYTA META O I3HKH AH YPCP HA I H W O 21.XII p 1973.

Shurin, A. K., "Phase Equilibria and Structure of Alloys Fe-TiB<sub>2</sub>, Fe-ZrB<sub>2</sub> and Fe-HfB"

Silva de, A.R.T., Tensile-Defromation Characteristics of Unidirectionally Solidified Eutectic Alloys. *Metal Science Journal*, Vol. 3, 1969, p.63.

Silva de, A.R.T., "The Fatigue Behaviour of the Unidirectionally Solidified Fibrous Fe-Fe<sub>2</sub>B Eutectic Alloy," *Metal Society J.*, Vol. 4, 1970, p.90.

Spear, K., "Phase Behavior and Related Properties of Rare-Earth Borides," Phase Diagrams Materials Science and Technology, A.M. Alper Ed. Vol IV, Academic Press, New York, 1976.

Sprenger, H., "Boride Und Sillizide Als Verstarkungsphasen in eutektishcen Hochtemperaturwerkstoffen," *Z. Metallkde*, Vol 68, No 4, 1977 pp 241-252.

Stanford Research Institute, "Examples of Submicron Structures Build By SRI Physical Electronics Group."

Stewart, D., "A Preliminary Study of Field Emission Cold Cathode Devices Prepared From Directionally Solidified Eutectic Materials."

Storms, Edmund, "The Vaporization Behavior of the Defect Carbides Part I: The Nb-C System" *High Temperature Sciencel*, 430-455, 1969.

Storms, Edmund, "Phase Relationship, Vaporization, and Thermodynamic Properties of the Lanthanum-Boron System," *The Journal of Physical Chemistry*, Vol. 82, No. 1, 1978 p 51.

Swanson L., "Angular Confinement of Field Electron and Ion Emission," *J. of Appl. Physics*, Vol 40, No 12, Nov 1969 p 4741.

Swanson, L., "Fabrication..... Converters," NASA Semiannual Report, NASA Grant No. NSG-3054, 1975, p 37.

Swanson, L., "Single-crystal Work-function and Evaporation Measurements of  $\text{LaB}_6$ ," Appl. Physics Letters, Vol 28, No 10. 15 May, p 578.

Swanson, L., "Fabrication.....Converters," NASA Interim Report #2, NASA Grant No. NSG 3054, p 38, Aug 1977.

Swanson, L., "Coadsorption Studies of Oxygen and Cesium on Lanthanum Hexaboride," NASA Interim Report #3, NASA Grant No. NSG-3054., p 18 Jan. 78.

Swanson, L., "Work Functions of the (001) Face of the Hexaborides of Ba, La, Ce and Sm.

Tanaka, T., "Growth of High Purity  $\text{LaB}_6$  Single Crystals By Multi-Float Passage," J. of Crystal Growth, Vol 30, 1975, pp 193-197.

Telegus, V. S., "Phase Equilibria In the Systems Vanadium-Manganese-Boron, Molybdenum-Manganese-Boron, and Tungsten-Manganese-Boron.

Vikhrev, "Composite Thermionic Emitters," Lenningradskii, Elektroteknicheskii Institut. Izvestiia, No. 104: 132-136, 1971

Wallace, T.C., Research Being Performed in the Chemistry and Materials Science Division of the Los Alamos Scientific Laboratory, Los Alamos, New Mexico. p 8, 1976.

Walter, J. (ed), "Conference on In Situ Composites-II," Xerox Individualized Publishing, Lexington, Mass. p 622, 1976.

Windsor, Eric Edward, "Field-Emission Cathode," Patent Specification 1 223 697.

Windsor, E.E., "Construction and Performance of Practical Field Emitters from Lanthanum Bexaboride," Proc. IEEE. Vol 116, No 3, March 1969, p 348.

Yen, C. F. "Enhancement of Mechanical Strength in Hot Pressed  $\text{TiB}_2$  Composites by the Addition of Fe and Ni." ORNL Report 38D, 1979.

Zybeck, I., "The Growth of Lanthanum Hexaboride Single Crystals by Molten Salt Electrolysis," J of Crystal Growth, Vol 34, 1976 pp 85-91.

MISSION  
of  
*Rome Air Development Center*

RADC plans and executes research, development, test and selected acquisition programs in support of Command, Control Communications and Intelligence (C<sup>3</sup>I) activities. Technical and engineering support within areas of technical competence is provided to ESD Program Offices (POs) and other ESD elements. The principal technical mission areas are communications, electromagnetic guidance and control, surveillance of ground and aerospace objects, intelligence data collection and handling, information system technology, ionospheric propagation, solid state sciences, microwave physics and electronic reliability, maintainability and compatibility.

# **SUPPLEMENTARY**

# **INFORMATION**

*AD-8101703*

ERRATA

10 August 1981

RADC-TR-81-92 dated May 1981

DEVELOPMENT OF BORIDE COMPOSITE MATERIALS FOR COLD CATHODE DEVICES

1. The authorship on the cover and in Block 7 of the DD Form 1473 should be corrected to read:

JOHN W. GOODRUM and KATHYRN V. LOGAN.

2. Pages 1 through 48 should be referenced to:

Kathryn Vance Logan, Feasibility of Directional Solidification of Lanthanum Hexaboride in a Boron Matrix. M.S. Thesis, Georgia Institute of Technology, December 1980.

Rome Air Development Center  
Air Force Systems Command  
Griffiss Air Force Base, New York 13441